ISBN 0-315-54923-8

THE UNIVERSITY OF MANITOBA

SYNTHESIS, CHARACTERIZATION AND COMPLEXATION OF SMALL AND LARGE CROWN THIOETHERS.

BY

BROER DE GROOT

A THESIS
SUBMITTED TO THE FACULTY OF GRADUATE STUDIES
IN PARTIAL FULFILLMENT OF THE REQUIREMENTS FOR THE
DEGREE OF MASTER OF SCIENCE

DEPARTMENT OF CHEMISTRY

WINNIPEG, MANITOBA

1989

SYNTHESIS, CHARACTERIZATION AND COMPLEXATION OF SMALL AND LARGE CROWN THIOETHERS.

BY

BROER DE GROOT

SYNTHESIS, CHARACTERIZATION AND COMPLEXATION OF SMALL AND LARGE CROWN THIOETHERS

BY

BROER DE GROOT

A thesis submitted to the Faculty of Graduate Studies of the University of Manitoba in partial fulfillment of the requirements of the degree of

MASTER OF SCIENCE

ABSTRACT

This thesis describes the synthesis, characterization, and complexation of several macrocyclic thioethers. The investigation of crown thioethers has been thwarted by the fact that in many cases they are accessible only with great difficulty. High dilution techniques had to be used, often affording only low yields of mixtures of products which required laborious separation. It was not until the early 1980's that the synthetic problems were overcome, when Kellogg and Buter introduced a new method, which employs cesium ions in the ring closure step[13,14]. Both synthetic methods are described in this thesis. Improved synthetic methods and the discovery of copper coordination to methionine in blue copper proteins, as well as the potential analogy to catalytically active phosphine complexes, revived the interest in thioether coordination chemistry and its electronic consequences. Two classes of ligands were prepared: tridentate and hexadentate macrocyclic thioethers. 'Rigid groups' (-CH_2-, *ortho*- and *meta*-xylyl) were incorporated in the rings to separate the two coordination sites, formed by $SCH_2CH_2SCH_2CH_2S$ strings. The potentially ditopic hexadentate thioether 1,3,6,9,11,14-hexathiacyclohexane(16S6) forms a mononuclear complex, $[Cu(16S6)][ClO_4]$, with $[Cu(CH_3CN)_4][ClO_4]$. The -CH_2- "spacing unit" appears to be too small for 16S6 to allow the coordination of two Cu(I) ions. Instead the ligand "wraps" around the Cu(I) ion, which uses only four of the six S atoms for coordination. The tridentate ligands 2,5,8-Trithia[9]-*o*-benzenophane (TTOB) and 2,5,8-Trithia[9]-*m*-benzenophane (TTMB) have one subunit for facial metal ion coordination. They serve as a probe for coordination of metals to the ditopic hexadentate ligands 2,5,8,13,16,19-Hexathia[9.9]-*ortho*-benzenophane (HTOB) and 2,5,8,13,16,19-Hexathia[9.9]-*meta*-benzenophane (HTMB), in which the chelating strings

are separated by *ortho*- and *meta*-xylyl units respectively. The CH_3CN ligand of the Cu(I) complex, $[Cu(TTOB)(CH_3CN)][ClO_4]$, is readily replaced by phosphines and other small molecules such as pyridine and benzonitrile. The small ring ligand TTOB can accomodate metals with a tetrahedral or octahedral geometry as evidenced by the structures of $[Cu(TTOB)(PPh_2Me)][ClO_4]$ and $Mo(TTOB)(CO)_3$. The meta analogue, TTMB, did not form complexes with Cu(I). The large macrocycle HTOB forms a binuclear complex $[Cu_2(HTOB)(CH_3CN)_2][ClO_4]_2$, with $[Cu(CH_3CN)_4][ClO_4]$ and its chemistry is analogous to the Cu(I) complex of TTOB. The ligands and complexes are studied through the use of $^{31}P\{^1H\}$, $^{13}C\{^1H\}$, and ^1H NMR, infrared and mass spectroscopy, and X-ray crystallography.

Erica....we thank you for the delight,

The joy and the love that you brought to us

in your short passage here.

Less is more.

Simplify, simplify, simplify.

Henry David Thoreau.

ACKNOWLEDGEMENTS

First of all I would like to thank Dr. Steve Loeb for accepting me as a graduate student and hence making it possible for me to realize a wish I've had for a long time. Thanks also to the Chemistry Department of the University of Winnipeg, a staff of wonderful people, each of whom I could depend on in times of hardship. I am grateful to the University of Manitoba for the use of their NMR facilities and to Dr. Doug Stephan at the University of Windsor for collecting all the X-ray diffraction data.

Furthermore, I am especially grateful to my wife Janine for her support and patience throughout my studies and in particular during the last four months of writing this thesis.

TABLE OF CONTENTS

CHAPTER 1

Introduction

CHAPTER 2

Chemistry of 16S6

CHAPTER 3

Synthesis, Characterization and Complexation of the Tridentate Ligands 2,5,8-Trithia[9]-*o*-benzenophane, TTOB and 2,5,8-Trithia[9]-*m*-benzenophane, TTMB.

Page

CHAPTER 4

The Ditopic Ligands 2,5,8,13,16,19-Hexathia[9.9]-*ortho*-benzenophane, HTOB and 2,5,8,13,16,19-Hexathia[9.9]-*meta*-benzenophane, HTMB.

LIST OF TABLES

LIST OF FIGURES

LIST OF ABBREVIATIONS

NMR	Nuclear Magnetic Resonance
MSD	Mass Selective Detector
GCMS	Gas Chromatography-Mass Spectroscopy
MS	Mass Spectroscopy
IR	Infra Red
ORTEP	Oak Ridge Thermal Ellipsoid Plot
mp	melting point
bp	boiling point
DMSO	DiMethylSulfOxide
DMF	DiMethylFormamide
16S6	1,3,6,9,11,14-Hexathiacyclohexadecane
TTOB	2,5,8-TriThia[9]-*Ortho*-Benzenophane
TTMB	2,5,8-TriThia[9]-*Meta*-Benzenophane
HTOB	2,5,8,13,16,19-HexaThia[9.9]-*Ortho*-Benzenophane
HTMB	2,5,8,13,16,19-HexaThia[9.9]-*Meta*-Benzenophane

CHAPTER 1

Introduction

1.1 Historical Background

Macrocyclic thioethers have been known for a long time. In 1934, Meadow and Reid[1] found that the reaction of sodium ethanedithiolate with ethylene bromide resulted in the formation of a lot of polymer and a small amount of the cyclic hexamer 1,4,7,10,13,16-hexathiacyclooctadecane (18S6). It was not until about 30 years later that the interest in the extensive chemistry of crown ethers was renewed. At that time, some new work by Pedersen[2,7] was published on crown oxaethers and by Rosen and Busch[3] on macrocyclic thioether ligands.

Since then, the chemistry of crown thioethers has undergone an explosive development. The reasons for this revived interest were the discovery of thioether coordination to copper in blue copper proteins[4,5,6] and improved synthetic methods. It is expected that the presence of S-donor atoms in the coordination sphere will lead to some novel chemistry that may further elucidate the binding of copper in bioinorganic complexes. The potential analogy to, and perhaps complement to, phosphine coordination chemistry led to investigation of the electronic consequences of thioether coordination. Industrial interest is geared towards the potential application of thioether complexes in homogeneous catalysis. A large quantity of homoleptic crown thioether complexes with a wide variety of metal ions has already been synthesized. The majority of them are mononuclear complexes. The research in this area has been focussed on the electronic consequences of an all sulfur coordination sphere, electrochemistry, ring size effects and conformational analysis.

1.2 Nomenclature

In its broadest sense, the definition of crown thio- or thia-ethers, would entail any medium sized or macrocyclic system having only one ring and containing only sulfur heteroatoms in the ring. As the work in thioether chemistry expanded, the system to indicate different structural types and/or functional groups became more complicated. The term "crown", was first invented by Pedersen and generally refers to macrocyclic polyethers having the ethyleneoxy unit as the basic repeating structure. Thus, for crown thioethers the repeating unit would be CH_2CH_2-S.

By analogy to the nomenclature convention for simple oxa-crowns, the description of simple thia-crowns involves two numbers; one to indicate the ring size and the other to indicate the number of heteroatoms that are present in the ring. The often long and cumbersome systematic names can be shortened considerably this way. For instance, 1,4,7,10,13,16-hexathiacyclooctadecane becomes hexathia-18-crown-6, indicating an eighteen-membered ring with six heteroatoms. Other systems to indicate that the heteroatoms are sulfur atoms can be used as well. Examples are 18-crown-S6, 18-ANE-S6 or 18S6.

Any substituents on the ring, or the presence of methylene- or propylene linking units between heteroatoms, complicate the systematic nomenclature considerably. For this reason, the simple "more convenient crown" descriptors persist, despite sometimes giving incomplete information and hence creating ambiguity, as shown in Figure 1.1.

Both structures are referred to as 20S6, but their systematic names differ. To indicate the length of the carbon chains between the sulfur atoms prefixes are inserted in the name. The two structures could be described as S_6-ethano-propano-ethano[20] or S_6-e-pr-e[20] and S_6-propano-methano-propano[20] or S_6-pr-m-pr[20] to denote a 20-membered ring containing six sulfur atoms separated by the sequence of alkyl chains as indicated[35,39]. However, this system is rarely used and the ambiguous nomenclature

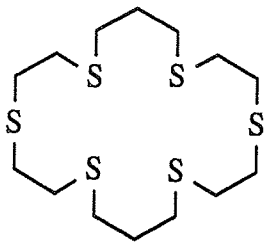

20S6.
1,4,7,11,14,17-hexathia-cycloeicosane.

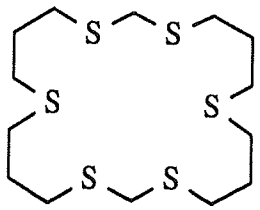

20S6
1,5,9,11,15,19-hexathia-cycloeicosane.

Figure 1.1 Ambiguity in "convenient" nomenclature.

prevails. Rigid groups included in the ring structure are indicated before the number giving the ring size, e.g. dibenzo-18S6 or dicyclohexano-18-crown-6. The fully descriptive systematic name would also include the placement of the group as in 2,3,11,12-dibenzo-1,4,7,10,13,16-hexathia-2,11-cyclooctadecadiene[16].

Once a molecule has been introduced, fully structurally characterized and described, the systematic names are often replaced by more "convenient" acronyms, e.g. 1,4,7-trithiacyclononane, (9S3), by TTCN and 1,4,7-trithianonane by TTN. Two numbering systems of the atoms are in use; (a) according to IUPAC conventions the atoms are numbered sequentially around the ring (S1, C2, C3, S4, etc.)[26] and (b) the system in which the sulfur and carbon atoms are numbered in separate sequences (S1, C1, C2, S2, etc.). The latter seems to be used more frequently in crystallographic descriptions of structures, whereas the first one is always used in the systematic nomenclature.

1.3 Synthesis

A drawback to the study of crown thioether ligands and their coordination chemistry was the lack of safe, general, high-yield synthetic routes to the ligands and their

subsequent purification. Some of the early syntheses required the use of very toxic intermediates[8] such as dichloroethylsulfide, which is a powerful vesicant. The formation of rings of different sizes in the one-pot reactions, often necessitated the use of complicated chromatographic methods[8-12] to separate the desired product.

The major problem is the formation of polymeric material. If the cyclization step proceeds through an ordinary S_N2 reaction, such as the thiolate anion attacking an activated carbon as shown schematically below, then the formation of linear polymer is

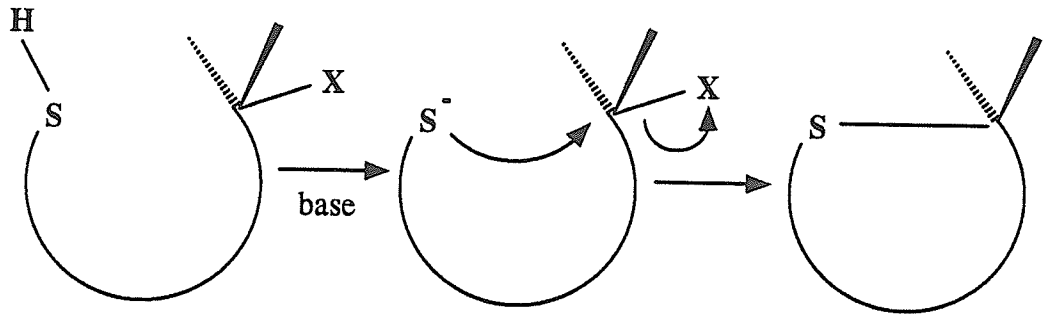

Figure 1.2 Schematic representation intramolecular ringclosure by a S_N2 mechanism.

favoured over the entropy constraints of cyclization[8]. Since this is a statistically defined process, high dilution techniques have to be employed to favor cyclization kinetically[8-14].

Another factor on which the ring closure depends is the so-called "template-effect". This is the ability of the linear polyether fragment to "wrap" itself around an alkali metal ion, thus facilitating its ring closure. In contrast to the strong template effect and corresponding high yields of macrocyclic polyoxaethers, it turns out that the low sulfur-active metal ion coordination renders template effects of little or no consequence[4,8]. In thioether chemistry, only two very specific multi-step syntheses are known that make use of some kind of template-effect; (1) the formation of dibenzo[18]-crown-S6 at an [$Fe^{II}CO$] center[16] by twice alkylating with $S(C_2H_4Br)_2$ and (2) the reaction at Mo(0), to form 9S3, which will be discussed later. It is obvious that the

rate of the S_N2-displacement reaction depends on factors like the nature of the leaving group, the solvent and the temperature at which the reaction is conducted.

In 1981, Kellogg and Buter[13,14] introduced a method that gave a dramatic increase in the yields of crown thioethers. The synthesis employs cesium salts in the the cyclization step. The role of the cesium ion in the cyclization step is not well understood. The formation of weak ion pairs with RS^- anions is suspected, thus making them exceptionally nucleophilic. Under high-dilution conditions this would favor the intra- over intermolecular S_N2 reaction of the open-chain ω-halo-α-thiolate intermediate[4]. For example, slow addition of a solution of 3-thiapentane-1,5-dithiol and 1,11-dichloro-3,6,9-trithiaundecane to a suspension of cesium carbonate in DMF gave 18S6 on the 20 g scale in 80%[20] yields. This method competes favorably with template routes because it involves less manipulation and it proceeds in one step from commercially available starting materials. Furthermore, the synthesis is general; modifications of the method provide 9-, 10-, 11-, 12-, 14-, 16-, 18-, and 24-membered crowns in high yields[4]. Examples of some of these macrocyclic thioethers are shown in Figure 1.3.

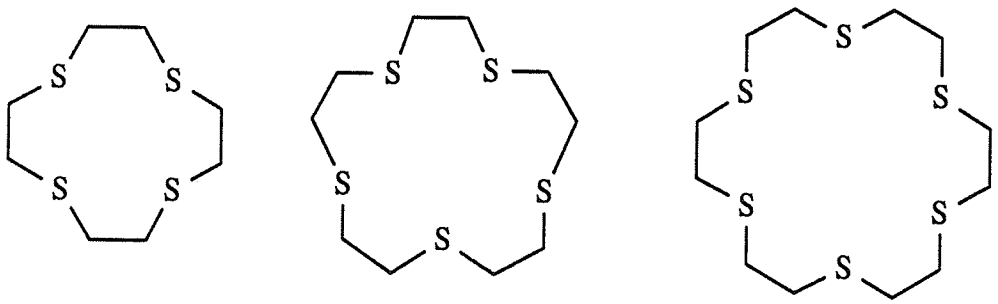

Figure 1.3 Crown thioethers.

To illustrate the effect synthetic developments have had on the availability of crown thioethers, the history of 1,4,7-trithiacyclononane (9S3) serves as a good example. This potentially tridentate ligand was first reported by Ochrymowycz[12] in 1977, at a yield

of 0.04%, from the reaction of the disodium salt of mercaptoethylsulfide with ethylene dichloride. In 1983, this was improved to 4% by using the bis(benzyltriethylammonium) salt of the dithiol under high-dilution conditions[6]. The first attempts to synthesize 9S3 using the Cs_2CO_3/DMF method gave a 20% yield[38], which has been improved to 50%[19]. In 1984, Sellmann[41] published a template reaction at Mo(0) involving the production of the intermediate disulfide complex $[NMe_4]_2[Mo(SCH_2CH_2SCH_2CH_2S)(CO)_3]$ and subsequent alkylation with 1,2-dibromoethane resulting in the formation of 9S3 at a 60% yield. The yields for 18S6 have likewise increased from a 5% yield in the reaction of the sodium salt of mercaptoethylsulfide with dibromoethane[8] to 89%[20] using the Cs_2CO_3 mediated cyclization method[13,14].

1.4 Conformational Analysis

One of the most important features that early structural studies on macrocyclic thioethers have revealed is that the sulfur atoms tend to point out of the macrocyclic ring[21,22,23,24]. This preference for an "exodentate" orientation contrasts sharply with that more commonly seen for oxa- and aza macrocycles[15]. However, more recent studies showed that the orientation of the sulfur donor atoms for a free macrocyclic ligand can be either out of the ring (exodentate) or into the ring (endodentate)[25].

In 1987, Cooper[72] introduced a new approach toward the description of macrocyclic thioethers. He recognized that the conformation of most cyclic thioethers with ethylene bridging units can be described in terms of the "bracket" units, defined by $S\text{-}CH_2CH_2\text{-}S\text{-}CH_2CH_2\text{-}S$, and their torsional angles.

The $-S\text{-}CH_2CH_2\text{-}S\text{-}CH_2CH_2\text{-}S-$ "bracket" unit resembles a right triangle in projection, with the central sulfur atom at the right angle. A cyclic structure then, is generated by the fusion of two or more bracket units. For example, the structure of 12S4 is obtained by the fusion of two bracket units and 18S6 has two bracket units fused by C-C fragments.

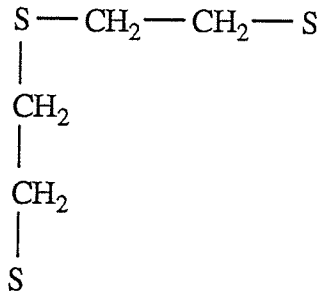

Figure 1.4 The $SCH_2CH_2SCH_2CH_2S$ "bracket" unit.

The torsional angles of these crown thioethers display a clear pattern. The C-S linkages adopt, without exception, a gauche placement with torsional angles of ± 60°, whereas the preferred placement at the C-C bonds is anti. As mentioned before, this is in sharp contrast with the placements of C-O and C-C bonds in oxa crown ethers. For example, 12 out of 12 C-S bonds in 18S6 are gauche, but only 2 out of 12 C-O bonds in 18-crown-6 are gauche. These conformational preferences of both C-S and C-O bonds manifest themselves very clearly in mixed oxa-thia crowns. For instance, 1,4-dithia-18-crown-6 has 4 out of 4 C-S bonds gauche and 0 out of 8 C-O bonds gauche.

Though ring size is an important factor, the main reason for these conformational preferences appears to be the different 1,4-interactions in gauche C-C-E-C and E-C-C-E (E = O, S) units. Consider the 1,4-interaction between the heteroatoms in the E-C-C-E units on the left side in Figure 1.5. For E = O dispersion forces (electron-nuclear attraction)[72] between the E-atoms stabilize gauche placement (the attractive gauche effect). However, when E = S the greater size of the atoms causes greater electron-electron repulsion between them which destabilizes gauche placement (the repulsive gauche effect). The 1,4-interaction in the C-C-E-C fragments on the right hand side in the figure reinforce the observed preferred placements in the E-C-C-E units. Due to the smaller size of the oxygen atom, gauche placement would cause repulsion between the terminal protons of the C-C-E-C chain. In the case where E = S, little or no repulsion exists,

because the greater length of the C-S bonds keeps the terminal H atoms relatively far apart. Hence, in crown ethers 1,4-interactions favor gauche placements at O-C-C-O bonds but disfavor them at C-C-O-C bonds and in crown thiaethers the opposite is true; S-C-C-S bonds disfavor gauche placements, whereas C-C-S-C bonds favor them. The above findings apply only to ethyl-linked systems of high symmetry. On the other hand, these systems are among those of greatest interest in the context of coordination chemistry.

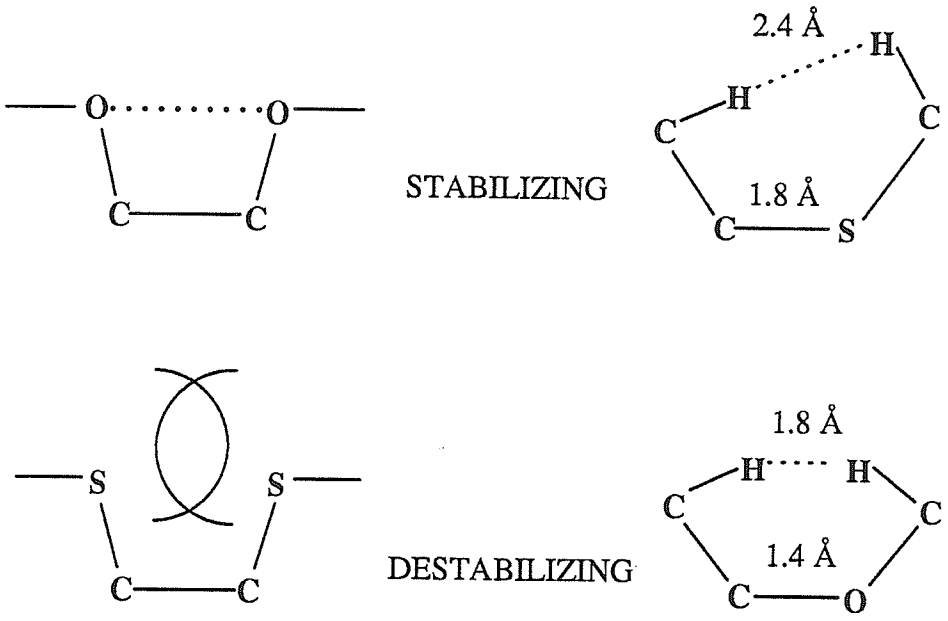

Figure 1.5 Schematic representation of 1,4-interactions in gauche CH_2-CH_2-E-CH_2 and E-CH_2-CH_2E linkages: (E = O, S).

1.5 Coordination Chemistry

i) general. The coordination chemistry of thioethers in transition metal complexes was reviewed extensively in 1981 by Hartley and Murray[21]. They reported six transition metal complexes of crown thioethers that had been fully characterized by X-ray

crystallography. Since that review the syntheses of complexes with crown thioethers have accelerated enormously. Complexes of 1st, 2nd and 3rd row transition metals with several crown thioethers have been fully characterized by X-ray crystallography: Ni(II)[3,6,22-26], Fe(II)[6,16,27-29], Co(II) and Co(III)[6,30-32], Cu(I) and Cu(II)[6,33-38,61], Nb(II)[39], Mo(0) and Mo(II)[40-43], Ru(II)[44-47], Rh(I) and Rh(III)[48-51], Pd(II) and Pd(III)[52-54], Ir(III)[60], Ag(I)[61,62], Pt(II)[63] and Mn(I)[74]. In the following paragraphs a few of these complexes and some of their unusual characteristics are discussed in more detail.

ii) 9S3 complexes. One ligand that has been used extensively in complexation studies is the potentially tridentate crown thioether ligand 1,4,7-trithiacyclononane (9S3). This ligand itself is rather unique, because its X-ray structure[64,65] shows that all three S atoms are endodentate. The enthalpic price for rearranging the S atoms for coordination to a trigonal face has been accounted for during the synthesis of the free ligand!

This ligand forms very stable ML_2 complexes with a variety of transition-metal ions; Ni(II)[6], Cu(II)[6], Co(II)[6], Co(III)[30], Fe(II)[28], Fe(III)[27], Pd(II)[54,17], Pd(III)[52], Rh(III)[51], Pt(II)[63], and Ru(II)[44-46], which have all been structurally characterized. The metal center is "sandwiched" between two ligand moieties (Figure 1.6). With exception of the

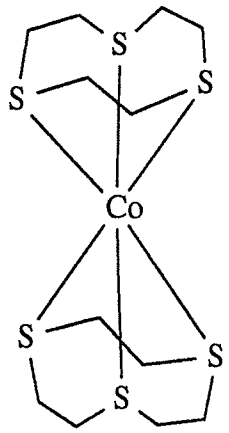

Figure 1.6 $[Co(9S3)_2]^{2+}$, "sandwiched" metal ion.

$[Pt(9S3)_2]^{2+}$ and $[Pd(9S3)_2]^{2+}$-complexes, the metal ions are coordinated to six S-donor

atoms from two 9S3 ligands. The resulting coordination sphere is octahedral or distorted octahedral. The metal ions of the Pt(II) and Pd(II) are coordinated to four thia donors from two ligands in an approximate square plane: the Pt(II)-ion showing apical interaction with one "dangling" S-atom and the Pd(II)-ion with both remaining sulfur atoms. The macrocyclic cavity of 9S3 is too small for the ligand to wrap around the metal ion. Hence most complexation reactions of 9S3 form ML_2 complexes when a 2:1 ligand to metal ratio is used. So far only five complexes, $Mo(9S3)(CO)_3$, $Mn(9S3)(CO)_3$, Cu(9S3)I, $[Fe(9S3)(C_5H_5)][BPh_4]$ and $Pd(9S3)Br_2$ are known where the ligand "caps" the metal, leaving other coordination sites open[41,61,29,17].

iii) electronic effects. These effects are best addressed in homoleptic complexes. An all sulfur coordination sphere limits the number of variables and simplifies the interpretation of the results. Thioethers generally bind weakly because they are both weak σ-donors and weak π-acceptors[21]. Crown thioethers, however, enhance coordination due to stabilizing factors like the chelate effect, the macrocyclic effect and the absence of steric repulsions between alkyl substituents[26]. Some unusual properties have been attributed to the low π-acidity of thioethers. In the $Co(9S3)_2^{2+}$, $Co(18S6)^{2+}$ and $Fe(9S3)_2^{2+}$ complexes[6,31,28] a stabilization of the low-spin states is observed. This is unexpected, since thioethers are weak field ligands (comparable in strength to ammonia[68]). Delocalization of t_{2g}-electron density into S-C σ* orbitals (because of the low π -acidity) is believed to reduce electron-electron repulsions and therefore the spin-pairing energy of the t_{2g} electrons[4]. The electronic effect of thioether coordination is also apparent comparing the reactivities of $RhCl(PPh_3)_3$ and RhCl(14S4) towards oxidative addition of CH_2Cl_2. RhCl(14S4) reacts rapidly at room temperature, while $RhCl(PPh_3)_3$ is inert. The increased nucleophilicity of the metal ion of the cyclic thioether complex, is probably due to the low π-acidity of the thioether ligand[50]. Another intriguing aspect of homoleptic thioether coordination is its ability to stabilize unusual oxidation states as in Pd(III)[52] and

Pt(III)[63]. This effect is also illustrated by the reduction of $[Rh(9S3)_2]^{3+}$ to the Rh(I) complex, in which a rare example of a monomeric Rh(II) species is observed[51].

iv) ring size effects. As the ring size and the number of S-donor atoms of the thioether ligand increase, some different modes of coordination result. Interesting studies on the effects of ring size have been performed by the group of Rorabacher[33,35]. They prepared a series of Cu(II)-complexes with macrocyclic thioether ligands of which the ring size gradually increased; 12S4, 13S4, 14S4, and 16S4 leaving the number of coordination sites unchanged. It was found that for 12S4 and 13S4 the copper atom is forced above the plane through the four sulfur atoms. However, when the ring contains 14 or more atoms the central cavity is large enough to accomodate a divalent, first-row transition metal ion such as Cu(II). Thus, in the 14S4- and 16S4-complexes the S-donor atoms lie in a square-planar arrangement around the central copper ion in an overall tetragonal geometry.

To illustrate the effect of ring size on coordination modes it is also appropriate to compare the structures of $Ni(18S6)^{2+}$ and $Ni(24S6)^{2+}$. Although the number of S donor atoms and potential coordination sites are the same in these complexes, the modes of coordination are different. In $Ni(18S6)^{2+}$ the crown is coordinated entirely in facial segments (each triad of adjacent S atoms occupies a trigonal face)[24]. In $Ni(24S6)^{2+}$, there still is an octahedral NiS_6 core, but the six sulfur atoms are bonded to the metal such that two loops of adjacent sulfurs coordinate meridionally[23] (Figure 1.7).

The Ni-S bonding distances in $Ni(18S6)^{2+}$ are shorter (0.06 Å) than the typical value of 2.44 Å found for other Ni(II)-thioether complexes[6,23]. Both 9S3 and 18S6 constrict the metal coordination sphere (macrocyclic constriction effect), a phenomenon which is not observed for the complexes $Ni(12S3)_2^{2+}$ and $Ni(24S6)^{2+}$, which have propyl linkages between the S donor atoms.

The orientation of the sulfur donor atoms in the free ligand has an important

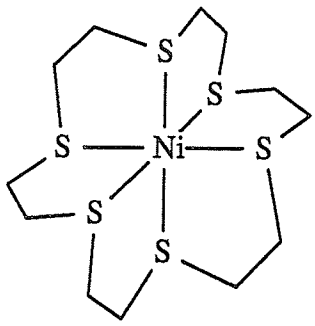

$[Ni(18S6)]^{2+}$

all sets of 3 adjacent S atoms are coordinated facially.

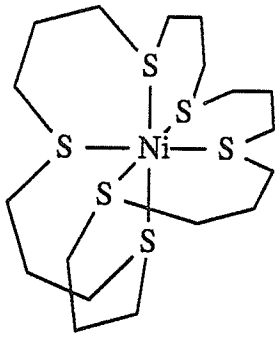

$[Ni(24S6)]^{2+}$

two sets of 3 adjacent S-atoms are coordinated meridionally.

Figure 1.7

influence on metal binding, since conformational changes on complex formation must be reflected in the thermodynamics of complexation. Several structures were characterized by X-ray crystallography, where the potentially multidentate macrocyclic thioether ligand coordinates in an "inside-out" manner (exo-coordination)[67] and forms a bridging unit between two metal centers. Some examples are $[(Cl_2Hg)_2(14S4)]$[66], $(NbCl_5)_2(14S4)$[39] and $[Rh_2(\eta^5\text{-}C_5Me_5)_2Cl_2(18S6)](BPh_4)_2$ [48]. Note that not all S-donor atoms are used for coordination (Figure 1.8). This feature is also observed in $[Cu(15S5)][ClO_4]$, where the ligand is wrapped around the distorted tetrahedral Cu(I) metal center, leaving one sulfur atom "dangling"[37]. The same ligand is capable of using all five donor atoms as shown in the square pyramidal $[Cu(II)(15S5)][ClO_4]_2$ complex[37], indicating that the coordination mode also depends on the oxidation state of the metal.

v) **18S6 complexes.** An increase in the number of coordination sites to six leads to the possibility of the ligand acting as a mono- or binuclear chelating ligand. The most studied thioether ligand in this class is without doubt the large flexible crown molecule 1,4,7,10,13,16-hexathiacyclooctadecane (18S6). It forms mononuclear complexes with

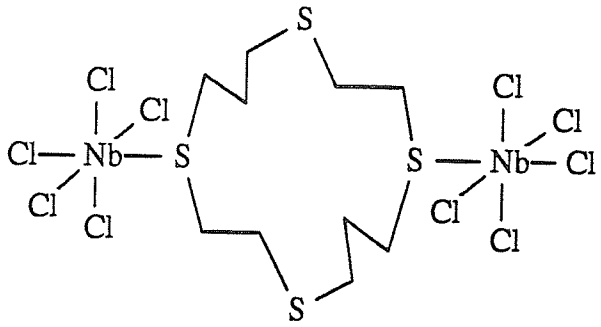

$Nb_2Cl_{10}14S4$

"inside-out" coordination.

$[Cu(I)18S6]^+$

tetrahedral coordination

Figure 1.8

Co(II)[31], Ni(II)[40] and Cu(II)[38] with the metal ion coordinated to all six S donor atoms in an octahedral geometry (cf. $M(9S3)_2$ complexes). The Pd(II) and Pt(II) complexes[53] of 18S6 are similar to the $M(9S3)_2$ complexes of these metals discussed earlier, with the metals being coordinated to four sulfurs while showing some interaction with the "dangling" apical S atoms. Co(II) is low spin and both the Co(II) and Cu(II) complexes show tetragonal distortion due to Jahn-Teller effects; the Ni(II) complex is high spin and exhibits almost perfect octahedral geometry.

When 18S6 is reacted with Cu(I) in a 1:1 ratio, a mononuclear complex results[38]. The complex adopts a severely distorted tetrahedral geometry and two neighbouring S-donor atoms are not used for coordination. Addition of a two-fold molar excess of $[Cu(CH_3CN)_4][ClO_4]$ to a solution of 18S6 in dichloromethane/acetonitrile, however, yielded the binuclear complex[36]. Each of the two copper(I) ions is facially coordinated to three S atoms and one acetonitrile molecule in an up and down conformation. Both centers have a slightly distorted tetrahedral geometry and each copper lies 1.08 Å above the plane of its coordinating S_3 set (Figure 1.9).

The same feature is observed for the binuclear Rh(I)(COD)-complex (COD =

$[Cu_2(CH_3CN)_2(16S6)]^{2+}$
complex, "up and down" conformation.

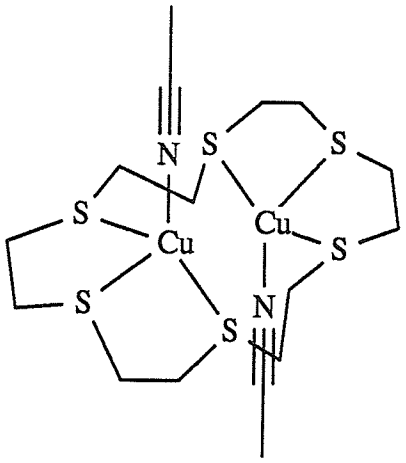

$[Rh_2(CO)_3(L)]^{2+}$
metal ions on the same side
of the ligand.

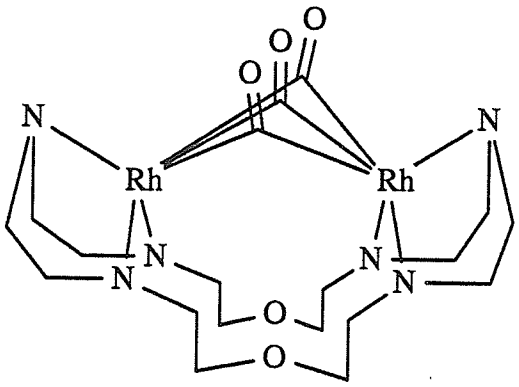

Figure 1.9

1.5-cyclooctadiene) of 20S6, where the two metal ions also coordinate to opposite sides of the ligand[49]. Thioether complexes with both metal centers residing on the same side of the ligand in close proximity to each other with the ligand in a "crown-like" conformation have yet to be isolated. Dinuclear complexes with this geometry are known for ditopic hexa-aza-macrocycles[75] as illustrated in Figure 1.9.

1.6 Reaction Chemistry

In the past decades, the research on crown thioethers has been directed towards their synthesis and their coordination chemistry. Many synthetic problems have been overcome and much more is known about how homoleptic thioether coordination affects the electronic properties. Research into the reaction chemistry of macrocyclc thioether complexes requires the presence of vacant coordination sites or labile ligands at the metal core. If the properties observed are to be used to generate unique reaction chemistry, then the research will have to focus on the preparation of these complexes. The analogy to phosphine chemistry seems to be evident and the possibilities are tremendous.

CHAPTER 2

Chemistry of 16S6

2.1 Introduction

While homoleptic crown thioether coordination modes are ideal for studying electronic effects, they do not allow for the possibility of reaction chemistry. Proper ligand design is essential to create a suitable environment, which allows for coordinative unsaturation and reaction chemistry at the metal center. 16S6 was designed for this reason; a macrocyclic thioether ligand, consisting of two S-CH_2CH_2-S-CH_2CH_2-S "brackets", joined by two methylene bridges.

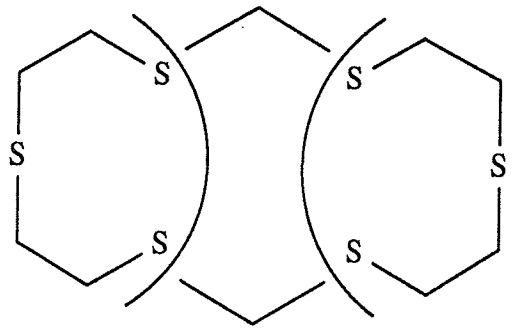

Figure 2.1 16S6 'building blocks'.

In order to prevent the ligand from "wrapping" around the metal center in an octahedral geometry, rigid S-CH_2-S groups were incorporated in the macrocyclic ring. Since the formation of a 4-membered chelating ring is energetically unfavorable because of the high ring strain, encapsulation of the metal ion in an octahedral geometry would be unlikely. Thus, 16S6 has the potential to act as a binucleating ligand. The S-CH_2-S unit serves as a "spacer" between two potentially tridentate coordination sites, suitable for facial

coordination to metal ions in either octahedral or tetrahedral geometries. 16S6 also has the potential to be a simple probe for tetrahedral coordination in a monomeric Cu(I) complex. In this case, encapsulation would occur, but two of the six donor atoms would not be involved in complexation.

In this chapter, the synthesis, characterization by X-ray diffraction and NMR, of 1,3,6,9,11,14-hexathiacyclohexadecane (16S6) and its Cu(I) complex $[Cu(16S6)][ClO_4]$ are described.

2.2 Experimental Section

i) General.

$[Cu(CH_3CN)_4][ClO_4]$ was prepared by the literature method[59]. 2-Mercaptoethanol, dibromomethane and 3-thiapentane-1,5-dithiol (bis-mercaptoethylsulfide) were purchased from Aldrich and used as received. Absolute ethanol was purified by distillation from CaH_2 under N_2. All reactions were conducted under an atmosphere of N_2 and solvents were degassed prior to use. Complexation reactions were done by standard Schlenk techniques[55,56]using a double gas/vacuum manifold, and syringes for transferring liquids. ^1H and $^{13}C\{^1H\}$ NMR spectra were recorded at 300.1 and 75.4 MHz respectively on a Bruker AM300 spectrometer locked to the deuterated solvent. ^1H NMR simulation calculations were performed using the program LAOCOON III. Infrared spectra were recorded on a Perkin-Elmer 781 grating spectrometer. GCMS experiments were performed routinely to monitor reaction progress using a HP 5970 series MSD coupled to a HP 5890 gas chromatograph. Elemental analyses were performed by Canadian Microanalytical Service Ltd., New Westminster, British Columbia, Canada.

ii) Preparation of 3,5-dithiaheptane-1,7-diol.

Na metal (11.64 g, 506 mmol) was dissolved in anhydrous ethanol (500 mL). 2-Mercaptoethanol (39.56 g, 506 mmol) was added and the resulting solution stirred for one hour. This solution was heated to reflux under N_2, and dibromomethane (44.01 g, 253 mmol) in anhydrous ethanol (100 mL) added dropwise over a period of 4 h. The mixture was refluxed for 12 h during which time a white solid precipitated and the solution color slowly changed to orange brown. The solvent was removed and the residue taken up in diethylether (300 mL). The solids were removed by filtration and the solution dried over $MgSO_4$. The diethylether was removed *in vacuo* and the resulting oily residue vacuum distilled (bp 149-152 °C, 1 mm Hg). Yield: 26.1 g (61 %). MS: m/e 168 (M^+). IR: ν(OH) 3340 cm^{-1} (vs, br). $^{13}C\{^1H\}$ NMR ($CDCl_3$): δ 60.74 (CH_2OH), 35.41 (CH_2S), 33.99 (SCH_2S); ^1H NMR ($CDCl_3$): δ 3.77 (t, 4H, CH_2O), 3.72 (s, 2H, SCH_2S), 2.91 (s, 2H, OH), 2.83 (t, CH_2S, 4H). Anal calculated for $C_5H_{12}O_2S_2$: C, 35.68; H, 7.20; S, 38.11. Found: C, 35.31; H, 7.20; S, 38.14.

iii) Preparation of 3,5-dithiaheptane-1,7-dithiol.

To a suspension of thiourea (6.74 g, 88.6 mmol) in 3,5-dithiaheptane-1,7-diol (7.45 g, 44.3 mmol) under N_2 was added HBr (aq, 48%) (22.4 g, 132.9 mmol). The mixture was refluxed for 9 h and then cooled to room temperature. Sodium hydroxide (5.32 g, 132.9 mmol) in H_2O (50 mL) was added dropwise during which time a white solid precipitated. Upon heating the solid dissolved. This solution was then refluxed for another 9 h during which time the product separated as an oil. The mixture was cooled to room temperature and extracted with CH_2Cl_2 (3 x 50 mL). The organic layer was dried over Na_2SO_4 and filtered. The solvent was removed *in vacuo* and the oily residue vacuum distilled. The fraction distilling from 120-155 °C (2 mm Hg) was collected and redistilled fractionally

(bp 135-140 °C, 2 mm Hg). Yield: 1.41 g (16%). MS: m/e 200 (M^+). IR: ν(SH) 2540 cm^{-1} (m). $^{13}C\{^1H\}$ NMR ($CDCl_3$): δ 36.06 (CH_2S), 34.52 (SCH_2S), 24.19 (CH_2SH); ^1H NMR ($CDCl_3$): δ 3.71 (s, 2H, SCH_2S), 2.82 (m, 8H,CH_2CH_2), 1.71 (t, 2H, SH). A satisfactory elemental analysis could not be obtained.

iv) Preparation of 1,7-dichloro-3,5-dithiaheptane.

Extreme Caution! Vesicant. Thionyl chloride (5.21 g, 40 mmol) was added via syringe to 3,5-dithiaheptane-1,7-diol (3.11 g, 18.5 mmol) dissolved in CH_2Cl_2 (15 mL) under N_2 in a 50 mL Schlenk flask. During the addition gas evolved and the solution developed an orange-brown color. The mixture was stirred for 1 h, after which the solvent was removed in vacuo. CH_2Cl_2 (10 mL) was added followed by a saturated solution (5 mL) of $NaHCO_3$ and the mixture stirred vigorously. The two phase system was then filtered through phase separation paper and the organic layer dried over $MgSO_4$. After filtration and removal of solvent *in vacuo*, the product was obtained as a pale orange-brown liquid. Due to the dangerous nature of this compound no further purification was attempted. However, the material was >97% pure by GCMS. MS: m/e 204. Yield: 2.50 g (66%). $^{13}C\{^1H\}$ NMR ($CDCl_3$): δ 43.24 (CH_2Cl), 36.08 (CH_2S), 34.11 (SCH_2S); ^1H NMR ($CDCl_3$): δ 3.75 (s, 2H, SCH_2S), 3.68 (t, 4H, CH_2Cl), 3.00 (t, 4H, CH_2S).

v) Preparation of 1,3,6,9,11,14-hexathiacyclohexadecane, 16S6.

Method A: 3-thiapentane-1,5-dithiol (15.9 g, 103 mmol) was added to anhydrous ethanol (250 mL) in which Na metal (4.73 g, 206 mmol) had been dissolved and the resulting solution was stirred for 1 h. Dibromomethane (17.9 g, 103 mmol) was then dissolved in anhydrous ethanol (250 mL) and both solutions were simultaneously added dropwise, using constant addition funnels, to anhydrous ethanol (500 mL). After 4 h, the

addition was complete and a white precipitate had formed. The mixture was stirred overnight and then filtered. The filtrate was concentrated and the residue extracted with CH_2Cl_2 (300 mL). The CH_2Cl_2 fraction was filtered through celite and the filtrate evaporated leaving an oily residue. The residue was then dissolved in a minimum amount of CH_2Cl_2 and added dropwise to boiling ethanol (100 mL). Upon cooling, a white solid precipitated which was recrystallized from $CHCl_3$. Yield: 1.44 g (8.4%).

Method B: Cs_2CO_3 (3.79 g, 12 mmol) was suspended in DMF (250 mL) under an atmosphere of N_2(g). A solution of 3,5-dithiaheptane-1,7-dithiol (2.12 g, 11 mmol) and 1,7-dichloro-3,5-dithiaheptane (2.17 g, 11 mmol) in DMF (45 mL) was added dropwise over a period of 6 h, while maintaining the temperature at 55 °C. After the addition period, the mixture was cooled to room temperature and stirred for another 12 h. The DMF was removed in vacuo and the resulting oily residue and white solid extracted with CH_2Cl_2. This was filtered and then washed with H_2O (2 × 50 mL). The CH_2Cl_2 solution was dried over $MgSO_4$, filtered, and taken to dryness. The resulting residue was then treated as in method A. Yield: 2.45 g (62%). mp: 92.5-94.5 °C. MS: m/e 332. $^{13}C\{^1H\}$ NMR ($CDCl_3$): δ 36.54 (SCH_2S); 32.02, 31.90 (SCH_2CH_2S); ^1H NMR ($CDCl_3$): δ 3.80 (s, 4H, SCH_2S), 2.91 (m, 16H, SCH_2CH_2S). Anal calculated for $C_{20}H_{20}S_6$: C, 36.10; H, 6.07; S, 57.83. Found: C, 36.05; H, 6.10; S, 58.47.

vi) Preparation of [Cu(16S6)][ClO_4].

Caution! Perchlorate salts of metal complexes with organic ligands are potentially explosive. 16S6 (246 mg, 0.74 mmol) was suspended in acetonitrile (3 mL) and dichloromethane was added until a clear solution resulted. [$Cu(CH_3CN)_4$][ClO_4] (242 mg, 0.74 mmol) dissolved in acetonitrile (4.5 mL) was added and the mixture warmed to 40 °C. The resulting clear, colorless solution was stirred for 1 hour, cooled to room temperature and the solvent removed in vacuo. The remaining white solid was

recrystallized from acetonitrile resulting in colorless needles. Yield: 324 mg (88%). IR: ν(ClO) 1090 cm^{-1} (vs, br). $^{13}C\{^1H\}$ NMR (CD_3CN): δ 38.91 (SCH_2S); 36.00, 35.87 (SCH_2CH_2S); ^1H NMR (CD_3CN): δ 3.91 (s, 4H, SCH_2S), 3.06 (s, 16H, SCH_2CH_2S). Anal calculated for $C_{10}H_{20}ClCuO_4S_6$: C, 24.23; H, 4.07; S, 38.82. Found: C, 24.37; H, 4.05; S, 37.95.

vii) General X-ray Diffraction Data Collection, Solution and Refinement.

Diffraction experiments were performed on a four-circle Syntex $P2_1$ diffractometer with graphite monochromatized MoKα radiation. The initial orientation matrices were obtained from 15 machine-centered reflections selected from rotation photographs. Partial rotation photographs around each axis were used to determine the crystal system. Ultimately, 30 high-angle reflections were used to obtain the final lattice parameters and orientation matrices. The intensities of three standard reflections were recorded every 197 reflections and showed no statistically significant changes over the duration of the data collections. The data were processed using the SHELX-76 program package. Refinement was carried out using full-matrix least-squares techniques on F minimizing the function $\Sigma w(|F_o|-|F_c|)^2$, where $w = 4F_o^2/\sigma^2$ (F_o^2) and F_o and F_c are the observed and calculated structure factors. Atomic scattering factors[69] and anomalous dispersion[70] terms were taken from the usual sources. Fixed H-atom contributions were included with C-H distances of 0.95 Å and the thermal parameters equal to 1.1 times the isotropic thermal parameter of the bonded C atoms. No H atoms were refined, but all values were updated as refinement continued.

viii) Structure Determination of 16S6.

Crystals of 16S6 were grown by slow evaporation of a $CHCl_3$ solution of the

compound. Preliminary photography was consistent with a monoclinic crystal system. Observed extinctions were consistent with space group $P2_1/n$. Machine parameters, crystal data, and data collection parameters are listed in Table 2.1. Intensity data ($\pm h,+k,+l$) were collected in one shell ($4.5°<2\theta<45°$). A total of 1940 reflections were collected and 1663 unique reflections with $F_o^2 > 3\sigma(F_o^2)$ were used in the refinement. The absorption coefficient was small and psi-scans recorded showed no significant absorption effects. Thus, no absorption correction was applied to the data. The six S atom positions were determined by direct methods from the E-map with highest figure of merit. The remaining non-hydrogen atoms were located from successive difference Fourier map calculations. In the final cycles of refinement, sulfur and carbon atoms were refined anisotropically. At final convergence this resulted in:

$R = \Sigma||F_o| - |F_c|/\Sigma|F_o|| = 0.0259$ and $R_w = (\Sigma w(|F_o| - |F_c|)^2/\Sigma wF_o^2)^{1/2} = 0.0295$

The Δ/σ value for any parameter in the final cycle was less than 0.004. A final difference Fourier map calculation showed no peaks of chemical significance; the largest was 0.25 electrons/Å^3 and was associated with the C1 carbon atom. Selected bond distances and angles are summarized in Table 2.2. Atomic positional parameters (Table B1), hydrogen atom parameters (Table B2) and anisotropic thermal parameters (Table B3) are given in appendix B.

ix) Structure Determination of [Cu(16S6)][ClO_4].

Crystals of [Cu(16S6)][ClO_4] were obtained by recrystallization from acetonitrile. Preliminary photography was consistent with an orthorhombic crystal system. Observed extinctions were consistent with space group $P2_12_12_1$. Machine parameters, crystal data, and data collection parameters are listed in Table 2.1. Intensity data ($+h,+k,+l$) were collected in one shell ($4.5°<2\theta<45°$). A total of 1862 reflections were collected and 1445 unique reflections with $F_o^2 > 3\sigma(F_o^2)$ were used in the refinement. The absorption

coefficient was small and psi-scans recorded showed no significant absorption effects. Thus, no absorption correction was applied to the data. The Cu atom position was determined by conventional heavy atom methods and the remaining non-hydrogen atoms were located from successive difference Fourier map calculations. In the final cycles of refinement, the copper, chlorine, sulfur and oxygen atoms were assigned anisotropic thermal parameters. The carbon atoms were assigned isotropic thermal parameters. The correct enantiomorph was determined by inversion of the atomic positions and comparison of resulting R and R_w values at convergence. At final convergence, this resulted in:

$R = \Sigma||F_o| - |F_c|/\Sigma|F_o|| = 0.0515$ and $R_w = (\Sigma w(|F_o| - |F_c|)^2/\Sigma wF_o^2)^{1/2} = 0.0551$.

The Δ/σ value for any parameter in the final cycle was less than 0.033. A final difference Fourier map calculation showed no peaks of chemical significance; the largest was 1.1 electrons/Å^3 and was associated with the chlorine atom. Selected bond distances and angles are summarized in Table 2.2. Atomic positional parameters (Table B4), hydrogen atom parameters (Table B5) and anisotropic thermal parameters (Table B6) are given in appendix B.

Table 2.1 Crystallographic Data for 16S6 and [Cu(16S6)][ClO_4].

Chemical formula	$C_{10}H_{20}S_6$	$C_{10}H_{20}ClCuO_4S_6$
Crystal color	colorless	colorless
Crystal form	needles	prisms
Formula weight	332.7	495.7
a, Å	16.386(4)	8.464(5)
b, Å	5.322(2)	18.321(9)
c, Å	17.986(3)	12.477(6)
β, deg	107.64(3)	-
Crystal system	monoclinic	orthorhombic

Space group	$P2_1/n$	$P2_12_12_1$
Vol, $Å^3$	1494.7(9)	1934(2)
ρ(calcd), g/cm^{-3}	1.48	1.70
Z	4	4
Crystal dimensions	.21x.28x.55	.34x.38x.44
μ, abs coeff, cm^{-1}	8.11	18.25
Radiation (λ, Å)	MoKα(.71069)	MoKα(.71069)
Temp, °C	24	24
Scan speed, deg/min	2.0-5.0 (θ-2θ scan)	
Scan range, deg	1.0 below $K\alpha_1$ and 1.0 above $K\alpha_2$	
Bkgd/scan time ratio	0.5	0.5
Data collected (2θ)	2272	1881
2θ	4.5 to 45°	4.5 to 45°
hkl range	$\pm h,+k,+l$	$+h,+k,+l$
Unique data ($F_o^2>3\sigma F_o^2$)	1663	1445
No. of variables	145	149
$R(F_o^2)$, %	2.59	5.15
$R_w(F_o^2)$, %	2.95	5.51

2.3 Results.

i) Synthesis.

The macrocyclic thioether ligand 16S6 was prepared using two different synthetic routes. The simplest method is a one-pot synthesis which employs high dilution techniques. This method is a slight modification of that previously described by Ochrymowycz for the preparation of a series of macrocyclic thioethers[8,12]. Although the yields are low, usually less than 10 %, the desired product was isolated with minimal manipulation. Employment of chromatographic techniques was never necessary, since the product could always be obtained by recrystallization. The reaction sequence to form 16S6 (eq 1) involves four reaction sites. The mechanism at each site is an ordinary S_N2 substitution. The cyclization step to form the 16-membered ring can take place through the coupling of two intermediate fragments or the ring closure of a longer linear fragment.

$$2\ \mathrm{HSEtSEtSH} \xrightarrow[\text{Ethanol}]{\mathrm{Na}} 2\ \mathrm{NaSEtSEtSNa} \xrightarrow[\text{Ethanol}]{\mathrm{CH_2Br_2}} 16\mathrm{S6} + 4\mathrm{NaBr} \qquad (1)$$

The potential problems in the cyclization step are polymerization and the possibility of the closure of intermediate fragments resulting in the formation of smaller and/or larger rings, depending on the size of the fragments. During the synthesis of 16S6 insoluble polymeric material was formed; the nature of this material (linear or macrocyclic) was not further investigated. Mass spectrometry showed that the formation of the smaller 8-membered ring (half the desired size) was negligible. The ratio of 8- to 16-membered ring formation was smaller than 1:1000. This may be due to the destabilizing effect of incorporating a rigid S-CH_2-S unit in a potentially strained,

8-membered ring system. The presence of the smaller 8-membered ring in the mass spectrum is more likely caused by a breakdown of 16S6 in the injection port of the mass spectrometer, since the NMR spectrum did not contain any peaks that could be attributed to the 8-membered ring species.

In order to get more control over the ring closure step, linear dithiol and dichloro fragments of desired length were synthesized (Figure 2.2). To form the desired ring only

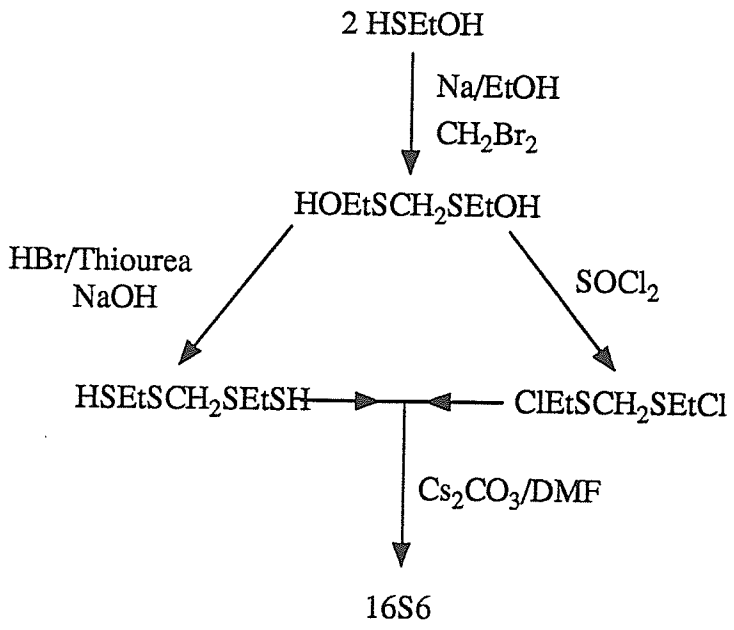

Figure 2.2 Reaction Scheme Synthesis of 16S6.

two fragments are needed now. For ring closure the Cs^+ mediated cyclization method of Kellogg and Buter[13,14] was employed. The reactions to form the diol and dichloro compounds are clean and give good yields. The conversion of the diol into the dithiol, however, was cumbersome and gave very poor yields. 3-Thiapentane-1,5-dithiol was a persistent side-product. The mechanism through which this proceeds must involve the cleavage of the S-CH_2-S unit, the protons of which are somewhat acidic due to the electron withdrawing capacities of the sulfur substituents. Though the literature[72] cites good yields for similar thiolization reactions (not involving the S-CH_2-S unit), the yield for this particular reaction never exceeded 16%. The final cyclization step proceeds

smoothly and gives a good yield; 62%. However, because of the poor yield in the thiolization step, the overall yield of 16S6 using this multi-step synthesis, is still low: 4%. Since the synthesis of the required starting materials in the cyclization step is elaborate and time consuming, the one-pot synthesis of 16S6 is recommended, because of its simplicity and easy work-up.

ii) X-ray Structure of 16S6.

The unit cell contains four discrete molecules of 16S6. The asymmetric unit contains two independent halves of a molecule, each on a crystallographic center of inversion. The closest intermolecular non-bonding contact is 2.39 Å between H3B and H10B. Sulfur-carbon bond distances range from 1.798(2) to 1.819(2) Å and carbon-carbon bond distances from 1.492(3) to 1.514(3) Å. These distances compare well to those found previously for other macrocyclic thioethers[18,65]. A complete listing of the interatomic distances and angles is given in Table 2.2. From the ORTEP diagrams (Figures 2.3 and 2.4) it can be noticed, that 16S6 crystallizes in two slightly different conformations (molecule 1 and molecule 2). This is also evident by examination of the torsional angles associated with the rings listed in Table 2.3. The only torsional angles in molecule 1 that differ appreciably from the corresponding angles in molecule 2 are S1-C1-S2-C2 (-169.8° vs. 64.8°) and S2-C2-C3-S3 (173.6° vs. 56.4°). In molecule 1, the two 'bracket' units joined by the methylene linkages are easily recognized. The preference of gauche-placement around S-C bonds is confirmed by the observation that four out of the six C-S bonds adopt this orientation. The conformation around the C-C bonds is anti. Four of the six sulfur atoms are exodentate to the ring, the other two point into the ring (endodentate). Overall the conformation of the molecule appears rectangular with sulfur atoms at the corners. In molecule 2, as well, four sulfur atoms are exodentate and two are endodentate. The conformation around the S-C and C-C bonds, however, differs slightly.

Five S-C bonds have a gauche placement and only one C-C bond has an anti placement. This results in distortion of the 'bracket' units and makes the rectangular shape of the molecule less recognizable. A slight degree of rotation about the S2-C2 bond in molecule 1 would essentially produce the conformation observed for molecule 2. Since both molecules crystallize in the same unit cell, the energy needed for this interconversion must be small.

Table 2.2 Selected Bond Distances and Angles for 16S6

	Distances (Å)		
S1-C1	1.798(2)	S4-C6	1.809(2)
S1-C5	1.807(2)	S4-C10	1.819(2)
S3-C3	1.810(2)	S6-C8	1.819(2)
S3-C4	1.810(2)	S6-C9	1.816(2)
S2-C2	1.817(3)	S5-C7	1.808(2)
C2-C3	1.492(3)	C7-C8	1.509(3)
C4-C5	1.514(3)	C9-C10	1.502(3)
	Angles (°)		
C1-S1-C5	101.3(1)	S3-C3-C2	114.2(2)
C3-S3-C4	100.3(1)	S3-C4-C5	112.5(2)
C6-S4-C10	100.9(1)	S1-C5-C4	114.9(2)
C8-S6-C9	100.1(1)	S5-C7-C8	111.1(2)
S2-C2-C3	109.3(2)	S6-C9-C10	111.3(2)

Table 2.3 Torsional Angles for 16S6.

S1-C1-S2-C2	-169.8	S4-C6-S5-C7	64.8
C1-S2-C2-C3	163.7	C6-S5-C7-C8	166.6
S2-C2-C3-S3	173.6	S5-C7-C8-S6	56.4
C2-C3-S3-C4	84.7	C7-C8-S6-C9	112.1
C3-S3-C4-C5	-74.1	C8-S6-C9-C10	-80.3
S3-C4-C5-S1′	170.4	S6-C9-C10-S4	172.6
C4-C5-S1′-C1′	-94.7	C9-C10-S4-C6	-103.6
C5-S1′-C1′-S2′	-72.0	C10-S4-C6-S5	-58.8

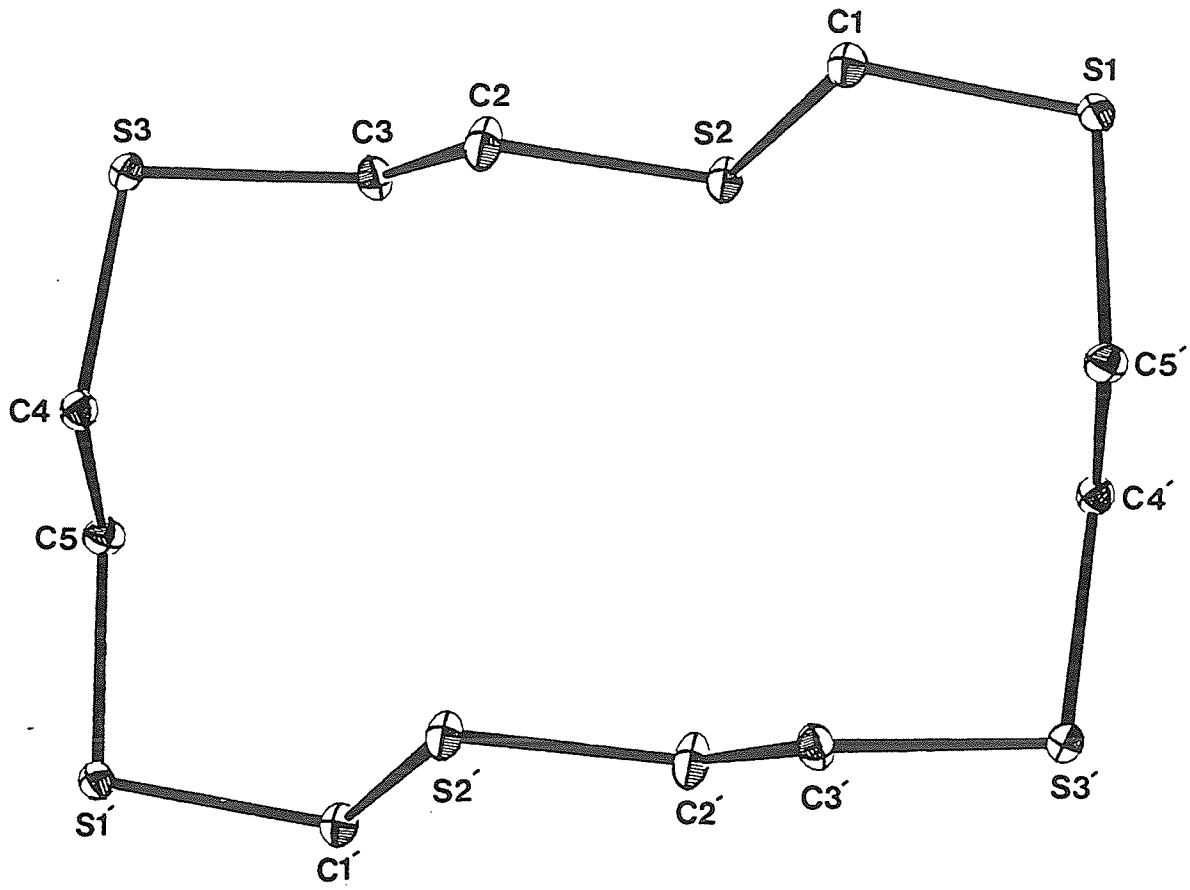

Figure 2.3 Perspective ORTEP drawing of 16S6, Molecule 1 showing the atom numbering scheme. 20% thermal ellipsoids are shown.

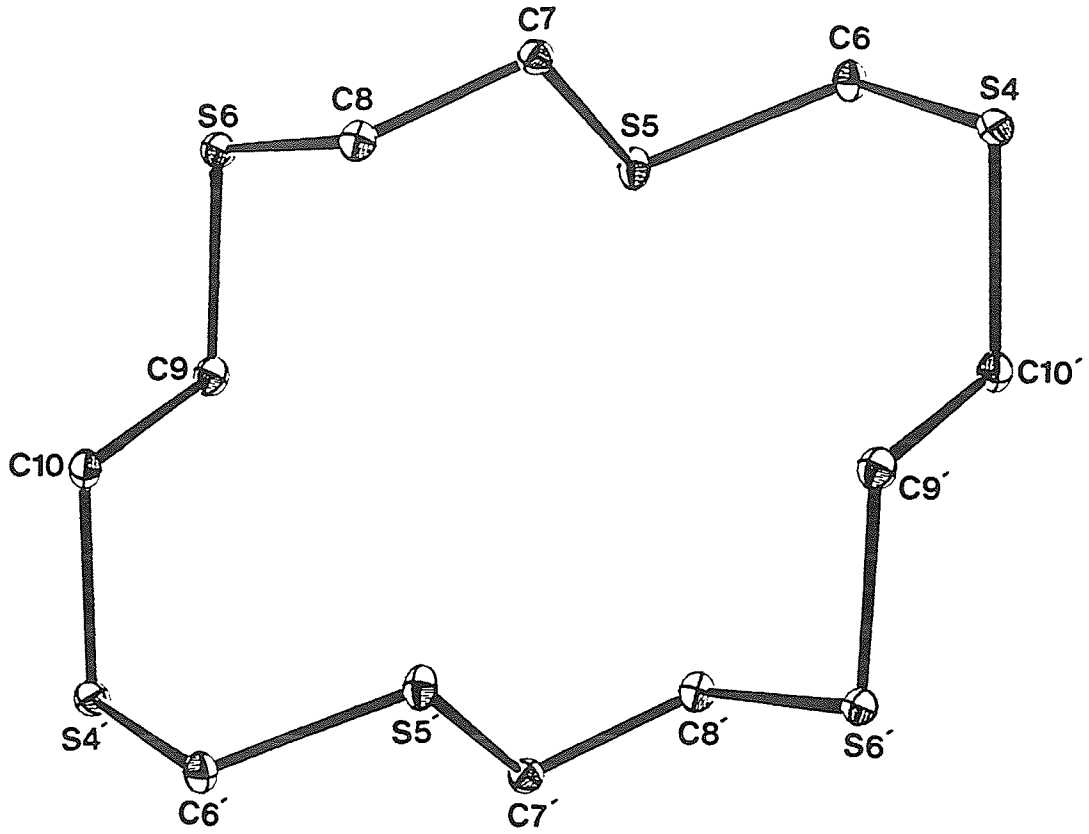

Figure 2.4 Perspective ORTEP drawing of 16S6, Molecule 2 showing the atom numbering scheme. 20% thermal ellipsoids are shown.

iii) X-ray Structure of $[Cu(16S6)][ClO_4]$.

The unit cell contains four $[Cu(16S6)]^+$ cations and four $[ClO_4]^-$ anions. The ORTEP diagram is shown in Figure 2.5 Complete listings of interatomic distances and angles are given in Table 2.4. The 16S6 ligand is wrapped around the Cu(I) ion, using four of the six sulfur atoms for coordination. The remaining two sulfur atoms are directed towards the Cu center, but at non-bonding distances of 3.555(3) Å for S2 and 3.413(3) Å for S5. The Cu(I) ion is in a tetrahedral environment. The S-Cu-S angles range from 93.6(1)° and 95.1(1)° for the five-membered chelate rings to 115.8(1)° and 119.2(1)° for the seven-membered chelate rings, giving an average S-Cu-S angle of 110(11)°. The sulfur-carbon bond distances range from 1.785(13) to 1.852(12) Å and the carbon-carbon bond distances from 1.499(16) to 1.522(18) Å. The perchlorate anion has the expected tetrahedral geometry. The angles around the chlorine atom in the anion range from 93.5(12) to 129.8(17) °, while the Cl-O bond distances vary from 1.311(19) to 1.418(18) Å. Although the large thermal parameters of the perchlorate anion indicate some degree of disorder, these values are comparable to those of other determinations[37].

Table 2.4 Selected Bond Distances and Angles for $[Cu(16S6)][ClO_4]$.

	Distances (Å)		
Cu-S1	2.305(3)	S5-C6	1.799(11)
Cu-S3	2.299(3)	S5-C7	1.821(14)
Cu-S4	2.306(3)	S6-C8	1.808(12)
Cu-S6	2.291(3)	S6-C9	1.820(13)
S1-C1	1.831(13)	C2-C3	1.501(19)
S1-C10	1.827(14)	C4-C5	1.499(16)
S2-C1	1.785(13)	C7-C8	1.499(18)

S2-C2	1.800(14)	C9-C10	1.522(18)
S3-C3	1.822(14)	Cl-O1	1.334(13)
S3-C4	1.852(12)	Cl-O2	1.410(18)
S4-C5	1.811(11)	Cl-O3	1.418(16)
S4-C6	1.837(11)	Cl-O4	1.311(19)
	Non-bonding Distances (Å)		
Cu-S2	3.555(3)	Cu-S5	3.413(3)
	Angles (°)		
S1-Cu-S3	119.2(1)	C3-S3-C4	100.6(6)
S1-Cu-S4	113.5(1)	S3-C4-C5	114.1(8)
S3-Cu-S4	95.1(1)	C4-C5-S4	116.2(8)
S1-Cu-S6	93.6(1)	C5-S4-C6	102.0(5)
S3-Cu-S6	121.1(1)	S4-C6-S5	116.5(6)
S4-Cu-S6	115.8(1)	C6-S5-C7	101.3(6)
Cu-S1-C1	108.7(4)	S5-C7-C8	116.3(9)
Cu-S1-C10	96.2(5)	C7-C8-S6	112.4(9)
Cu-S3-C3	103.6(5)	C8-S6-C9	99.3(6)
Cu-S3-C4	98.1(4)	S6-C9-S1	110.8(9)
Cu-S4-C5	97.0(4)	C9-C10-S1	109.9(9)
Cu-S4-C6	107.4(4)	C10-S1-C1	98.5(6)
Cu-S6-C8	102.8(4)	O1-Cl-O2	107.1(11)
Cu-S6-C9	97.6(4)	O1-Cl-O3	105.8(14)
S1-C1-S2	115.8(8)	O1-Cl-O4	116.9(18)
C1-S2-C2	104.5(7)	O2-Cl-O3	93.5(12)
S2-C2-C3	117.5(10)	O2-Cl-O4	129.8(17)
C2-C3-S3	112.6(10)	O3-Cl-O4	96.5(12)

Table 2.5 Torsional Angles for Cu(16S6)][ClO_4]

S1-C1-S2-C2	102.8	S4-C6-S5-C7	95.2
C1-S2-C2-C3	61.7	C6-S5-C7-C8	63.6
S2-C2-C3-S3	52.8	S5-C7-C8-S6	54.8
C2-C3-S3-C4	-170.2	C7-C8-S6-C9	-173.9
C3-S3-C4-C5	72.2	C8-S6-C9-C10	147.5
S3-C4-C5-S4	53.4	S6-C9-C10-S1	-65.7
C4-C5-S4-C6	-69.6	C9-C10-S1-C1	-158.3
C5-S4-C6-S5	-87.2	C10-S1-C1-S2	-66.9

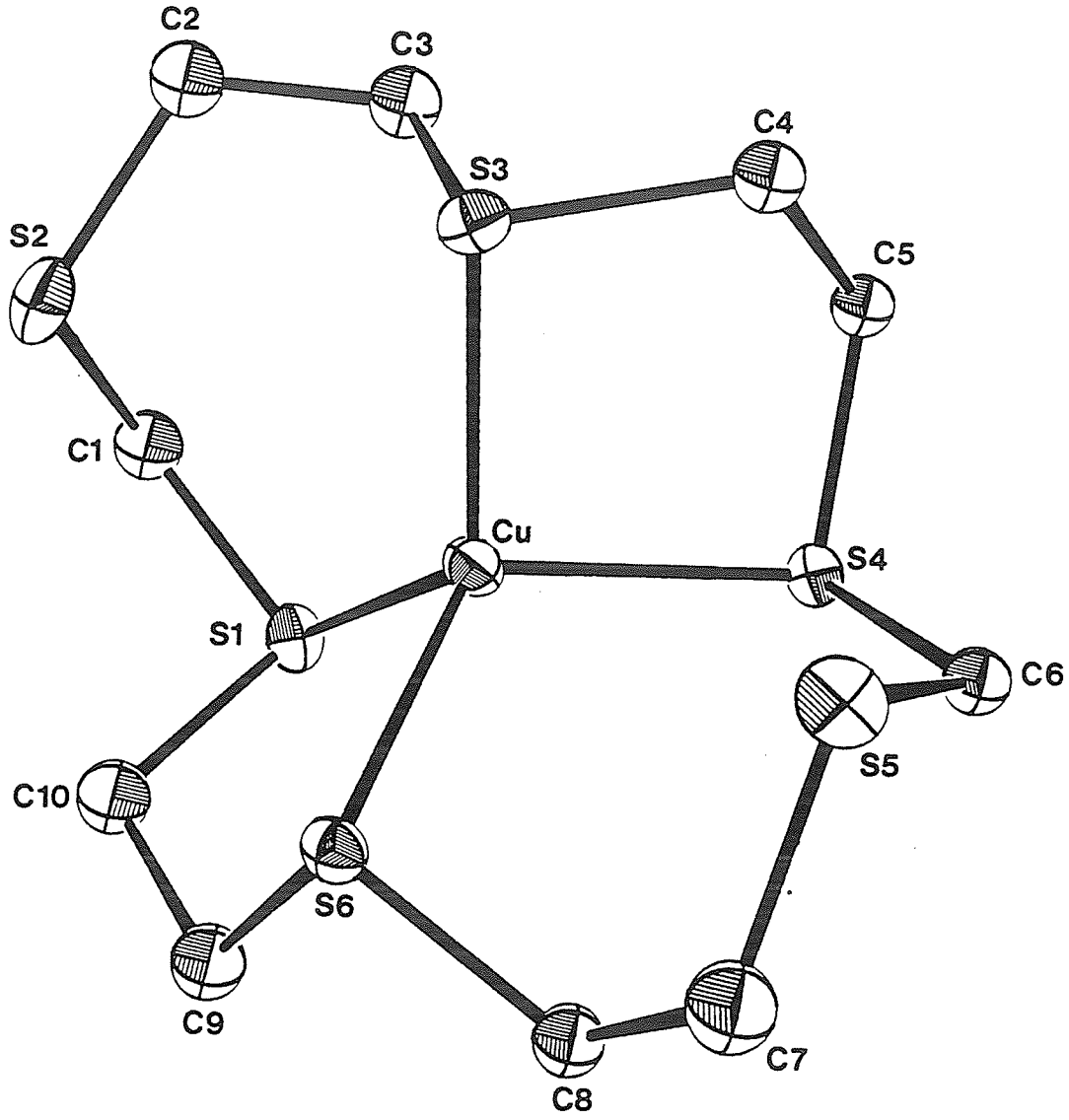

Figure 2.5 Perspective ORTEP drawing of $[Cu(16S6)]^+$ cation showing the atom numbering scheme. 20% thermal ellipsoids are shown.

2.4 Discussion.

The torsional angles of the 16S6 ligand in $[Cu(16S6)]^+$ (Table 2.5) are useful for a comparison to those observed for the free 16S6 ligand (Table 2.3) since they give some indication of the amount of conformational adjustment required for the ligand to coordinate in a tetrahedral geometry. This is of interest since the majority of the sulfur atoms in crown thioethers are exodentate and must be converted to endodentate for complexation to be favorable[6,8,26]. The torsional angle analysis of the complexed ligand shows that 8 out of 12 S-C bonds are in gauche placements and 4 out of 4 C-C bonds are in gauche placements. The major change from the free ligand form is the need for the C-C bonds (anti-placement) to convert to gauche placements in the bonded conformation. This is simply the result of placing a C-C linkage in the back-bone of a metal chelate ring. However, this entirely disrupts the 'bracket' formations favored in the uncomplexed ligand and may restrict the coordinating ability of certain crown thioether ligands. The formation of the Cu(I) complex, however, proves that 16S6 is mechanically quite flexible and the energy needed for the conformational change is accounted for during complexation.

16S6 is a potentially ditopic ligand. In order to explain why binuclear coordination was not observed, it is useful to examine the Cu(I) complexes formed by other crown thioether ligands; 18S6, 15S5 and 14S4. The mononuclear complexes $[Cu(18S6)][BF_4]$, $[Cu(15S5)][ClO_4]$ and $[Cu(14S4)][ClO_4]$ and the dinuclear complex $[Cu_2(CH_3CN)_2(18S6)][ClO_4]_2$ have been structurally characterized[38,37,34,36]. In $[Cu(18S6)][BF_4]$ and $[Cu(15S5)][ClO_4]$, the thioether ligand coordinates the Cu(I) ion via four S-atoms from one continuous section ($-SCH_2CH_2SCH_2CH_2SCH_2CH_2S-$) of the macrocyclic ligand in a severely distorted tetrahedral geometry leaving the remaining S-atoms uncoordinated. In the complex $[Cu(14S4)][ClO_4]$, three S-atoms are coordinated from one macrocycle in a similar manner, with the fourth site occupied by the fourth

S-atom from a neighbouring complex, to give a distorted tetrahedral geometry in a polymeric form.

In the dicopper complex, the six S donor sites are coordinated to two $(Cu\text{-}CH_3CN)^+$ fragments in identical tetrahedral geometries. The two copper atoms are bonded to opposite sides of the macrocyclic ligand in an *in-out* conformation. A similar coordination could also be expected for 16S6. In describing the solid state structure of $[Cu_2(CH_3CN)_2(18S6)][ClO_4]_2$, it was noted that there was a close intramolecular contact between two S atoms (3.64 Å), one from each coordination site, through the center of the complex. It is possible that this interaction would be severe in a similar $[Cu_2(CH_3CN)_2(16S6)][ClO_4]_2$ complex, since only a methylene group would separate the two coordination sites. This potential destabilization of the dinuclear complex and the ability of the 16S6 ligand to form a homoleptic thioether complex using four S atoms from the same macrocyclic ligand, by 'wrapping' around the metal center, without appreciable distortion from tetrahedral geometry, are possible explanations for the observed coordination mode of 16S6.

2.5 NMR.

The ^1H NMR spectrum ($CDCl_3$) of 16S6 shows a singlet (4H) at δ = 3.80 ppm, which was assigned to the methylene protons of the rigid S-CH_2-S units, and a multiplet (16H) at δ = 2.91 ppm, consisting of 16 peaks and associated with the S-CH_2CH_2-S-CH_2CH_2-S brackets. The observation of this well resolved multiplet may be related to the retention of the S-CH_2CH_2-S-CH_2CH_2-S bracket in solution. The latter portion of the spectrum forms an AA′BB′pattern and was simulated (Fig 2.6) using the program LAOCOON III. This program starts with a trial set of molecular parameters (coupling constants and chemical shifts) and calculates from these a trial spectrum. The user then assigns certain transitions of the experimental spectrum to those in the calculated

spectrum. The program then iterates the parameters to find the best fit between observed and calculated spectrum. Only well-resolved, sharp peaks in the observed spectrum were used in the assignments. A list of observed/assigned and calculated transitions is given in Table B7.

The results of the final iteration gave as best values: geminal coupling constant ($^2J_{HH}$) = -13.0 Hz and vicinal coupling constants ($^3J_{HH}$) of 6.1 and 9.1 Hz. To assess the validity of the statement that the retention of the configuration of the S-CH_2CH_2-S-CH_2CH_2-S bracket is retained in solution, the coupling constants ($^3J_{HH}$) were also calculated using the dihedral angles from the X-ray data. There are two formulae in use to do this. Both formulae, $^3J_{HH}= 10\cos^2\theta$ [57] and $^3J_{HH}= 4.22-0.5\cos\theta+4.5\cos2\theta$ [58], where θ is the dihedral angle, give comparable results (5.9 and 9.9[57] compared to 2.6 and 9.1[58] Hz, respectively). Ideally the torsional angles for gauche and anti placement of the coupled protons would be 60° and 180°, corresponding to calculated coupling constants of 2 and 10 Hz depending on which formula one uses. These values are consistent with an anti placement of the sulfur atoms around a C-C bond. To account for the observed differences, it should be noted that the above formulae are approximations and that the magnitude of the coupling constants also depends on the nature of substituents and the hybridization of the CH_2-groups; effects that have not been taken into account. In the ^1H NMR spectrum of the Cu complex, the multiplet has collapsed into a slightly broadened singlet. Since there are five inequivalent methylene groups in the solid state conformation, this might indicate that some kind of fluxional process is occurring in solution. A possible explanation is that the coordinating S-atoms (S1 and S4) of the SCH_2S group exchange with the corresponding non-coordinating S-atoms (S2 and S5), which are already oriented towards the Cu center. This would make all the methylene units of the S-CH_2CH_2-S-CH_2CH_2-S brackets equivalent and account for the two observed singlets in the spectrum. Variable temperature NMR (solvent CD_2Cl_2) showed that the singlet due to the protons of the SCH_2S unit splits into a quartet

at 190 K, whereas a complicated broad multiplet results for the resonance due to the protons of the ethylene linkages. The low temperature limit could not be reached.

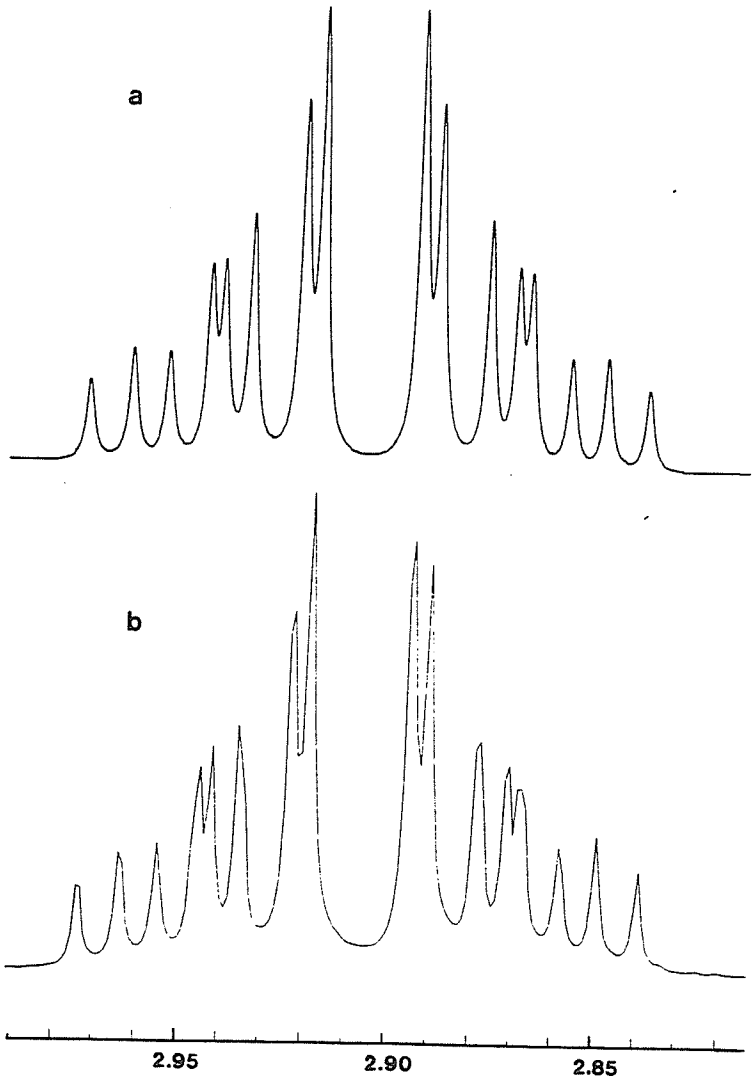

Figure 2.6 ^{1}H-NMR spectrum of the S-CH_2CH_2-S-CH_2CH_2-S bracket of 16S6 at 300 MHz. (a) simulated and (b) observed.

2.6 Summary and Conclusions.

In this chapter the synthesis, characterization by X-ray diffraction and NMR of the macrocyclic hexadentate thioether ligand 1,4,7,9,11,14-hexathiacyclohexadecane (16S6) and the $[Cu(16S6)][ClO_4]$ complex were described.

In the free ligand four out of six S donor atoms are exodentate. However, the flexibility of 16S6 proved to be large enough to undergo the necessary conformational rearrangement for complexation. Therefore, endodentate conformation of S donor atoms in the free ligand is not always an essential criterion for complexation.

Although designed to act as a binucleating ligand and therefore not 'wrap-around' a metal ion, the results with Cu(I) show that 16S6 encapsulated the metal ion to form a mononuclear complex. 16S6 appears to be ideally suited for encapsulating and providing a homoleptic coordination sphere for metal ions in a tetrahedral geometry.

Appendix B

Table B1. Positional Parameters[a] for 16S6.

Atom	x	y	z
S1	2709(1)	6907(1)	3243(1)
S2	6317(1)	11464(1)	5147(1)
S3	5395(1)	6094(1)	3216(1)
S4	2733(1)	8562(1)	8307(1)
S5	6386(1)	7959(1)	10299(1)
S6	5455(1)	7970(1)	8392(1)
C1	2869(1)	9367(5)	3958(1)
C2	6161(2)	8486(5)	4629(1)
C3	5700(2)	8933(5)	3787(1)
C4	4393(1)	5402(4)	3402(1)
C5	3678(1)	7146(5)	2967(1)
C6	2736(2)	1450(5)	8838(1)
C7	6542(1)	10479(5)	9681(1)
C8	5764(1)	10799(5)	8977(1)
C9	4446(2)	7273(5)	8571(1)
C10	3732(1)	8867(5)	8071(1)

[a] Multiplied by 10^4

Table B2. Hydrogen Atom Parameters[a] for 16S6.

Atom	x	y	z	U[b]
H1A	3024	10854	3763	47
H1B	2340	9667	4078	47
H2A	5832	7395	4843	68
H2B	6702	7740	4679	68
H3A	5196	9866	3752	50
H3B	6063	9887	3752	50
H4A	4473	5562	3945	42
H4B	4232	3724	3243	42
H5A	3883	8824	3059	40
H5B	3539	6780	2426	40
H6A	2228	11457	9001	45
H6B	2723	12784	8502	45
H7A	7024	10107	9512	38
H7B	6641	11999	9972	38
H8A	5297	11304	9151	47
H8B	5884	12077	8685	47
H9A	4504	7589	9104	50
H9B	4309	5553	8457	50
H10A	3907	10576	8137	46
H10B	3633	8392	7542	46

[a] Multiplied by 10^4. [b] Multiplied by 10^3.

Table B3. Thermal Parameters[a] for 16S6.

Atom	U11	U22	U33	U23	U13	U12
S1	32.7(4)	44.3(4)	33.3(4)	-7.0(3)	9.9(3)	-7.0(3)
S2	47.9(4)	35.4(4)	33.7(4)	-5.9(3)	4.5(3)	5.4(3)
S3	36.5(4)	42.5(4)	36.2(4)	-11.5(3)	12.8(3)	-1.0(3)
S4	32.5(4)	42.8(4)	37.1(4)	-7.9(3)	10.2(3)	-7.6(3)
S5	47.8(4)	34.3(4)	37.1(4)	-0.6(3)	7.4(3)	-8.4(3)
S6	34.2(44)	47.2(4)	36.0(4)	-11.0(3)	10.5(3)	-1.1(3)
C1	43.3(15)	37.0(14)	34.8(14)	-2.0(11)	9.5(12)	1(1)
C2	61.8(18)	40.9(16)	37.3(15)	-10.7(12)	-1(1)	13.0(13)
C3	45.8(15)	37.0(14)	37.1(15)	-4.9(12)	11.2(12)	-10.3(12)
C4	38.0(14)	29.5(13)	37.2(13)	-1(1)	13.6(11)	-2.1(11)
C5	36.6(14)	47.4(15)	30.7(14)	2.5(12)	12.4(11)	-1(1)
C6	41.7(14)	37.3(14)	29.6(13)	2.9(11)	5.9(11)	3.5(11)
C7	34.9(13)	35.0(14)	34.2(13)	-3.1(11)	12.7(11)	-5.2(11)
C8	42.7(14)	32.7(13)	34.2(13)	1(1)	11.1(11)	-2.3(11)
C9	45.7(15)	38.4(15)	37.8(15)	-2.0(12)	12.8(12)	-2(1)
C10	41.4(14)	47.9(16)	28.6(13)	1(1)	7.2(11)	-2.6(12)

[a] Multiplied by 10^3.

Table B4. Positional Parameters[a] for $[Cu(16S6)][ClO_4]$

Atom	x	y	z
Cu	5786(1)	8716(1)	6402(1)
Cl	9897(3)	11078(2)	5586(3)
S1	7668(3)	8174(2)	7475(2)
S2	5212(5)	6947(2)	7506(3)
S3	3175(3)	8404(2)	6620(2)
S4	5419(3)	9939(1)	6762(2)
S5	4566(4)	9819(2)	4359(2)
S6	7107(3)	8451(1)	4847(2)
O1	11279(18)	10830(10)	5221(12)
O2	9995(18)	11846(10)	5610(22)
O3	8859(28)	11072(10)	4693(19)
O4	9069(31)	10632(17)	6186(13)
C1	6750(15)	7416(7)	8201(11)
C2	3418(17)	7283(8)	8101(12)
C3	3079(17)	8084(7)	8001(11)
C4	2360(14)	9336(6)	6771(10)
C5	3451(13)	9861(6)	7321(9)
C6	5033(12)	10398(6)	5480(9)
C7	6498(16)	9718(8)	3734(12)
C8	7738(14)	9341(6)	4388(9)
C9	8945(15)	8140(7)	5451(10)
C10	8618(17)	7649(8)	6410(11)

[a] Multiplied by 10^4.

Table B5. Hydrogen Atom Parameters[a] for $[Cu(16S6)][ClO_4]$.

Atom	x	y	z	U[b]
H1A	7553	7072	8370	69
H1B	6313	7605	8844	69
H2A	2565	7028	7776	71
H2B	3458	7167	8843	71
H3A	3835	8345	8413	64
H3B	2050	8176	8275	64
H4A	2132	9525	6079	56
H4B	1412	9306	7176	56
H5A	3559	9703	8043	47
H5B	2975	10030	7306	47
H6A	4165	10720	5583	47
H6B	5946	10673	5299	47
H7A	6365	9453	3086	73
H7B	6878	10194	3576	73
H8A	7990	9633	4994	52
H8B	8653	9281	3956	52
H9A	9547	7879	4935	66
H9B	9529	8552	5690	66
H10A	9580	7447	6667	69
H10B	7935	7266	6189	69

[a] Multiplied by 10^4. [b] Multiplied by 10^3.

Table B6. Thermal Parameters[a] for Cu[(16S6)][ClO_4].

Atom	U11	U22	U33	U23	U13	U12
Cu	39.7(7)	40.7(7)	39.6(7)	0.0(6)	5.4(5)	6.2(6)
Cl	42(2)	87(3)	71(2)	-4(2)	7(2)	4(2)
S1	51(2)	46(2)	45(2)	-2(1)	-7(1)	6(1)
S2	94(3)	40(2)	65(2)	7(2)	-7(2)	-8(2)
S3	45(1)	49(1)	39(1)	-3(1)	0(1)	-7(1)
S4	39(1)	37(1)	33(1)	-6(1)	-6(1)	1(1)
S5	55(2)	71(2)	35(1)	-2(1)	-14(1)	5(1)
S6	44(2)	43(1)	37(1)	-10(1)	2(1)	-1(1)
O1	100(9)	208(18)	109(10)	57(11)	33(9)	71(10)
O2	125(13)	113(12)	301(32)	-75(15)	-52(17)	3(10)
O3	240(21)	131(12)	234(21)	76(14)	-168(19)	-65(15)
O4	276(28)	343(32)	69(9)	17(14)	14(14)	-174(26)
C1	61(3)					
C2	67(4)					
C3	63(3)					
C4	53(3)					
C5	43(2)					
C6	44(2)					
C7	64(3)					
C8	47(3)					
C9	58(3)					
C10	62(3)					

[a] Multplied by 10^3. Note: here only U_{11} is given, this refers to the isotropic temperature factor.

Table B7. Data for NMR simulation of 16S6 (S-CH_2CH_2-S-CH_2CH_2-S bracket).*

Expt Freq	Calc Freq	Intensity	Error
851.700	851.705	.785	-.005
854.760	854.747	1.074	-.013
	857.399	1.041	
	860.321	.851	
	860.321	.851	
	861.288	1.697	
	863.314	1.149	
	863.314	1.149	
866.970	866.982	3.215	-.012
	868.315	4.155	
875.520	875.517	4.155	.003
	876.851	3.215	
	880.518	1.149	
	880.518	1.149	
882.540	882.544	1.697	-.004
	883.511	.851	
	883.511	.851	
886.440	886.434	1.041	.006
	889.085	1.074	
	892.127	.785	

*Frequencies are in Hz. Simulation at 300 MHz.

CHAPTER 3

Synthesis, Characterization and Complexation of the Tridentate Ligands 2,5,8-Trithia[9]-*ortho*-benzenophane, (TTOB), and 2,5,8-Trithia[9]-*meta*-benzenophane, (TTMB).

3.1 Introduction

The tridentate crown thioether ligand 9S3 has proven to be an excellent ligand for facial coordination to a variety of transition metals. The exceptional ligating properties of this ligand have often been attributed to the endodentate conformation of the S donor atoms. It forms very stable ML_2 complexes[6,28,44], with the metal ion "sandwiched" between two ligand molecules in an octahedral geometry. The homoleptic coordination sphere, however, makes reaction chemistry impossible. In our search for "capping" ligands, we replaced one of the ethylene linkages in 9S3 by a xylyl group. Introducing steric hindrance in the ligand may prevent the coordination of two ligands to the metal center, thus leaving sites open for reaction chemistry. In this chapter the synthesis and characterization of two tridentate ligands and their complexation capacities are reported.

3.2 Experimental Section

i) Preparation of 2,5,8-trithia[9]-*ortho*-benzenophane, TTOB.

3-Thiapentane-1,5-dithiol (16.08 g, 104 mmol) was added to anhydrous ethanol (250 mL) in which K metal (8.15 g, 208 mmol) had been dissolved. The resulting solution was equilibrated for one h. α,α′-dibromo-*ortho*-xylene (27.51 g, 104 mmol) was dissolved

in anhydrous ethanol (500 mL). Both solutions were added dropwise and simultaneously to EtOH (500 mL) over a period of 72 h using constant addition funnels. During this time a white precipitate formed. The mixture was then stirred overnight and filtered. The filtrate was concentrated and the residue extracted with benzene (300 mL). After filtering, the solvent was removed from the filtrate to give a semi-solid residue. The crude product was dissolved in a minimum amount of hot anhydrous ethanol, filtered and the filtrate cooled to give the product as colorless needles. Yield: 5.55 g, (21%). mp: 98.5-100.0 °C. MS: m/e 256 (M^+). $^{13}C\{^1H\}$ NMR ($CDCl_3$): δ 136.91, 130.26, 127.60 (aromatic); 32.27 (benzylic CH_2S); 32.10, 31.80 (SCH_2CH_2S). ^1H NMR ($CDCl_3$): δ 7.39 (m, 4H, aromatic), 3.94 (s, 4H, benzylic CH_2), 2.68 (m, 8H, SCH_2CH_2S). Anal calculated: C, 56.19; H, 6.30; S, 37.51. Found: C, 56.21; H, 6.14; S, 37.29.

ii) Preparation of 2,5,8-trithia[9]-*meta*-benzenophane, TTMB.

3-Thiapentane-1,5-dithiol (13.50 g, 87 mmol) was added to anhydrous ethanol (200 mL) in which K metal (6.84 g, 175 mmol) had been dissolved. The resulting solution was equilibrated for one h. α,α′-dibromo-*meta*-xylene (22.96 g, 87 mmol) was dissolved in anhydrous ethanol (500 mL). Both solutions were added dropwise and simultaneously to EtOH (300 mL) over a period of 4 h using constant addition funnels . During this time a white precipitate formed. The mixture was concentrated and the residue extracted with benzene (300 mL). After filtration, the benzene solution was left to stand, upon which colorless prism-shaped crystals formed. Yield: 10.14 g, (46%). mp: 144-145 °C (lit: 143-144 °C)[11]. MS: m/e 256 (M^+). $^{13}C\{^1H\}$ NMR ($CDCl_3$): δ 137.06, 130.65, 130.54, 128.13 (aromatic); 35.51 (benzylic CH_2S); 30.98, 30.09 (SCH_2CH_2S). ^1H NMR ($CDCl_3$): δ 7.00-7.47(m, 4H, aromatic), 3.77 (s, 4H, benzylic CH_2), 2.19-2.41 (m, 8H, SCH_2CH_2S). Anal calculated: C, 56.19; H, 6.30; S, 37.51. Found: C, 56.21; H, 6.14; S, 37.29.

iii) Preparation of $[Cu(TTOB)(CH_3CN)][ClO_4]$.

TTOB (1.12 g, 4.36 mmol) was dissolved in CH_3CN (5 mL) under N_2. A solution of $[Cu(CH_3CN)_4][ClO_4]$ (1.43 g, 4.36 mmol) in CH_3CN (30 mL) was added by syringe. The temperature was kept at 45 °C. The resulting mixture turned tea-colored almost immediately, but this color faded as the reaction progressed. The mixture was stirred for two h and then cooled to room temperature, during which time a white crystalline solid precipitated. The CH_3CN was removed *in vacuo* and the product recrystallized from CH_3CN. Yield: 1.85 g (94%). Anal calculated: C, 36.51; H, 4.16; S, 20.89. Found: C, 36.57; H, 4.24; S, 21.27. $^{13}C\{^1H\}$ NMR (Acetone-d6): δ 134.85, 132.57, 129.84, 37.92, 35.67, 35.22. ^1H NMR (Acetone-d6): δ 7.39-7.46 (m, 4H), 4.18 (s, 4H, broad), 2.85 (s, 8H, broad). IR: ν(ClO) 1088 cm^{-1}(vs, br).

iv) Preparation of $[Cu(TTOB)(PPh_2Me)][ClO_4]$.

To a solution of $[Cu(TTOB)(CH_3CN)][ClO_4]$ (382 mg, 0.83 mmol) in CH_3CN (10 mL) under N_2 was added, by syringe, PPh_2Me (166 mg, 0.83 mmol) dissolved in CH_3CN (5 mL). No visible change occured as the two colorless solutions were mixed. The mixture was stirred for 3 h at room temperature. Crystals formed after approximately 10 days by diffusion of diethylether into the reaction mixture. Yield: 329 mg (64%). Anal calculated: C, 48.46; H, 4.72; S, 15.52. Found: C, 48.38; H, 4.74; S, 15.52. $^{13}C\{^1H\}$ NMR (CD_3CN, 300 K): δ 129.7-133.7 (aromatic), 37.16, 36.34, 34.98, 12.84, 12.55. ^1H NMR (CD_3CN): δ 7.0-7.5 (m, 14H), 3.8-4.4 (q, 4H, broad), 2.8-3.5 (m, 8H, broad), 1.6 (d, 3H, broad). $^{31}P\{^1H\}$ NMR δ -12.80 (s,broad). IR: ν(ClO) 1090 cm^{-1}(vs, br).

v) Preparation of [Cu(TTOB)(PPh_3)][ClO_4].

To a solution of TTOB (0.70 g, 2.7 mmol) in 20 mL CH_2Cl_2 under N_2 was added [$Cu(CH_3CN)_4$][ClO_4] (0.89 g, 2.7 mmol) in CH_3CN (20 mL). The mixture was stirred for two h at a temperature of 48 °C and then cooled to room temperature. An extra quantity (10 mL) of CH_3CN was added to dissolve the white solid that precipitated. While stirring vigorously, a solution of triphenylphosphine (0.71 g, 2.7 mmol) in CH_3CN (15 mL) was added slowly by syringe. Approximately one min into the addition, a white precipitate formed. Stirring was continued for five more min after which the solid was allowed to settle. The CH_3CN was syringed off and the white solid residue dried *in vacuo*. Crystals were obtained by slow diffusion of either acetone or diethylether into a CH_3CN solution of the product. Yield: 1.15 g (65%). Anal calculated: C, 52.86; H, 4.58; S, 14.11. Found: C, 53.07; H, 4.46; S, 13.54. $^{13}C\{^1H\}$ NMR (CD_3CN, 300 K): δ 134.5-129.5 (aromatic), 37.19, 35.44, 34.92. ^1H NMR (CD_3CN): δ 7.5-6.9 (m, 19H), 4.3-3.9 (q, 4H, broad), 3.6-2.8 (m, 8H, broad). $^{31}P\{^1H\}$ NMR δ 5.55 (s,broad). IR: ν(ClO) 1094 cm^{-1}(vs, br).

vi) Preparation of [Cu(TTOB)(Pyridine)][ClO_4].

To a solution of TTOB (238 mg, 0.9 mmol) in CH_3CN (10 mL) at a temperature of 45 °C, under N_2, was added dropwise by syringe, [$Cu(CH_3CN)_4$][ClO_4] (304 mg, 0.9mmol) dissolved in CH_3CN (5 mL). The colorless mixture was stirred for two h. After cooling to room temperature, pyridine (237 mg, 3 mmol; 3 x excess assuming 100% reaction yield) was added by syringe. The mixture was again warmed to 45 °C and stirred for one more h. The solvent was removed *in vacuo* and the off-white solid recrystallized from CH_3CN. Yield: 390 mg (87%). Anal calculated: C, 40.96; H, 4.25; S, 19.29. Found: C, 37.83; H, 4.40; S, 18.63. $^{13}C\{^1H\}$ NMR (CD_3CN): δ 137.98, 132.57, 129.94, 37.48, 35.59, 35.39. ^1H NMR (CD_3CN): δ 8.6-7.3 (m, 9H), 3.99 (s, 4H, broad), 3.00 (s, 8H,

broad). IR: ν(ClO) 1090 cm^{-1}(vs, br).

vii) Preparation of [Cu(TTOB)(C_6H_5CN)][ClO_4].

This compound was obtained by recrystallization of [Cu(TTOB)(CH_3CN)][ClO_4] from C_6H_5CN (benzonitrile). ^1H NMR (CD_3CN): δ 7.8-7.3 (m, 9H), 3.95 (s, 4H, broad), 3.6-2.7 (s, 8H, very broad). Anal calculated: C, 43.67; H, 4.05; S, 18.41. Found: C, 40.31; H, 3.78; S, 19.91.

viii) Preparation of Mo(TTOB)($CO)_3$.

$Mo(CO)_6$ (634 mg, 2.4 mmol) was dissolved in CH_3CN (20 mL) under N_2. The initially colorless solution turned yellow after a few minutes and was refluxed for four h. To the resulting yellow solution of *fac*-Mo($CH_3CN)_3(CO)_3$, TTOB (487 mg, 1.9 mmol) dissolved in CH_3CN (10 mL) was added dropwise by syringe, while stirring vigorously. The color of the solution changed to a yellow-brown and after a few minutes into the addition a dirty yellow precipitate started to form. The mixture was refluxed for one more hour and cooled to room temperature. The solvent was removed *in vacuo* leaving a shiny beige colored residue. Yield: 802 mg (97%). Recrystallization from a DMSO/Et_2O mixture yielded yellow crystals suitable for X-ray diffraction. Anal calculated: C, 39.69; H, 4.31; S, 24.93. Found: C, 39.57; H, 3.91; S, 22.87. $^{13}C\{^1H\}$ NMR (DMSO-d6): δ 134.96, 130.85, 128.26, 37.42, 34.77, 31.85. ^1H NMR (CD_3CN): δ 7.28 (s, 4H), 4.13-3.77 (q, 4H), 3.3-2.6 (m, 8H). IR : ν(CO) 1818, 1935 cm^{-1}(CH_3NO_2) ; ν(CO) 1810, 1925 cm^{-1} (KBr).

ix) General X-ray Diffraction Data Collection, Solution and Refinement.

In order to avoid repetition, the reader is referred to the relevant paragraph in chapter 2 for general comments on X-ray diffraction data collection, solution and refinement. This paragraph applies to all subsequent structures unless stated otherwise.

x) Structure Determination of 2,5,8-Trithia[9]-*meta*-benzenophane, TTMB.

Colorless crystals of TTMB were grown by slow evaporation of an acetone solution of the compound. Preliminary photography was consistent with an orthorhombic crystal system. Observed extinctions were consistent with space group $P2_12_12_1$. Intensity data ($+h,+k,+l$) were collected in one shell ($4.5°<2\theta<45°$). A total of 1972 reflections were collected and 1384 unique reflections with $F_o^2 > 3\sigma(F_o^2)$ were used in the refinement. The six S atom positions were determined by direct methods from the E-map with highest figure of merit. The remaining non-hydrogen atoms were located from successive difference Fourier map calculations. In the final cycles of refinement, sulfur atoms were refined anisotropically and the carbon atoms were assigned isotropic thermal parameters. The correct enantiomorph was determined by inversion of the atomic positions and comparison of the resulting R and R_w values for the possible enantiomorphs at convergence. At final convergence this resulted in:

$R = \Sigma||F_o| - |F_c|/\Sigma|F_o|| = 0.0659$ and $R_w = (\Sigma w(|F_o| - |F_c|)^2/\Sigma wF_o^2)^{1/2} = 0.0704$

The Δ/σ value for any parameter in the final cycle was less than 0.002. A final difference Fourier map calculation showed no peaks of chemical significance; the largest was 0.35 electrons/Å^3 and was associated with the C2 and C3 carbon atoms. Machine parameters, crystal data and data collection parameters are given in Table 3.1. Selected bond distances and angles are summarized in Table 3.4. Atomic positional parameters (Table C1), hydrogen atom parameters (Table C2) and anisotropic thermal parameters (Table C3) are given in appendix C.

xi) Structure Determination of 2,5,8-Trithia[9]-*ortho*-benzenophane, TTOB.

Colorless crystals of TTOB were grown by slow diffusion of diethylether into an acetone solution of the compound. Preliminary photography was consistent with a monoclinic crystal system. Observed extinctions were consistent with space group $P2_1/n$. Intensity data ($\pm h,+k,+l$) were collected in one shell ($4.5^\circ<2\theta<45^\circ$). A total of 1827 reflections were collected and 1034 unique reflections with $F_o^2 > 3\sigma(F_o^2)$ were used in the refinement. The three S atom positions were determined by direct methods from the E-map with highest figure of merit. The remaining carbon atoms were located from successive difference Fourier map calculations. In the final cycles of refinement, sulfur atoms were refined anisotropically and the carbon atoms were assigned isotropic thermal parameters. At final convergence this resulted in:

$R = \Sigma||F_o| - |F_c|/\Sigma|F_o|| = 0.0480$ and $R_w = (\Sigma w(|F_o| - |F_c|)^2/\Sigma wF_o^2)^{1/2} = 0.0551$

The Δ/σ value for any parameter in the final cycle was less than 0.001. A final difference Fourier map calculation showed no peaks of chemical significance; the largest was 0.26 electrons/Å^3 and was associated with the C3 and C4 carbon atoms. Atomic positional parameters are summarized in Table C4 and selected bond distances and angles in Table 3.6. Hydrogen atom parameters (Table C5) and anisotropic thermal parameters (Table C6) are given in appendix C. Table 3.1 gives the crystal data and machine and collection parameters.

Table 3.1 Crystallographic Data for 2,5,8-Trithia[9]-*meta*-benzenophane (TTMB) and 2,5,8-Trithia[9]-*ortho*-benzenophane (TTOB).

Chemical formula	$C_{12}H_{16}S_3(m)$	$C_{12}H_{16}S_3(o)$
Crystal color	colorless	colorless
Crystal form	prisms	prisms

Formula weight	256.5	256.5
a, Å	9.107(5)	8.840(2)
b, Å	8.851(7)	15.866(5)
c, Å	31.897(21)	10.600(2)
β, deg	-	119.34(6)
Crystal system	orthorhombic	monoclinic
Space group	$P2_12_12_1$	$P2_1/n$
Vol, $Å^3$	2571(1)	1295.9(6)
ρ(calcd), g/cm^{-3}	1.33	1.31
Z	8	4
Cryst dimens, mm	.24x.33x.16	.42x.23x.25
μ, abs coeff, cm^{-1}	4.85	4.81
Radiation (λ, Å)	MoKα(0.71069)	MoKα(0.71069)
Temp, °C	24	24
Scan speed, deg/min	2.0-5.0 (θ-2θ scan)	
Scan range, deg	1.0 below $K\alpha_1$ and 1.0 above $K\alpha_2$	
Bkgd/scan time ratio	0.5	0.5
Data collected (2θ)	1972	1827
2θ	4.5 to 45°	4.5 to 45°
hkl range	$+h,+k,+l$	$\pm h,+k,+l$
Unique data ($F_o^2>3\sigma F_o^2$)	1384	1034
No. of variables	183	96
$R(F_o^2)$, %	6.59	4.80
$R_w(F_o^2)$, %	7.04	5.51

xii) Structure determination of $[Cu(TTOB)(PPh_2Me)][ClO_4]$

Colorless crystals of the complex were grown by slow diffusion of diethylether into an acetonitrile solution of the compound. Preliminary photography was consistent with a triclinic crystal system. Observed extinctions were consistent with the space groups P1 and $P\bar{1}$. The spacegroup $P\bar{1}$ was confirmed by successful solution refinement. Intensity data ($\pm h,\pm k,+l$) were collected in one shell ($4.5° < 2\theta < 45°$). A total of 7193 reflections were collected and 5091 unique reflections with $F_o^2 > 3\sigma(F_o^2)$ were used in the refinement. The position of the Cu atoms were determined by direct methods from the E-map with highest figure of merit. The remaining non-hydrogen atoms were located from successive difference Fourier map calculations. In the final cycles of refinement, the heteroatoms were refined anisotropically and the carbon atoms were assigned isotropic thermal parameters. At final convergence this resulted in:

$R = \Sigma||F_o| - |F_c|/\Sigma|F_o|| = 0.0643$ and $R_w = (\Sigma w(|F_o| - |F_c|)^2/\Sigma wF_o^2)^{1/2} = 0.0697$

The Δ/σ value for any parameter in the final cycle was less than 0.412. A final difference Fourier map calculation showed no peaks of chemical significance; the largest was 0.89 electrons/Å^3 and was associated with the C44 atom of one of the phosphine phenyl groups of molecule 2. The data were absorption corrected (μ=11.83) empirically by interpolation in 2θ and ϕ between Ψ-scans of reflections (3,-4,10), (2,-3,7) and (2,-4,9). Selected bond distances and angles are summarized in Table 3.8. Atomic positional parameters (Table C7), hydrogen atom parameters (Table C8) and anisotropic thermal parameters (Table C9) are given in appendix C. Table 3.2 gives the crystal data and machine and data collection parameters.

Table 3.2 Crystallographic Data for $[Cu(TTOB)(PPh_2Me)][ClO_4]$

Chemical formula	$C_{25}H_{29}ClCuO_4PS_3$
Crystal color	colorless
Crystal form	prisms
Formula weight	619.64
a, Å	12.888(4)
b, Å	8.156(2)
c, Å	31.575(8)
α, deg	115.64(2)
β, deg	104.56(2)
γ, deg	99.73(2)
Crystal system	triclinic
Space group	$P\bar{1}$
Vol, $Å^3$	2745(1)
ρ(calcd), g/cm^{-3}	1.50
Z	4
Cryst dimens, mm	.26x.32x.22
μ, abs coeff, cm^{-1}	11.38
Radiation (λ, Å)	MoKα(0.71069)
Temp, °C	24
Scan speed, deg/min	2.0-5.0 (θ-2θ scan)
Scan range, deg	1.0 below $K\alpha_1$ and 1.0 above $K\alpha_2$
Bkgd/scan time ratio	0.5
Data collected (2θ)	7193
2θ	4.5 to 45°
hkl range	$\pm h,\pm k,+l$

Unique data ($F_o^2 > 3\sigma F_o^2$)	5091
No. of variables	167
$R(F_o^2)$, %	6.43
$R_w(F_o^2)$, %	6.97

xiii) Structure Determination of $Mo(CO)_3$(TTOB).DMSO

Yellow crystals of the complex were grown by slow diffusion of diethylether into a DMSO solution of the compound. Preliminary photography was consistent with a monoclinic crystal system. Observed extinctions were consistent with space group $P2_1/c$. Intensity data ($\pm h, +k, +l$) were collected in one shell ($4.5° < 2\theta < 45°$). A total of 2904 reflections were collected and 2174 unique reflections with $F_o^2 > 3\sigma(F_o^2)$ were used in the refinement. The position of the molybdenum atom was determined by the heavy atom method from analysis of a Patterson map and the remaining non-hydrogen atoms were located from successive difference Fourier map calculations. This also resulted in the location of a disordered solvent molecule in the crystal lattice. In the final cycles of refinement, all non-hydrogen atoms, except for the solvent molecule, were refined anisotropically. The solvent molecule was refined isotropically with site occupancy factors of 78 and 22% respectively. At final convergence this resulted in:

$R = \Sigma||F_o| - |F_c|/\Sigma|F_o|| = 0.0452$ and $R_w = (\Sigma w(|F_o| - |F_c|)^2/\Sigma w F_o^2)^{1/2} = 0.0544$

The Δ/σ value for any parameter in the final cycle was less than 0.002. The largest peak in the final difference Fourier map calculation was 1.23 electrons/Å^3 and was associated with the solvent molecule. Selected bond distances and angles are summarized in Table 3.10. Atomic positional parameters (Table C10), hydrogen atom parameters (Table C11) and anisotropic thermal parameters (Table C12) are given in appendix C. Table 3.3 gives the crystal data and machine and data collection parameters.

Table 3.3 Crystallographic Data for $Mo(TTOB)(CO)_3$.DMSO.

Chemical formula	$C_{17}H_{22}MoO_4S_4$
Crystal color	yellow
Crystal form	prisms
Formula weight	514.37
a, Å	7.732(4)
b, Å	18.693(16)
c, Å	14.996(10)
β, deg	104.05(5)
Crystal system	monoclinic
Space group	$P2_1/c$
Vol, $Å^3$	2103(1)
ρ(calcd), g/cm^{-3}	1.62
Z	4
Cryst dimens, mm	.24x.38x.20
μ, abs coeff, cm^{-1}	9.39
Radiation (λ, Å)	MoKα(0.71069)
Temp, °C	24
Scan speed, deg/min	2.0-5.0 (θ-2θ scan)
Scan range, deg	1.0 below $K\alpha_1$ and 1.0 above $K\alpha_2$
Bkgd/scan time ratio	0.5
Data collected (2θ)	2904
2θ	4.5 to 45°
hkl range	±*h*,+*k*,+*l*
Unique data ($F_o^2>3\sigma F_o^2$)	2174
No. of variables	215

$R(F_o^2)$, %	4.52
$R_w(F_o^2)$, %	5.44

3.3 Results

i) Synthesis.

The macrocyclic thioether ligands TTMB and TTOB were prepared by a slight modification of the general synthesis described by Ochrymowycz[8,12] for macrocyclic thioethers. High dilution techniques are employed. The simple one pot synthesis requires minimal manipulation of the reagents. Separation and purification of the products by column chromatography was never necessary, since the desired products could always be obtained by fractional recrystallization. The reaction (Figure 3.1) is a simple S_N2 substitution as described previously in chapter 2 for 16S6.

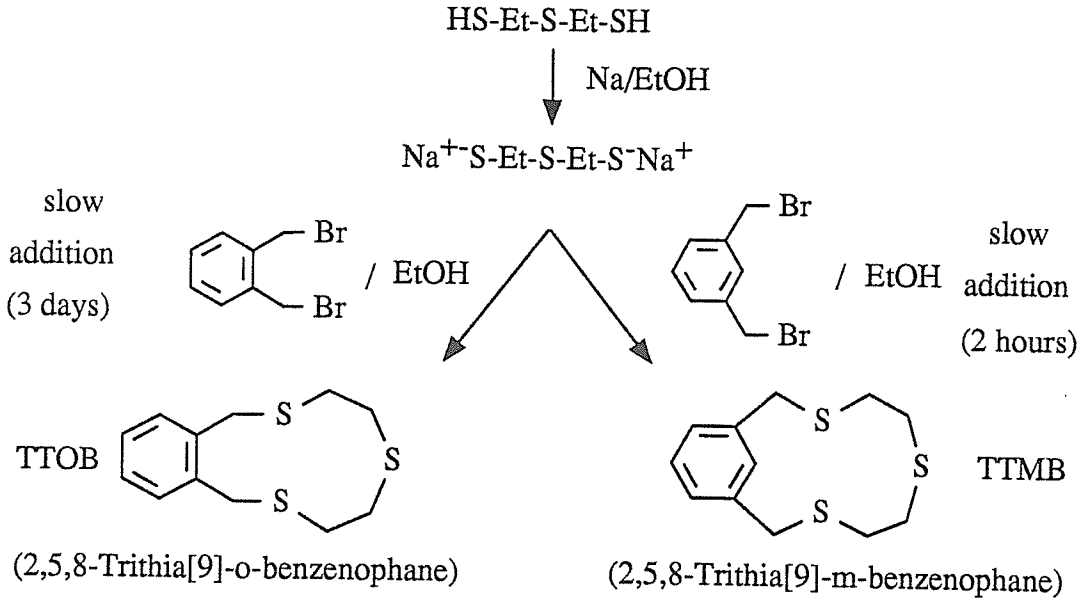

Figure 3.1 Synthesis of TTOB and TTMB.

The high yield of TTMB (45%) and the independence of the yield on the addition rate probably result from the near perfect fit of the S-CH_2CH_2-S-CH_2CH_2-S "bracket" and the meta-xylyl fragment. This is in sharp contrast to the results obtained for TTOB. Yields depend very strongly on the addition rate of the dithiolate. If the addition is completed within a few hours, then the yields of TTOB are usually very low (<5%). Most of the product is polymeric material and one can isolate small amounts of 2,5,8,17,20,23-hexathia[9.9]-*ortho*-benzenophane (HTOB), the dimer of TTOB, which will be discussed in chapter 4 . Yields improve significantly (>20%) when the addition period is stretched over three days. Both ligands are quite air-stable and can be stored on the shelf for months without decay.

The labile CH_3CN ligand on the Cu(I) complex, [Cu(TTOB)(CH_3CN)][ClO_4], is easily replaced by a variety of ligands. The addition of triphenylphosphine or diphenylmethylphosphine gave the phosphine complexes in almost quantitative yields. The CH_3CN molecule is spontaneously exchanged when the [Cu(TTOB)(CH_3CN)][ClO_4] complex is recrystallized from benzonitrile to give [Cu(TTOB)(C_6H_5CN)][ClO_4].

The molybdenum tricarbonyl complex precipitates as a grey-yellow powder from the reaction mixture and seems to be less sensitive to air in this form than after recrystallization from DMSO. The color of the crystals changes gradually from yellow to green and the composition of the complex becomes powdery. Whether these observations are due to evaporation of solvent from the crystal lattice or oxidation by air, was not further investigated.

ii) X-ray structure of 2,5,8-trithia[9]-*meta*-benzenophane, TTMB.

The compound 2,5,8-trithia[9]-*meta*-benzenophane (TTMB) was previously synthesized by Vögtle[11], but not structurally characterized by X-ray diffraction.

The unit cell contains eight distinct molecules of TTMB and therefore the

asymmetric unit consists of two independent molecules. Perspective ORTEP drawings of these molecules are shown in Figures 3.2 and 3.3. Both molecules show a high degree of disorder. Sulfur-carbon bond distances range from 1.774(12) to 2.00(3) Å and carbon-carbon bond distances from 1.42(3) to 1.59(3) Å for the aliphatic carbons and from 1.336(12) to 1.407(13) Å for the carbons in the aromatic ring. The C-S-C angles range from 89.7(10) to 107.3(10)°. A complete listing of the interatomic distances and angles is given in Table 3.4.

The S-atoms are exodentate and form a triangular cavity with a non-bonding distance between S1 and S3 across the meta-xylyl linkage of 6.84 Å. The torsional angles associated with the ring (Table 3.5) show that the S-CH_2CH_2-S-CH_2CH_2-S "bracket" spans the gap between the benzylic xylene carbons almost perfectly. There is almost no distortion from the ideal conformation for these "bracket" units as predicted by Cooper[26]. The torsional angles of most interest are those of S1-C8-C9-S2 (180.0°) and S2-C10-C11-S3 (179.1°), clearly indicating the preferred anti-placement along the C-C bonds. The trend for preferred gauche placement along the C-S bonds can be derived from the torsional angles of the appropriate C-C-S-C fragments. Eight out of twelve (two molecules!) C-S bonds have torsional angles that range from 61.9° to 88.6°. The plane through the S-atoms of the thioether portion of the ligand is almost perpendicular to the plane through the aromatic part of the molecule (104.4° for molecule 1 and 98.1° for molecule 2).

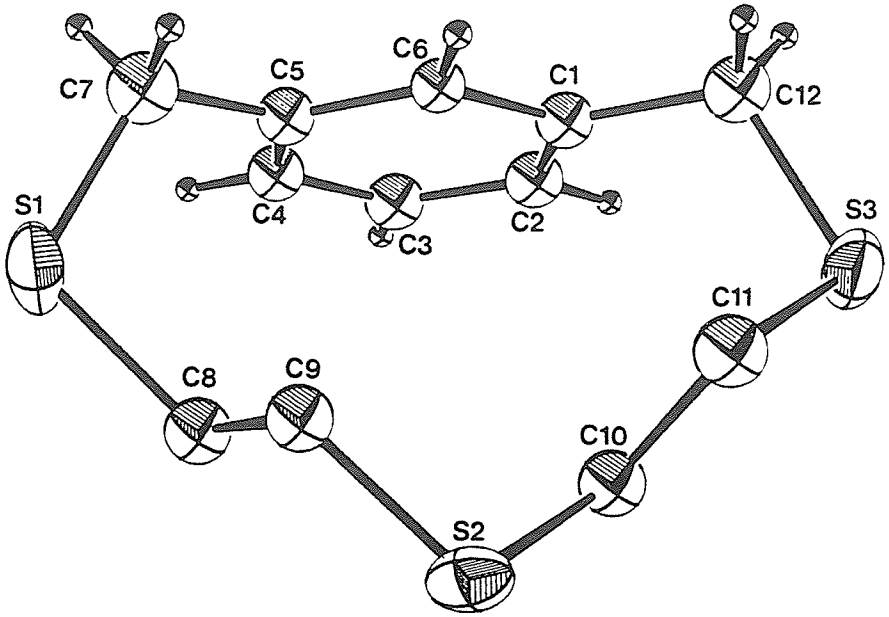

Figure 3.2 Perspective ORTEP drawing of TTMB, Molecule 1 showing the atom numbering scheme. 20% thermal ellipsoids are shown.

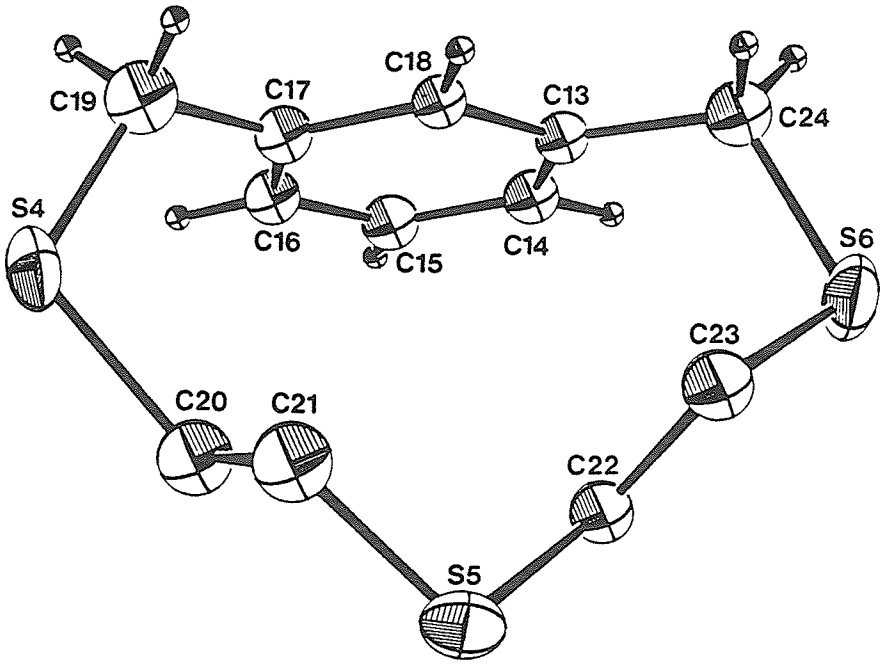

Figure 3.3 Perspective ORTEP drawing of TTMB, Molecule 2 showing the atom numbering scheme. 20% thermal ellipsoids are shown.

Table 3.4 Selected Bond Distances and Angles for 2,5,8-Trithia[9]-*meta*-benzenophane.

Molecule 1:

Distances (Å)			
S1-C7	1.781(13)	C2-C3	1.373(14)
S1-C8	1.95(2)	C3-C4	1.370(13)
S1-C8d	1.86(3)	C4-C5	1.407(13)
S2-C9	1.80(2)	C5-C6	1.393(13)
S2-C9d	1.79(3)	C1-C6	1.403(12)
S2-C10	1.79(2)	C5-C7	1.521(15)
S2-C10d	1.85(4)	C1-C12	1.523(14)
S3-C11	1.87(2)	C8-C9	1.48(2)
S3-C11d	1.91(4)	C8d-C9d	1.58(4)
S3-C12	1.820(11)	C10-C11	1.48(3)
C1-C2	1.354(13)	C10d-C11d	1.53(5)
Angles (°)			
C7-S1-C8	105.0(7)	S1-C3d-C9d	110(2)
C7-S1-C8d	89.7(10)	C8-C9-S2	111.5(14)
C9-S2-C10	103.3(8)	C8d-C9d-S2	113(2)
C9B-S2-C10d	100.9(13)	S2-C10-C11	112.2(14)
C11-S3-C12	96.2(7)	S2-C10d-C11d	106(2)
C11d-S3-C12	107.3(10)	C10-C11-S3	109.7(14)
C5-C7-S1	113.4(8)	C10d-C11d-S3	105(2)
S1-C8-C9	110.5(13)	S3-C12-C1	115.5(7)

Molecule 2:

Distances (Å)

S4-C19	1.774(12)	C14-C15	1.336(12)
S4-C20	2.00(3)	C15-C16	1.342(13)
S4-C20d	1.80(2)	C16-C17	1.392(13)
S5-C21	1.81(3)	C17-C18	1.385(13)
S5-C21d	1.78(3)	C13-C18	1.342(12)
S5-C22	1.84(2)	C17-C19	1.500(14)
S5-C22d	1.83(3)	C13-C24	1.498(13)
S6-C23	1.92(2)	C20-C21	1.42(3)
S6-C23d	1.88(3)	C20d-C21d	1.59(3)
S6-C24	1.798(11)	C22-C23	1.49(3)
C13-C14	1.395(12)	C22d-C23d	1.48(4)

Angles (°)

C19-S4-C20	108.2(1)	S4-C20d-C21d	108.2(1)
C19-S4-C20d	104.1(7)	C20-C21d-S5	105(2)
C21-S5-C22d	103.2(1)	C20d-C21d-S5	113.6(16)
C21d-S5-C22d	99.6(11)	S5-C22-C23	105.8(15)
C23-S6-C24	97.5(1)	S5-C22d-C23d	105(2)
C23d-S6-C24	106.9(9)	C22-C23-S6	103.3(15)
C17-C19-S4	116.3(8)	C22d-C23d-S6	107(2)
S4-C20-C21	108(2)	S6-C24-C13	115.9(7)

d = atom for minor component in disorder model.

Table 3.5 Torsional Angles for TTMB.

Molecule 1			
C7-C5-C6-C1	-175.7	C11-C10-S2-C9	81.2
C5-C6-C1-C12	177.7	C10-S2-C9-C8	77.1
C6-C1-C12-S3	104.9	S2-C9-C8-S1	180.0
C1-C12-S3-C11	-63.4	C9-C8-S1-C7	-72.8
C12-S3-C11-C10	101.7	C8-S1-C7-C5	32.2
S3-C11-C10-S2	179.1	S1-C7-C5-C6	110.4
Molecule 2			
C19-C17-C18-C13	178.0	C23-C22-S5-C21	-74.9
C17-C18-C13-C24	175.3	C22-S5-C21-C20	75.7
C18-C13-C24-S6	107.4	S5-C21-C20-S4	173.0
C13-C24-S6-C23	61.9	C21-C20-S4-C19	-88.6
C24-S6-C23-C22	103.3	C20-S4-C19-C17	21.1
S6-C23-C22-S5	-176.5	S4-C19-C17-C18	105.0

iii) X-ray structure of 2,5,8-trithia[9]-*ortho*-benzenophane, TTOB.

The unit cell contains four discrete molecules of TTOB. Sulfur-carbon bond distances range from 1.793(7) to 1.822(7) Å and carbon-carbon bond distances from 1.499(8) to 1.515(6) Å for the aliphatic carbons and from 1.359(7) to 1.399(7) Å for the carbons in the aromatic ring. The C-S-C angles range from 99.2(3) to 101.3(3)° and are all smaller than the ideal tetrahedral angle, due to the repulsion between the lone pairs on the sulfur atoms (Gillespie-Nyholm approach)[7]. These values are in good agreement with those found for other macrocyclic thioethers reported in the literature[18,65] and those

reported for 16S6. A complete listing of the interatomic distances and angles is given in Table 3.6.

From the ORTEP diagram (Figure 3.4) it can be seen, that the S-atoms are all exodentate to the ring and the S-CH_2CH_2-S-CH_2CH_2-S "bracket" is again easily recognized. Although less pronounced than is the case for the meta analogue of the ligand, the magnitude of the torsional angles (Table 3.7) for the S-C-C-S fragments (158.5° and 166.7°) still indicate the preferred anti-placement of the C-S bonds along the C-C axis. The conformation of the "bracket" is slightly distorted because of the smaller ring size due to the ortho-xylyl fragment . The torsional angles of the C-C-S-C fragments are clearly indicative of the preferred gauche placement along C-S bonds. The S-atoms form a triangular cavity with a non-bonding distance between S1 and S3 across the ortho-xylyl fragment of 5.76 Å. The thioether portion (the S-CH_2CH_2-S-CH_2CH_2-S bracket) of the ligand is almost perpendicular to the plane through the aromatic part of the molecule (96.1°).

Table 3.6 Selected Bond Distances and Angles for 2,5,8-Trithia[9]-*ortho*-benzenophane.

Distances (Å)			
S1-C7	1.807(5)	C3-C4	1.361(7)
S1-C8	1.801(6)	C4-C5	1.364(7)
S2-C9	1.822(7)	C5-C6	1.394(6)
S2-C10	1.816(6)	C6-C7	1.502(7)
S3-C11	1.793(7)	C1-C6	1.394(6)
S3-C12	1.803(5)	C8-C9	1.499(8)
C1-C2	1.399(7)	C10-C11	1.495(7)
C2-C3	1.359(7)	C1-C12	1.515(6)

Angles (°)			
C7-S1-C8	99.5(2)	C8-C9-S2	113.2(5)
C9-S2-C10	99.2(3)	S2-C10-C11	113.9(4)
C11-S3-C12	101.3(3)	C10-C11-S3	114.7(4)
C6-C7-S1	116.0(3)	S3-C12-C1	116.1(3)
S1-C8-C9	113.5(4)		

Table 3.7 Torsional Angles for TTOB.

S1-C7-C6-C1	138.6	C11-C10-S2-C9	-74.5
C7-C6-C1-C12	5.0	C10-S2-C9-C8	75.3
C6-C1-C12-S3	127.9	S2-C9-C8-S1	158.5
C1-C12-S3-C11	79.5	C9-C8-S1-C7	-74.4
C12-S3-C11-C10	80.4	C8-S1-C7-C6	58.4
S3-C11-C10-S2	166.7		

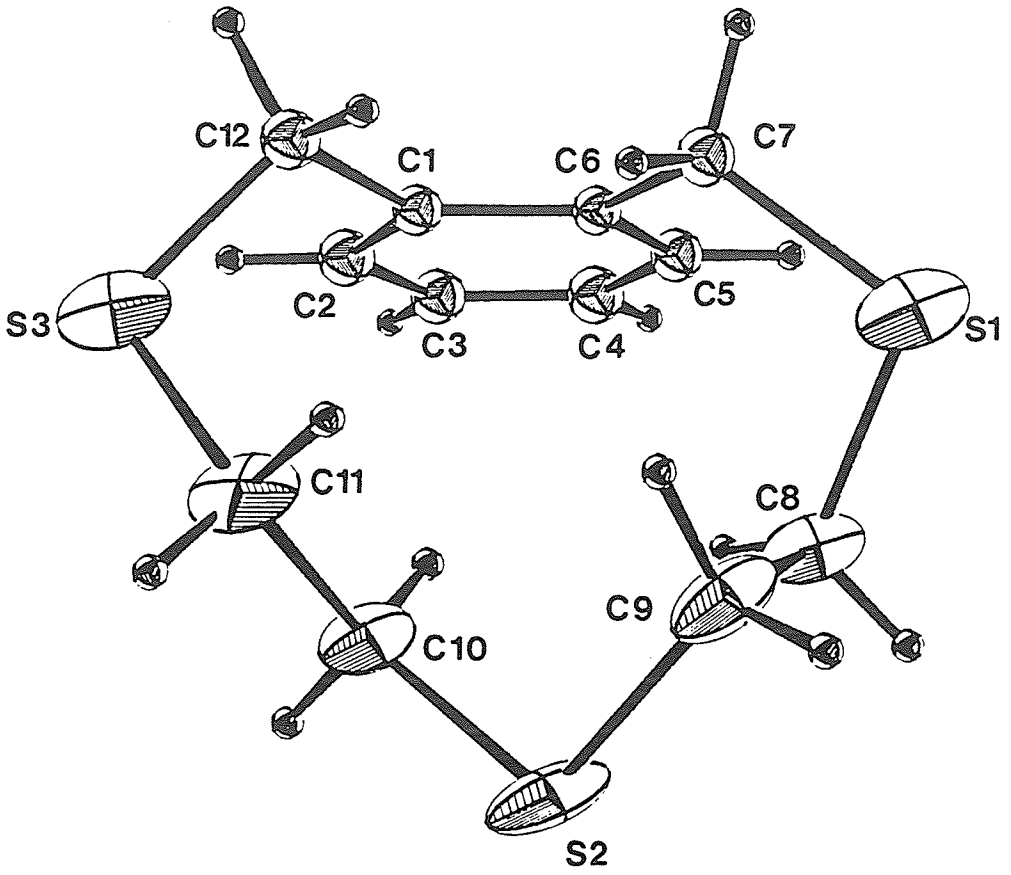

Figure 3.4 Perspective ORTEP drawing of TTOB showing the atom numbering scheme. 20% thermal ellipsoids are shown.

iv) X-ray structure of $[Cu(TTOB)(PPh_2Me)][ClO_4]$.

The unit cell contains four $[Cu(TTOB)(PPh_2Me)]^+$ cations and four $[ClO_4]^-$ anions. The asymmetric unit contains two distinct molecules, differing only in the orientation of the diphenylmethyl phosphine groups with respect to the TTOB ligand. The ORTEP diagrams are shown in Figures 3.5 and 3.6, while Figure 3.7 gives a top-view (down the P-Cu axis) of both cations to illustrate the rotation of the phosphorus substituents. Complete listings of interatomic distances and angles are given in Table 3.8.

The TTOB ligand is facially coordinated to the Cu(I) ion. The Cu(I) ion is in a tetrahedral environment. In molecule 1 the S-Cu-S angles for the five-membered chelate rings are both 92.6(1)° and the seven-membered chelate ring has a S-Cu-S angle of 113.5(1)°. The S-Cu-P angles range from 113.6(1)° (S1-Cu1-P1) and 114.6(1)°(S2-Cu1-P1) to 123.4(1)°(S3-Cu1-P1), indicating that the Cu1-P1 axis deviates slightly from the normal of the plane through the three S-atoms. The Cu1-S distances range from 2.294(3) to 2.376(2) Å. The sulfur-carbon bond distances range from 1.799(8) to 1.824(12) Å and the carbon-carbon bond distances from 1.490(12) to 1.521(11) Å for the aliphatic carbon and from 1.321(16) to 1.403(12) Å for the aromatic carbons. These distances compare well with those reported in the literature for other Cu-thioether complexes[33-38]. The Cu1-P1 distance is 2.234(2) Å. The angles around the chlorine atom in the anion range from 101.6(10)° to 115.3(10)°, while the Cl-O bond distances vary from 1.316(18) to 1.407(13) Å. These distances and angles for the perchlorate anion indicate that it is well behaved, though the large thermal parameters do suggest some disorder. The angle between the plane through the three S-atoms and the plane of the phenyl ring of the ligand is 167.6°.

Molecule 2 shows basically the same features as molecule 1. The S4-Cu2-S6 angle in the seven membered chelating ring is considerably larger (115.5(1)°) than the chelating angles in the five-membered rings (93.0(1)° and 93.4(1)° for S4-Cu2-S5 and S5-Cu2-S6, respectively). The S-Cu-P angles range from 112.6(1)° to 120.2(1)°, which means that the Cu2-P2 axis is tilted with respect to the plane through the sulfur atoms. The Cu2-S bond distances range from 2.284(2) Å to 2.355(4) Å, the longest bond being the one from Cu2 to the central S-atom(S5) opposite the ortho-xylyl fragment of the ligand. The C-C bond distances range from 1.478(18) to 1.510(13) Å. The aromatic carbon-carbon bond distances vary from 1.305(20) to 1.402(19) Å. The Cu2-P2 bond distance is 2.222(2) Å. The angle between the plane through the sulfur atoms and the plane of the phenyl ring of the ligand for molecule 2 is 162.9°, indicating the ligand is slightly more "flattened" in this

conformation. The perchlorate shows the expected tetrahedral geometry with O-Cl-O angles ranging from 99.1(8)° to 115.2(7)° and Cl-O bond distances from 1.349(10) to 1.424(16) Å.

The torsional angles of the coordinated ligand on both molecules (Table 3.9) show the same trends. Since both conformations crystallize in the same unit cell, the energy required to interconvert the molecules (rotation of the diphenylmethylphosphine group around the Cu-P axis) must be small.

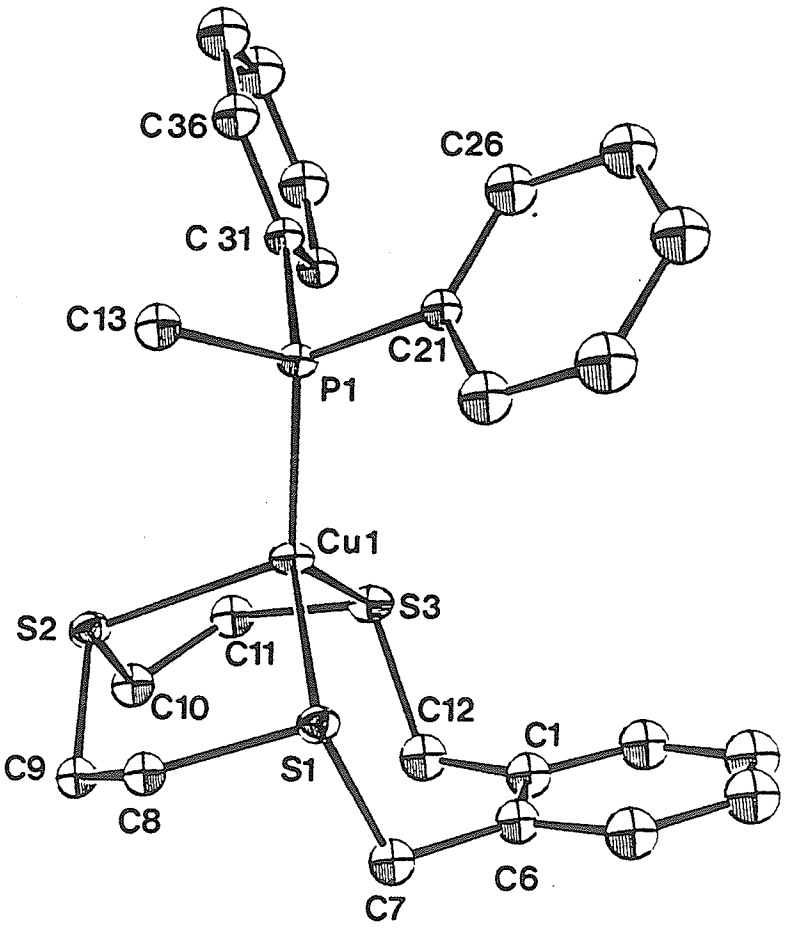

Figure 3.5 Perspective ORTEP drawing of the $[Cu(TTOB)(PPh_2Me)]^+$ cation, Molecule 1 showing the atom numbering scheme. 20% thermal ellipsoids are shown.

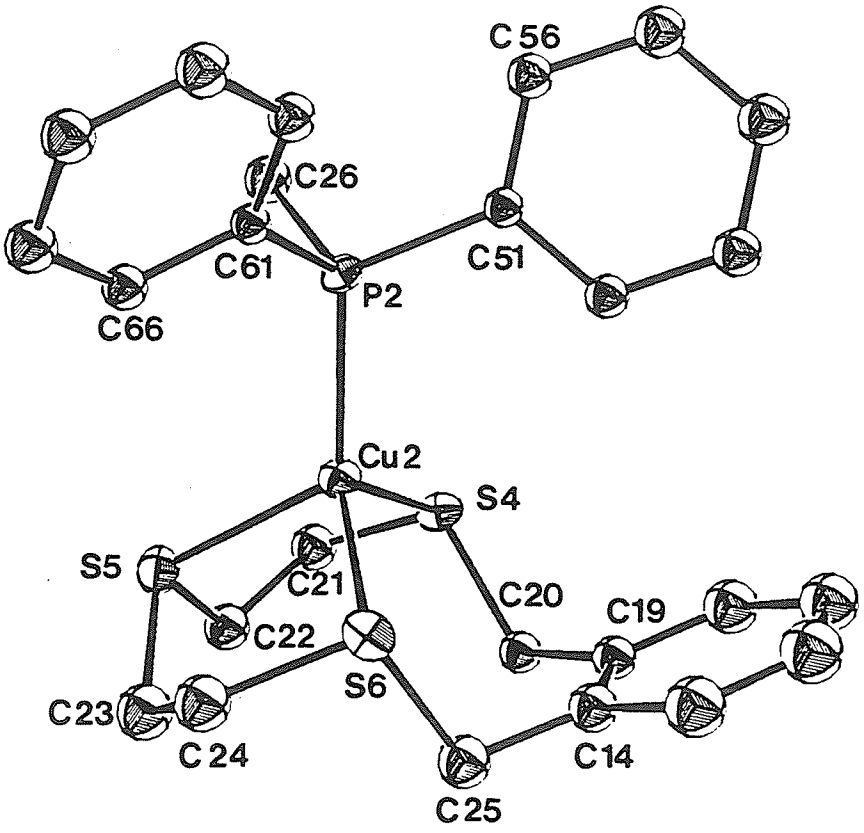

Figure 3.6 Perspective ORTEP drawing of the $[Cu(TTOB)(PPh_2Me)]^+$ cation, Molecule 2 showing the atom numbering scheme. 20% thermal ellipsoids are shown.

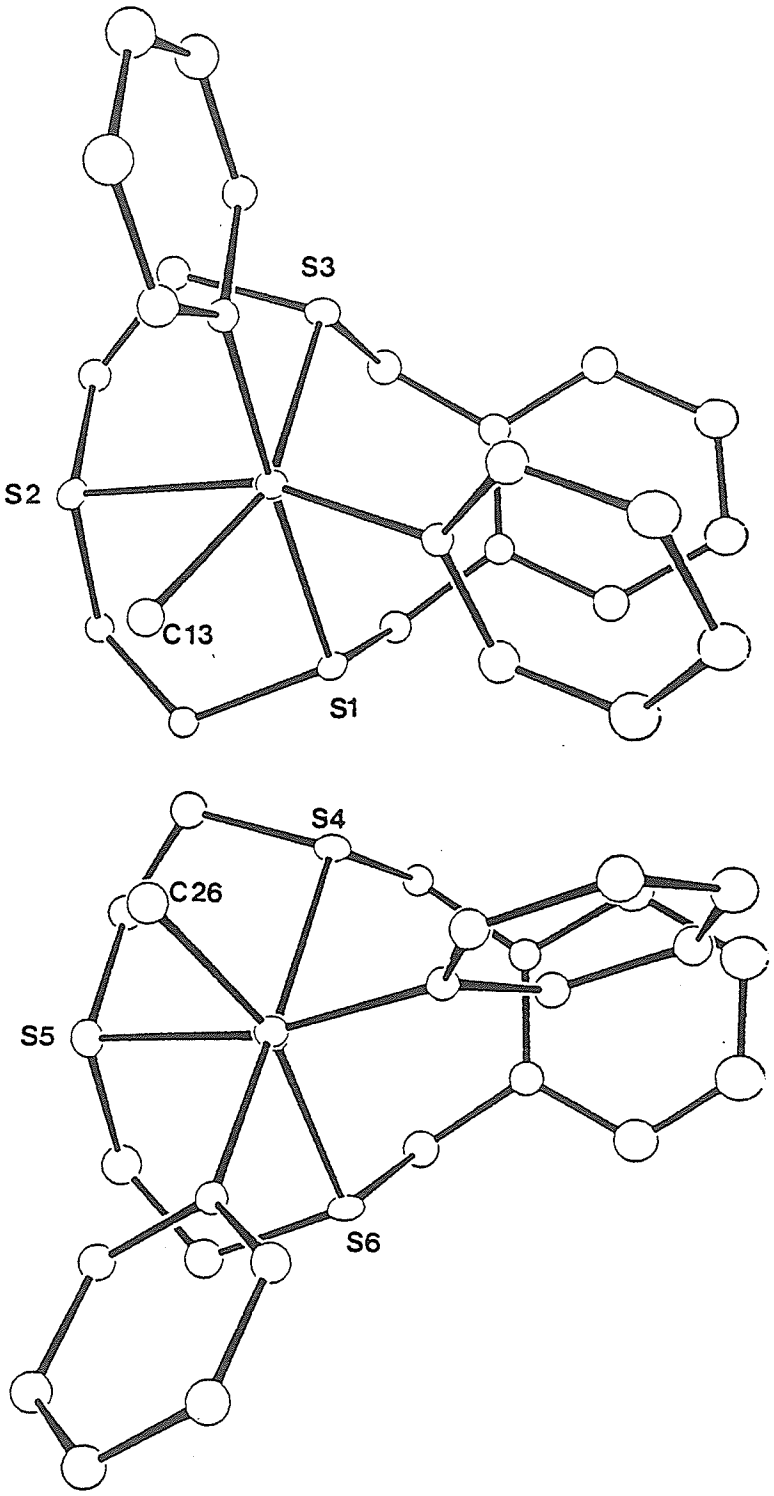

Figure 3.7 Perspective ORTEP drawing of the $[Cu(TTOB)(PPh_2Me)]^+$ cations of Molecule 1 and Molecule 2 showing top view down the P-Cu axis. Note the rotation of the phosphine group with respect to the TTOB ligand.

Table 3.8 Selected Bond Distances and Angles for $[Cu(TTOB)(PPh_2Me)][ClO_4]$.

	Distances (Å)		
Molecule 1			
Cu1-S1	2.300(3)	C8-C9	1.521(11)
Cu1-S2	2.376(2)	C10-C11	1.509(14)
Cu1-S3	2.294(3)	C12-C1	1.490(12)
Cu1-P1	2.234(2)	C1-C2	1.396(15)
S1-C7	1.828(12)	C2-C3	1.359(14)
S1-C8	1.799(8)	C3-C4	1.329(21)
S2-C9	1.820(9)	C4-C5	1.391(16)
S2-C10	1.824(12)	C5-C6	1.403(12)
S3-C11	1.803(8)	C6-C1	1.362(16)
S3-C12	1.824(12)	CL1-O1	1.327(17)
P1-C13	1.828(12)	CL1-O2	1.404(8)
P1-C31	1.825(5)	CL1-O3	1.316(18)
P1-C41	1.822(6)	CL1-O4	1.407(13)
C6-C7	1.491(14)		
	Angles (°)		
S1-Cu1-S2	92.6(1)	C10-C11-S3	116.9(7)
S1-Cu1-S3	113.5(1)	S3-C12-C1	109.4(7)
S2-Cu1-S3	92.6(1)	C12-C1-C6	122.5(9)
S1-Cu1-P1	113.6(1)	C1-C6-C7	123.6(7)
S2-Cu1-P1	114.6(1)	C6-C7-S1	110.2(6)
S3-Cu1-P1	123.4(1)	C13-P1-C31	100.9(4)
Cu1-S1-C7	109.6(4)	C13-P1-C41	104.2(4)
Cu1-S1-C8	97.9(3)	C31-P1-C41	104.5(2)

C7-S1-C8	103.4(4)	Cu1-P1-C13	111.7(3)
Cu1-S2-C9	99.2(2)	Cu1-P1-C31	117.3(2)
Cu1-S2-C10	99.4(3)	Cu1-P1-C41	116.4(2)
C9-S2-C10	102.0(5)	O1-CL1-O2	108.8(7)
Cu1-S3-C11	97.7(4)	O1-CL1-O3	115.3(10)
Cu1-S3-C12	109.6(4)	O1-CL1-O4	101.6(10)
C11-S3-C12	101.9(4)	O2-CL1-O3	113.4(8)
S1-C8-C9	116.2(7)	O2-CL1-O4	112.2(6)
C8-C9-S2	112.7(5)	O3-CL1-O4	105.0(10)
S2-C10-C11	112.3(6)		

Distances (Å)

Molecule 2

Cu2-S4	2.298(3)	C21-C22	1.478(18)
Cu2-S5	2.355(4)	C23-C24	1.495(17)
Cu2-S6	2.284(2)	C25-C14	1.482(19)
Cu2-P2	2.222(3)	C14-C15	1.399(15)
S4-C20	1.813(7)	C15-C16	1.337(25)
S4-C21	1.808(12)	C16-C17	1.305(20)
S5-C22	1.825(11)	C17-C18	1.402(19)
S5-C23	1.820(11)	C18-C19	1.399(20)
S6-C24	1.815(15)	C19-C14	1.384(14)
S6-C25	1.823(11)	CL2-O5	1.407(10)
P2-C26	1.805(7)	CL2-O6	1.349(10)
P2-C51	1.817(8)	CL2-O7	1.366(13)
P2-C61	1.821(7)	CL2-O8	1.424(16)
C19-C20	1.510(13)		

Angles (°)

S4-Cu2-S5	93.0(1)	C23-C24-S6	116.9(7)
S4-Cu2-S6	115.5(1)	S6-C25-C14	109.4(7)
S5-Cu2-S6	93.4(1)	C25-C14-C19	122.5(9)
S4-Cu2-P2	112.6(1)	C14-C19-C20	123.6(7)
S5-Cu2-P2	120.2(1)	C19-C20-S4	110.2(6)
S6-Cu2-P2	118.3(1)	C26-P2-C51	104.6(4)
Cu2-S4-C20	111.0(3)	C26-P2-C61	100.6(4)
Cu2-S4-C21	97.9(4)	C51-P2-C61	107.6(3)
C20-S4-C21	102.0(5)	Cu2-P2-C26	113.9(4)
Cu2-S5-C22	97.5(4)	Cu2-P2-C51	113.2(2)
Cu2-S5-C23	99.5(5)	Cu2-P2-C61	115.6(2)
C22-S5-C23	102.7(5)	O5-CL2-O6	112.1(7)
Cu2-S6-C24	97.8(3)	O5-CL2-O7	113.9(6)
Cu2-S6-C25	107.1(3)	O5-CL2-O8	104.0(7)
C24-S6-C25	103.8(6)	O6-CL2-O7	115.2(7)
S4-C21-C22	116.2(7)	O6-CL2-O8	99.1(8)
C21-C22-S5	112.7(5)	O7-CL2-O8	111.0(10)
S5-C23-C24	112.3(6)		

Table 3.9 Torsional Angles Associated with [Cu(TTOB)(PPh_2Me][ClO_4].

Molecule 1		Molecule 2	
S2-C9-C8-S1	55.0	S4-C21-C22-S5	58.3
C10-S2-C9-C8	133.6	C21-C22-S5-C23	139.6
C11-C10-S2-C9	133.3	C22-S5-C23-C24	127.0

S3-C11-C10-S2	-54.8	S5-C23-C24-S6	-49.1
C12-S3-C11-C10	67.9	C23-C24-S6-C25	69.0
C1-C12-S3-C11	166.1	C24-S6-C25-C14	166.8
C6-C1-C12-S3	93.4	S6-C25-C14-C19	95.9
C7-C6-C1-C12	-1.4	C25-C14-C19-C20	-1.2
S1-C7-C6-C1	93.8	C14-C19-C20-S4	90.7
C8-S1-C7-C6	163.9	C19-C20-S4-C21	160.0
C9-C8-S1-C7	68.4	C20-S4-C21-C22	71.3

v) X-ray structure of $Mo(CO)_3$(TTOB).DMSO.

The unit cell contains four $Mo(CO)_3$(TTOB) molecules each associated with one DMSO solvent molecule. The oxygen atom of the Me_2SO solvent molecule points into the rear cone/cavity formed by the axial hydrogen atoms on the carbons atoms C7, C8, C10 and C12. The O..H non-bonding distances range from 2.42 to 2.64 Å. A similar inclusion of Me_2SO in the crystal lattice has been reported before by Schröder and co-workers[33], who found that $Ru(9S3)^{2+}$ has an oxygen atom of a DMSO solvent molecule pointing into the rear cavity of each coordinated 9S3 ligand, with O..H non-bonding distances ranging from 2.20 to 3.29 Å. The ORTEP diagram is shown in Figure 3.8. Complete listings of interatomic distances and angles are given in Table 3.9.

The TTOB ligand is facially coordinated to the Mo(0) atom. The environment around the metal is pseudo-octahedral with three facial carbonyl ligands and the three thioether donor atoms. The S-Mo-S angles for the five-membered chelating rings are 81.3(1)° and 81.9(1)°, whereas the chelating angle for the seven-membered ring is much larger: 96.5(1)°. The angles of the metal center with the carbon atoms of the carbonyl groups range from 84.4(3)° to 88.9(3)°. With the exception of S1-Mo-C13 (85.9(2)°), the

angles between the carbonyl carbons and the chelating S-atoms range from 93.0(2)° to 96.9(2)°. The S-Mo-C "trans" angles vary from 170.0(2)° to 175.1(2)°. Thus the Mo coordination sphere deviates slightly from octahedral geometry by virtue of a trigonal elongation. The Mo-S distances range from 2.531(2) to 2.546(2) Å. The metal-carbon distances vary from 1.931(8) to 1.958(7) Å and are approximately 0.1 Å shorter than the reported distance in $Mo(CO)_6$ (2.06(2) Å)[73]. The sulfur-carbon bond distances range from 1.810(7) to 1.844(8) Å and the carbon-carbon bond distances from 1.471(10) to 1. 515(10) Å for the aliphatic carbon and from 1.366(11) to 1.431(10) Å for the aromatic carbons. The carbonyl C-O bonds are between 1.173(8) and 1.149(9) Å. These distances are very similar to those reported in the literature for $Mo(9S3)(CO)_3$[42]. The angle between the plane through the three S-atoms and the plane of the phenyl ring of the ligand is 148.5°.

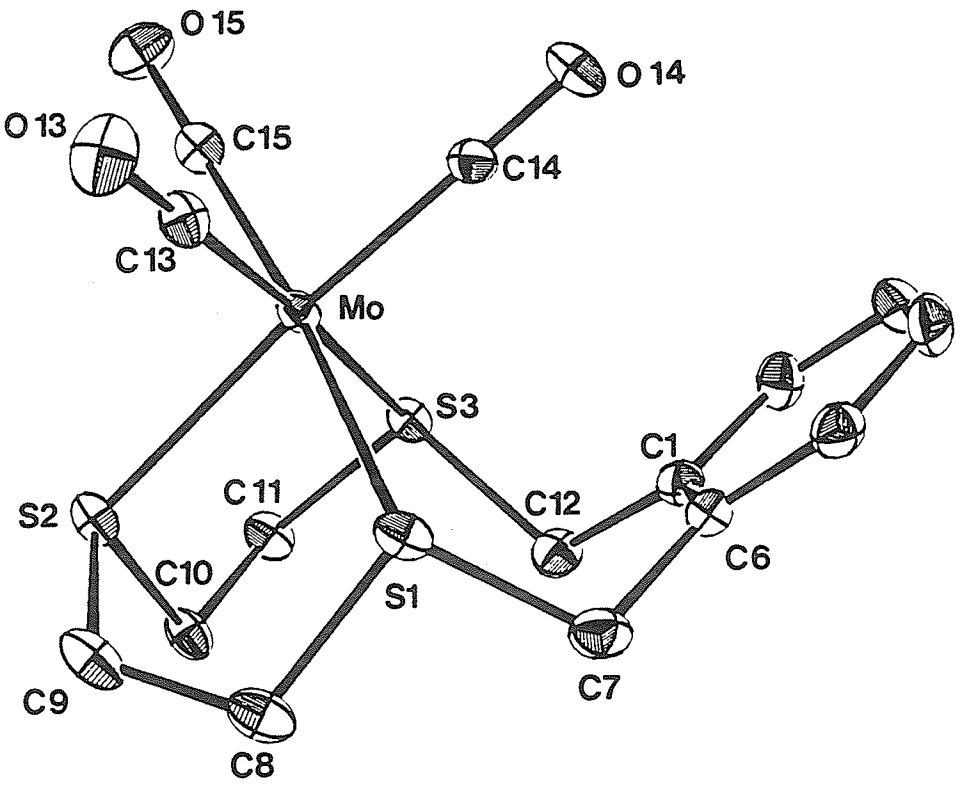

Figure 3.8 Perspective ORTEP drawing of $Mo(CO)_3$(TTOB) showing the atom numbering scheme. 20% thermal ellipsoids are shown.

Table 3.10 Selected Bond Distances and Angles for $Mo(TTOB)(CO)_3$.

	Distances (Å)		
Mo-S1	2.546(2)	C12-C1	1.471(10)
Mo-S2	2.531(2)	C1-C6	1.431(10)
Mo-S3	2.545(2)	C6-C7	1.488(10)
Mo-C13	1.931(8)	C7-S1	1.844(8)
Mo-C14	1.958(7)	C1-C2	1.391(9)
Mo-C15	1.954(7)	C2-C3	1.360(11)
S1-C8	1.831(7)	C3-C4	1.364(12)
C8-C9	1.503(11)	C4-C5	1.366(11)
C9-S2	1.820(8)	C5-C6	1.386(10)
S2-C10	1.817(7)	C13-O13	1.173(8)
C10-C11	1.515(10)	C14-O14	1.149(9)
C11-S3	1.810(7)	C15-O15	1.155(8)
S3-C12	1.831(7)		
	Angles (°)		
S1-Mo-S2	81.3(1)	Mo-S3-C12	111.4(2)
S1-Mo-S3	96.5(1)	Mo-S1-C7	118.5(2)
S2-Mo-S3	81.9(1)	Mo-S3-C11	103.7(2)
C13-Mo-C14	88.9(3)	Mo-S2-C9	103.1(3)
C14-Mo-C15	87.7(3)	Mo-S2-C10	104.8(2)
C15-Mo-C13	84.4(3)	C1-C6-C7	120.8(6)
S1-Mo--C13	85.9(2)	C6-C7-S1	111.8(5)
S1-Mo-C14	94.7(2)	C7-S1-C8	100.9(4)
S1-Mo-C15	170.0(2)	S1-C8-C9	112.5(5)

S2-Mo-C13	94.3(2)	C8-C9-S2	115.7(5)
S2-Mo-C15	96.9(2)	C9-S2-C10	101.1(4)
S2-Mo-C14	174.6(2)	S2-C10-C11	110.7(5)
S3-Mo-C14	95.2(2)	C10-C11-S3	113.9(4)
S3-Mo-C15	93.0(2)	C11-S3-C12	101.9(3)
S3-Mo-C13	175.1(2)	S3-C12-C1	108.1(5)
Mo-S1-C8	107.6(3)	C12-C1-C6	121.9(6)

Table 3.11 Torsional Angles for Mo(TTOB)$(CO)_3$.

S1-C7-C6-C1	84.1	C11-C10-S2-C9	150.1
C7-C6-C1-C12	-0.8	C10-S2-C9-C8	61.0
C6-C1-C12-S3	101.8	S2-C9-C8-S1	49.8
C1-C12-S3-C11	166.0	C9-C8-S1-C7	150.0
C12-S3-C11-C10	74.4	C8-S1-C7-C6	149.5
S3-C11-C10-S2	-58.7		

vi) NMR.

The ^1H NMR spectra for TTMB and TTOB are shown in Figure 3.9. In the aromatic region they show the characteristic pattern for meta- and ortho-substituted benzene rings, respectively. The benzylic protons in both molecules are assigned to the singlet just below 4 ppm, and the protons of the S-CH_2CH_2-S-CH_2CH_2-S bracket are associated with the complex second order multiplet at 2.10-2.50 ppm (TTMB) and at 2.50-2.85 ppm (TTOB). A ^1H NMR simulation of this portion (AA'BB' system) of the

spectrum was carried out for both ligands (Figure 3.10). Tables C13 and C14 in the appendix list the observed/assigned and calculated frequencies. The coupling constants thus obtained are given in Table 3.12 and compare well to those calculated by using the dihedral angles from the X-ray data, indicating that the solid state conformation is preserved in solution. The results of the final iteration for TTMB gave as best values: geminal coupling constant (^{2}J) = -14.34 Hz and vicinal coupling constants (^{3}J) of 4.54 and 13.14 Hz with a RMS error of .02. The retention of conformation is most evident from the results obtained from TTOB. The X-ray data show no disorder in the molecule and low R-values. These are indications that the dihedral angles obtained from the X-ray data and used to calculate the coupling constants are very reliable. The $^3J_{HH}$ values thus calculated (8.8 and 5.9 Hz.[57];8.1 and 4.6[58]), are very close to those obtained from the simulation. The NMR simulation calculations with LAOCOON III give a geminal coupling constant of -14.85 Hz and vicinal coupling constants of 8.74 and 6.04 Hz, while the RMS error was down to 0.004.

Table 3.12 Calculated coupling constants, $^2J_{HH}$ and $^3J_{HH}$ for TTMB and TTOB

J(Hz)	TTMB		TTOB	
	LAOCOON	X-ray	LAOCOON	X-ray
$^2J_{HH}$(geminal)	-14.3		-14.8	
$^3J_{HH}$(vicinal)	13.1	10.0	8.7	8.8
	4.5	2.5	6.0	5.9

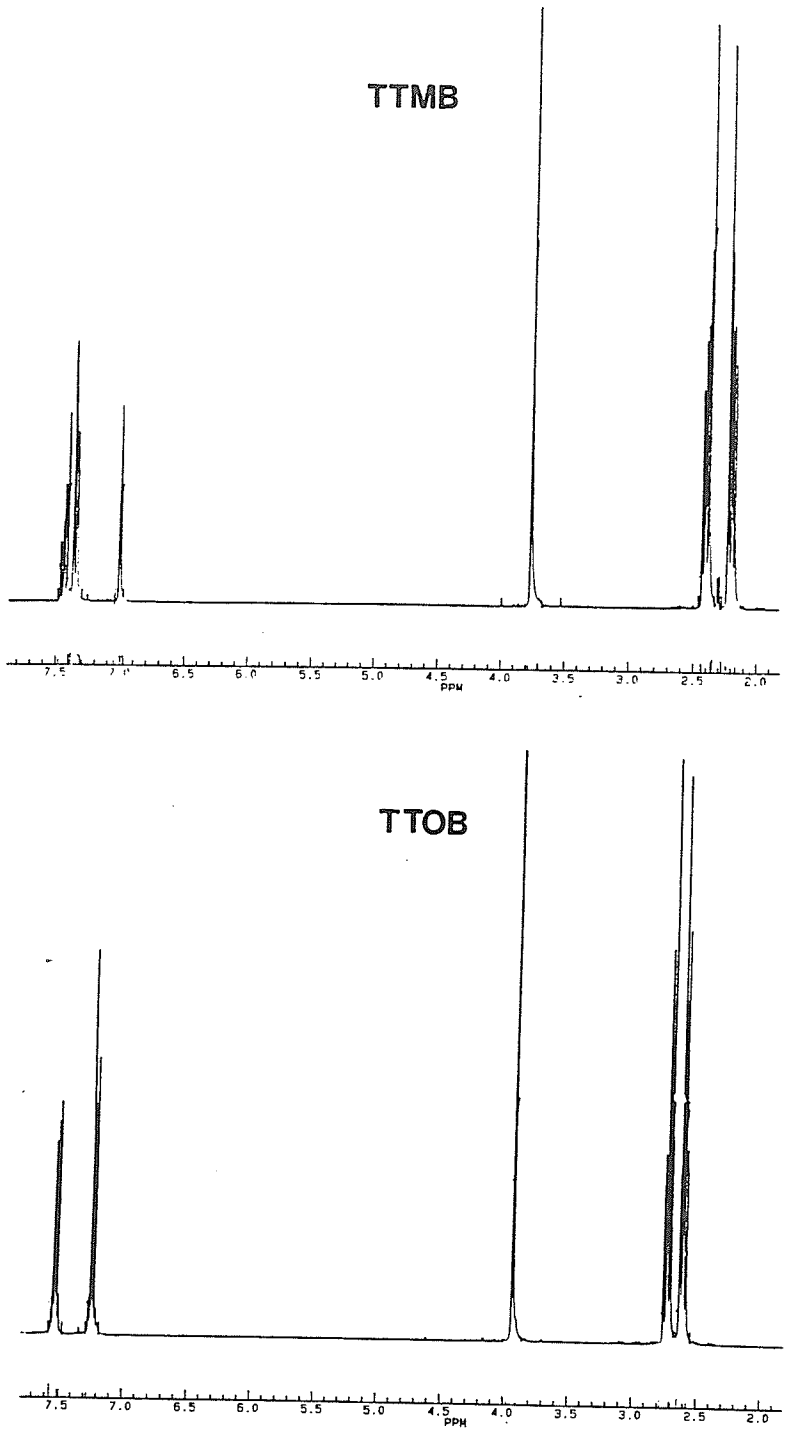

Figure 3.9 ^{1}H-NMR spectra of TTMB and TTOB, at 300 MHz

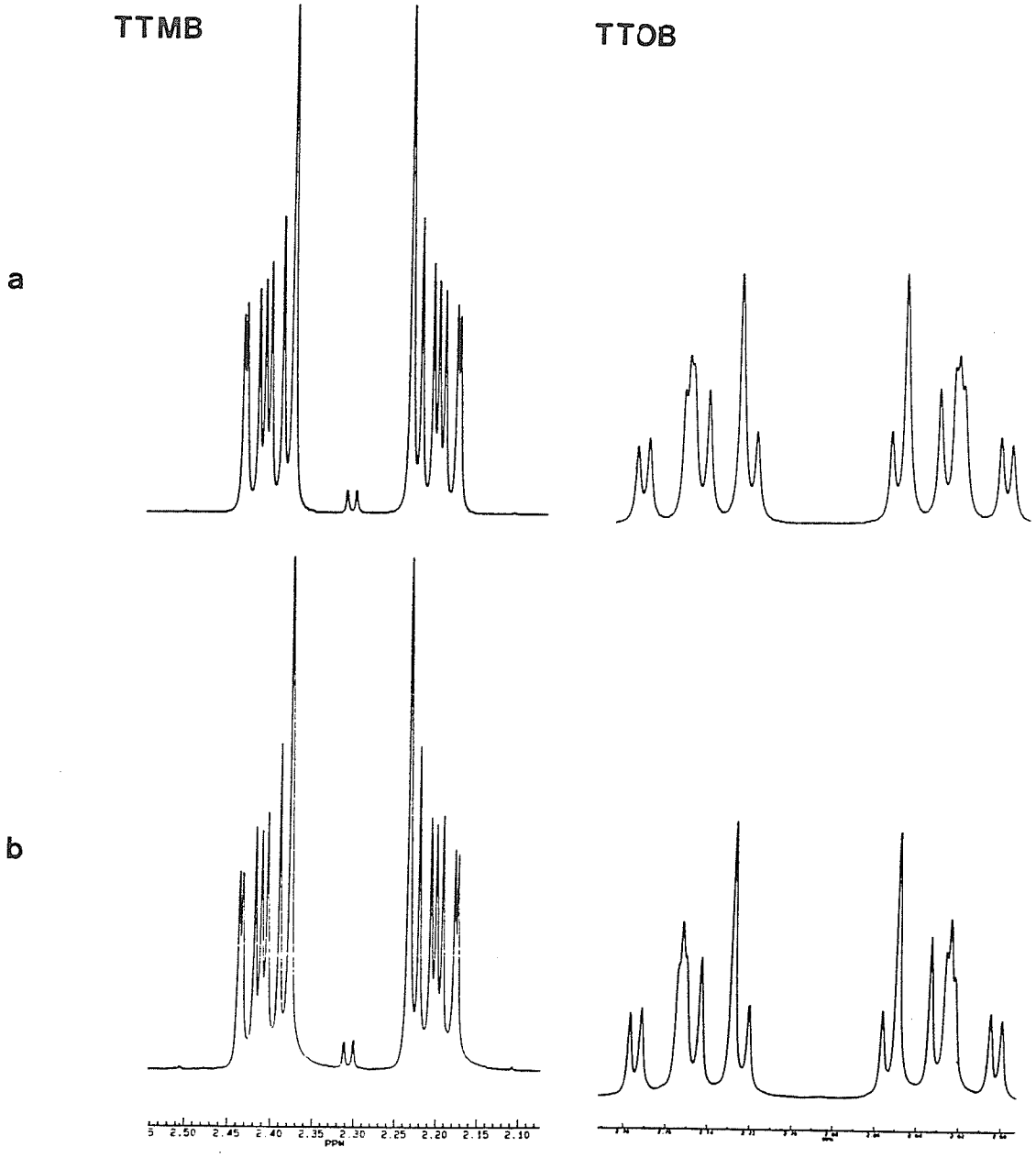

Figure 3.10 ^{1}H-NMR spectra of the $SCH_2CH_2SCH_2CH_2S$ "bracket" of TTMB and TTOB. (a) simulated and (b) observed.

The spectra of both the Cu and the Mo complex of TTOB show some interesting features. At room temperature the resonance of the benzylic protons for the Cu complex is split into a quartet and the multiplet of the ethylene linkages has collapsed into a singlet and a triplet. The multiplet of the aromatic protons has collapsed as well. All peaks are severely broadened and this might indicate some kind of fluxional process. Upon cooling to 235 K the signal due to the ethylene linkage consisted of a well resolved complex multiplet. Sharpening of the peaks associated with the aromatic protons has also occured and some additional splitting was observed in the low field portion of the signal due to the benzylic protons (Figure 3.11).

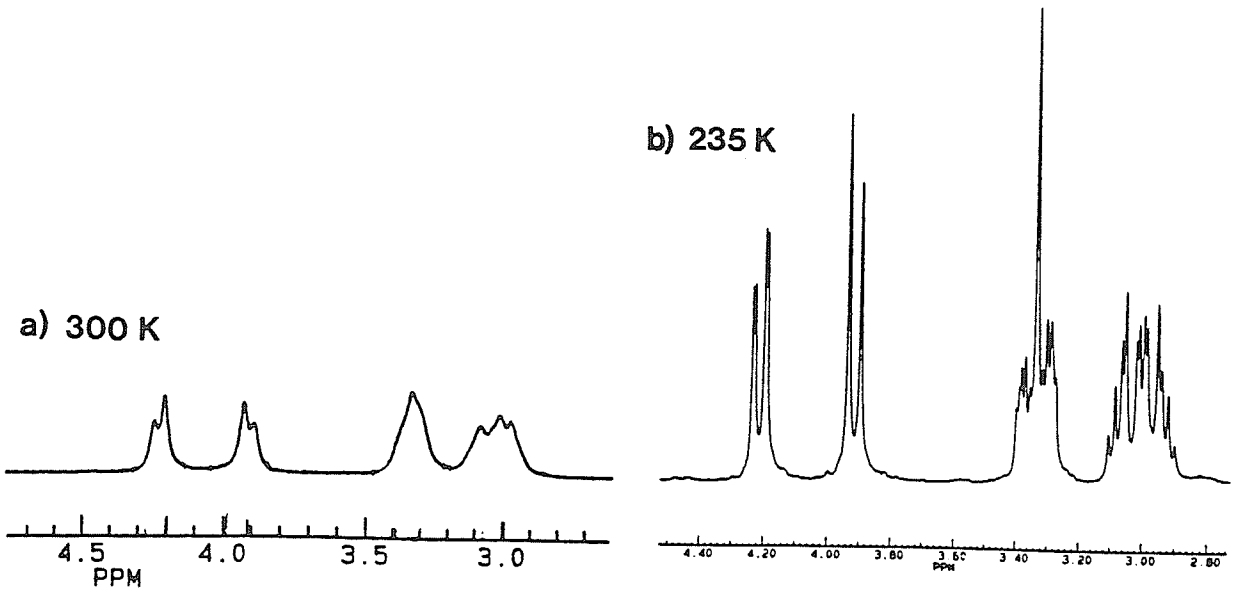

Figure 3.11 ^{1}H NMR spectrum showing the -$CH_2SCH_2CH_2SCH_2CH_2SCH_2$- string of TTOB in [Cu(TTOB)(PPh_2Me)][ClO_4] at a) 300 and b) 235 K.

This coupling can also be seen in the aromatic part of the spectrum. The same phenomenon is observed when the ancillary ligand is PPh_3 instead of PPh_2Me, whereas the additional splitting is absent when the ancillary ligand is CH_3CN, PhCN, or Pyridine. This splitting is due to the π-contributions to the H-H coupling between the benzylic and

the aromatic protons of the ligand. The magnitude of this long range ($^4J(\pi)$) coupling can be estimated from the product of the e.s.r. hyperfine coupling constants and is proportional to $\cos^2 \phi$, where ϕ is the torsional angle between the benzylic proton and the p-orbitals of the unsaturated system[58].

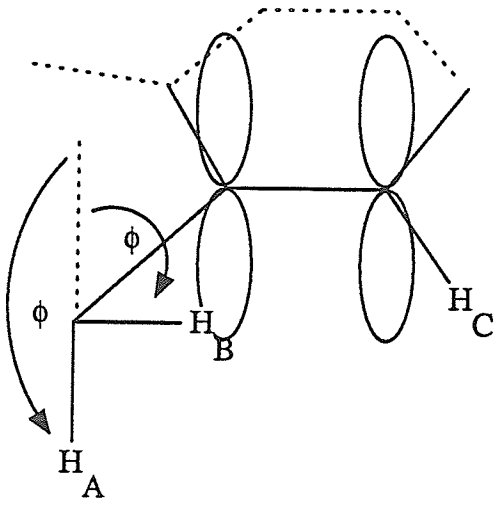

Figure 3.12

ϕ = 0° or 180° $^4J(\pi)$ is maximal
ϕ = 90° or 270° $^4J(\pi)$ is zero

The dependence on the $\cos^2$ term results in a large π-contribution when ϕ = 0° and ϕ = 180° (Figure 3.12). The π-contribution totally disappears when ϕ approaches 90° or 270°. It may therefore be concluded that the downfield resonance at 4.2 ppm is due to the axial benzylic proton and the upfield signal can safely be assigned to the equitorial benzylic proton (in the same plane as the aromatic ring and therefore forming a 90° angle with the p-orbital system). The experimental value (1.4 Hz) compares well to the ^4J coupling observed in the literature for similar basic structures[58]. The fact that this coupling is not observed when the ancillary ligand is CH_3CN, C_6H_5CN, or pyridine possibly indicates that the low temperature limit for these complexes was not reached or may have to to do

with the quadrupolar relaxation properties of nitrogen. The peaks in the aromatic part of the ^1H NMR spectra of the phosphine complexes also sharpen considerably at low temperature, which might indicate that the aromatic part of the ligand is flipping up and down at room temperature.

The ^1H NMR spectrum of $MoTTOB(CO)_3$ at room temperature shows basically the same relevant features as the spectra for the Cu complexes at low temperature, though no broadening is observed. The signal assigned to the benzylic protons is a sharp quartet and the "bracket" methylenes form a complicated multiplet of a slightly different pattern than the Cu complexes. The aromatic region shows only one sharp resonance. This is in contrast to the broadened signal for the Cu complexes. The amount of movement for the coordinated TTOB in the Mo-complex seems therefore much more restricted than for the Cu complexes. The ^1H NMR spectra of the other $[Cu(TTOB)(L)]^+$ complexes, where L= CH_3CN, PPh_3, C_6H_5CN, or pyridine all show severe broadening at room temperature, indicating fluxionality and of course when the coordinating atom is nitrogen, quadrupolar relaxation effects.

3.4 Discussion

The subtle differences between TTMB and TTOB seem to be large enough to create a totally different coordination chemistry for the two molecules. X-ray crystallography shows that the S atoms in both ligands are exodentate in the solid state. Therefore, rearrangement of the S atoms to an endodentate conformation must occur in order for complexation to be possible.

In TTMB the distance between the two S atoms S1 and S3, across the meta-xylyl fragment, is relatively large: 6.84 Å. The torsional angles (Tables 3.5 and 3.7) show that the S-CH_2CH_2-S-CH_2CH_2-S "bracket" has the ideal conformation (see introduction). The placement around the S-C bonds is gauche and the torsional angles of the S-C-C-S

fragments (S1-C8-C9-S2 = 180.0° and S2-C10-C11-S3 = 179.1°) clearly indicate anti placement around the C-C bonds. This makes TTMB quite rigid. Attempts to synthesize a complex of Cu(I) with TTMB analogous to $[Cu(CH_3CN)(TTOB)][ClO_4]$, resulted in the isolation of starting materials.

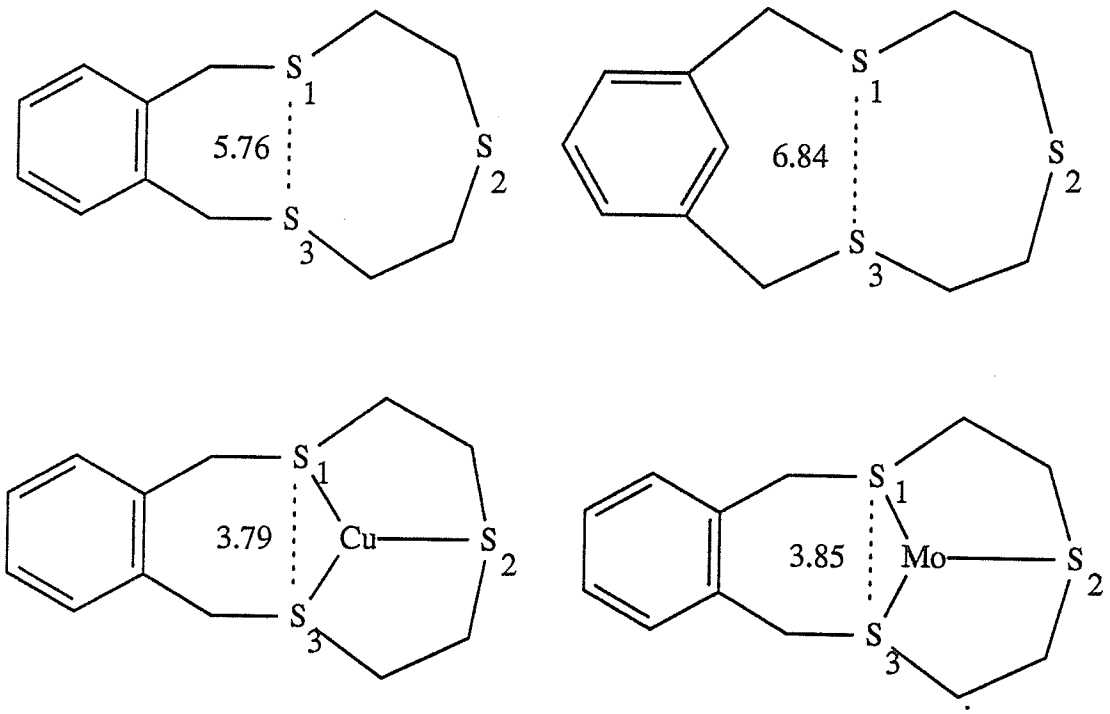

Figure 3.13 distances between S1 and S3 (ångström).

The S1-S3 non-bonding distance in TTOB is 5.76 Å, which is more than one Ångström shorter than in the meta-analogue. Anti-placement around the C-C bonds is definitely less pronounced in TTOB (S1-C8-C9-S2 = 158.5° and S2-C10-C11-S3 = 166.7°). However, in contrast to TTMB, this molecule proves to be remarkably flexible. Upon complexation the S-atoms S1 and S3 are forced into an endodentate position and approach each other quite closely as Figure 3.13 indicates schematically.

A good indication of the conformational adjustment required for the TTOB ligand to coordinate in a tetrahedral or an octahedral geometry is a comparison of the torsional

angles in the free and coordinated ligand (Table 3.13). Except for C10-S2-C9-C8 and C9-C8-S1-C7, the torsional angles of the ligand in the complexed conformation are very similar. Big differences occur, especially for the S-C-C-S fragments, which are rearranged from an anti- to gauche-placement upon chelation. The reduction of the S-C-C-S torsion angles is the result of stabilization provided by the formation of the metal-sulfur bonds[42], which partly overcomes the repulsion by the sulfur lone pairs.

The increased susceptibility in TTOB towards complexation can probably be attributed to the slightly higher ring strain and the conformation of the S-CH_2CH_2-S-CH_2CH_2-S "bracket" being less than ideal. This gives TTOB a higher internal energy than TTMB and lowers the energy barrier that has to be overcome for the essential rearrangement. The failure of TTMB to form a complex with $[Cu(CH_3CN)_4][ClO_4]$ could indicate that the energy needed to "distort" the preferred conformation of the "bracket" and rearrange the sulfur atoms to an endodentate conformation is substantial and/or that the gap between the donor atoms S1 and S3 across the meta-xylyl linkage is just too large for the Cu(I) ion to span even when the S atoms are endodentate to the ring.

Table 3.13 Comparison of Torsional Angles of Uncomplexed TTOB to those in [CuTTOB)(PPh_2Me)]$^+$ and Mo(TTOB)$(CO)_3$.

torsional angle	free TTOB*	compl. (Mo)	compl. (Cu)
S1-C7-C6-C1	127.9	84.1	93.8
C7-C6-C1-C12	5.0	-0.8	-1.4
C6-C1-C12-S3	138.6	101.8	93.4
C1-C12-S3-C11	58.4	166.0	166.1
C12-S3-C11-C10	-74.4	74.4	67.9

S3-C11-C10-S2	158.5	-58.7	-54.8
C11-C10-S2-C9	75.3	150.1	133.3
C10-S2-C9-C8	-74.5	61.0	133.6
S2-C9-C8-S1	166.7	49.8	55.0
C9-C8-S1-C7	80.4	150.0	68.4
C8-S1-C7-C6	79.5	149.5	163.9

* numbering scheme TTOB reversed to get corresponding torsional angles.

3.5 Summary and Conclusions.

This chapter described the synthesis and characterization of the tridentate crown thioether ligands 2,5,8-Trithia[9]-*meta*-benzenophane (TTMB) and 2,5,8-Trithia[9]-*ortho*-benzenophane (TTOB). All three S atoms in both molecules are exodentate to the ring. In an attempt to synthesize the Cu(I) complexes both ligands were reacted with $[Cu(CH_3CN)_4][ClO_4]$. These attempts proved to be successful only for TTOB. The molecule turns out to be very flexible and an excellent ligand to accommodate a first row transition metal in a tetrahedral environment. The reaction of TTOB with $Mo(CH_3CN)_3(CO)_3$ shows that the ligand is also capable of coordinating facially to a metal in an octahedral environment. The inertness of TTMB towards complexation is probably due to the "near perfect" conformation of the S-CH_2CH_2-S-CH_2CH_2-S "bracket" in the molecule and the gap between the benzylic S-atoms, which is too large for the Cu(I) ion to span.

The facial coordination of the macrocyclic tridentate crown thioether TTOB to a metal ion in a tetrahedral geometry infers that the ligand can possibly stabilize other ions like Ni(0), Pd(0) and Pt(0), which prefer a tetrahedral environment. The labile CH_3CN ligand of the Cu(I) complexes proves to be easily substituted by other ligands like

phosphines, pyridine and benzonitrile. Furthermore, this may lead to novel chemistry at open reaction sites and perhaps to the synthesis of new alkylating agents, such as organocuprates, in organic chemistry.

Also, the study of the conformational, electronic and coordination properties of these two ligands provides information, which may serve as a useful guideline for the chemistry of the potentially ditopic ligands containing similar donor groups and skeletal frameworks.

Appendix C

Table C1. Positional Parameters[a] for 2,5,8-Trithia[9]-*m*-benzenophane.

Atom	x	y	z
S1	6986(4)	1395(4)	1360(1)
S2	2731(3)	3897(3)	1524(1)
S3	0797(4)	1322(4)	2575(1)
S4	9291(5)	-1768(3)	4961(1)
S5	11591(4)	0472(4)	3911(1)
S6	9248(4)	4772(3)	4000(1)
C1	3370(10)	-0367(11)	2405(3)
C2	2884(12)	-1568(11)	2182(3)
C3	3761(12)	-2150(12)	1872(3)
C4	5101(11)	-1550(11)	1770(3)
C5	5629(11)	-0267(10)	1982(3)
C6	4738(9)	0264(10)	2305(3)
C7	7058(13)	0504(15)	1860(4)
C8	4952(20)	2021(20)	1293(6)
C8d	5642(35)	2796(32)	1571(9)
C9	4617(20)	3307(19)	1574(6)
C9d	4063(35)	2493(31)	1379(9)
C10	1751(20)	2516(20)	1825(6)
C10d	2275(36)	3285(37)	2064(11)
C11	1871(21)	2828(21)	2281(6)
C11d	1175(36)	1992(39)	2017(11)

C12	2415(12)	0297(13)	2751(3)
C13	7479(10)	3087(10)	4544(3)
C14	6261(10)	2698(11)	4301(3)
C15	5659(11)	1330(11)	4342(3)
C16	6249(10)	0346(12)	4614(3)
C17	7442(11)	0713(11)	4867(3)
C18	8058(10)	2136(9)	4827(3)
C19	8152(13)	0334(14)	5177(4)
C20	9910(27)	-1126(28)	4388(8)
C20d	10705(22)	-0745(21)	4688(6)
C21	11220(26)	-0267(28)	4428(8)
C21d	10294(25)	-0588(26)	4205(8)
C22	10187(21)	1950(23)	3847(6)
C22d	11113(29)	2375(31)	4087(8)
C23	10688(24)	3243(24)	4110(7)
C23d	9812(30)	2817(32)	3835(9)
C24	8229(12)	4575(12)	4480(3)

[a] Multiplied by 10^4. d = Atom for minor component in disorder model.

Table C2. Hydrogen Atom Parameters[a] for 2,5,8-Trithia[9]-*m*-benzenophane.

Atom	x	y	z	U[b]
H2	1952	-2004	2240	73
H3	3424	-3009	1721	79
H4	5672	-1997	1553	74
H6	5074	1099	2466	55
H7A	7280	1249	2065	97
H7B	7816	-0234	1856	97
H12A	2098	-0509	2926	85
H12B	3004	0974	2910	85
H14	5853	3406	4110	66
H15	4827	1056	4179	72
H16	5830	-0634	4637	71
H18	8866	2436	4996	54
H19A	8731	0254	5363	99
H19B	7386	-0814	5329	99
H24A	7497	5340	4485	78
H24B	8891	4724	4706	78

[a] Multiplied by 10^4. [b] Multiplied by 10^3.

Table C3. Thermal Parameters[a] for 2,5,8-Trithia[9]-*m*-benzenophane.

Atom	U11	U22	U33	U23	U13	U12
S1	102(3)	104(3)	119(3)	17(2)	55(2)	11(2)
S2	87(2)	63(2)	95(2)	22(2)	-17(2)	2(2)
S3	72(2)	112(3)	109(3)	25(2)	33(2)	22(2)
S4	140(3)	59(2)	121(3)	28(2)	13(3)	23(2)
S5	77(2)	97(2)	100(2)	-6(2)	28(2)	20(2)
S6	117(3)	65(2)	125(3)	38(2)	31(2)	-1(2)
C1	59(3)					
C2	66(3)					
C3	71(3)					
C4	68(3)					
C5	62(3)					
C6	50(2)					
C7	90(4)					
C8	75(5)					
C8d	63(8)					
C9	67(4)					
C9d	53(7)					
C10	70(5)					
C10d	70(9)					
C11	80(5)					
C11d	74(9)					
C12	77(3)					
C13	49(2)					

C14	60(3)
C15	67(3)
C16	64(3)
C17	62(3)
C18	50(2)
C19	93(4)
C20	92(7)
C20d	48(5)
C21	93(7)
C21d	54(6)
C22	63(5)
C22d	73(7)
C23	73(6)
C23d	78(8)
C24	73(3)

[a] Multiplied by 10^3. d = atom for minor component in disorder model.

Table C4. Positional Parameters[a] for 2,5,8-Trithia[9]-*o*-benzenophane.

Atom	x	y	z
S1	-0550(2)	2673(1)	4969(2)
S2	1351(3)	1758(1)	2087(2)
S3	3502(2)	4339(1)	2784(2)
C1	0610(5)	4626(3)	3175(5)
C2	-0312(7)	5121(3)	1937(6)
C3	-2064(6)	5208(3)	1290(6)
C4	-2966(7)	4803(3)	1844(6)
C5	-2106(6)	4307(3)	3039(5)
C6	-0312(6)	4201(3)	3735(5)
C7	0548(6)	3650(3)	5054(5)
C8	-0576(8)	2204(4)	3411(6)
C9	1155(9)	1870(4)	3712(7)
C10	1615(7)	2860(4)	1773(6)
C11	3361(7)	3212(4)	2801(7)
C12	2573(6)	4633(3)	3903(5)

[a]multiplied by 10^4

Table C5. Hydrogen Atom Parameters[a] for 2,5,8-Trithia[9]-*o*-benzenophane.

Atom	x	y	z	U[b]
H2	0303	5405	1538	55
H3	-2657	5550	0452	56
H4	-5672	4867	1400	62
H5	-2752	4024	3410	48
H7A	1675	3514	5214	49
H7B	0642	3965	5851	49
H8A	-0938	2619	2673	92
H8B	-1384	1752	3084	92
H9A	2013	2246	4355	112
H9B	1322	1332	4156	112
H10A	0762	3179	1861	76
H10B	1439	2915	0818	76
H11A	3649	3041	3752	62
H11B	4180	2984	2560	62
H12A	2955	5188	4251	50
H12B	3001	4253	4696	50

[a] Multiplied by 10^4. [b] Multiplied by 10^3.

Table C6. Thermal Parameters[a] for 2,5,8-Trithia[9]-o-benzenophane.

Atom	U11	U22	U33	U23	U13	U12
S1	88(2)	68(1)	61(1)	11(1)	46(1)	-17(1)
S2	120(2)	62(1)	72(1)	-23(1)	39(1)	15(1)
S3	52(1)	99(1)	65(1)	-9(1)	40(1)	-16(1)
C1	35(1)					
C2	50(1)					
C3	51(1)					
C4	56(1)					
C5	44(1)					
C6	34(1)					
C7	45(1)					
C8	83(5)	50(4)	59(4)	0(3)	24(4)	-18(3)
C9	102(5)	58(4)	74(5)	5(4)	30(4)	18(4)
C10	69(4)	82(5)	43(3)	-11(3)	22(3)	10(3)
C11	56(4)	121(6)	63(4)	-33(4)	30(3)	15(4)
C12	45(1)					

[a] Multiplied by 10^3. Note: Where only U_{11} is given, this refers to the isotropic temperature factor.

Table C7. Positional Parameters[a] for [Cu(TTOB)(PPh_2Me)][ClO_4].

Atom	x	y	z
Molecule 1			
Cu1	7066(1)	4959(1)	3552(1)
S1	5746(2)	6543(3)	3593(1)
S2	5923(2)	2442(3)	2720(1)
S3	6914(2)	2959(3)	3883(1)
P1	8717(2)	6647(3)	3621(1)
C1	5819(7)	4848(13)	4468(3)
C2	6394(8)	5374(15)	4968(3)
C3	6567(9)	7141(16)	5354(5)
C4	6235(9)	8459(16)	5267(4)
C5	5631(8)	7963(14)	4774(4)
C6	5421(7)	6138(12)	4369(3)
C7	4781(7)	5728(12)	3850(3)
C8	4925(7)	5337(11)	2928(3)
C9	4660(6)	3171(10)	2643(3)
C10	5516(7)	0520(12)	2855(3)
C11	6422(7)	0712(12)	3299(3)
C12	5673(8)	2900(13)	4061(4)
C13	8562(7)	7156(12)	3102(3)
C32	8728(4)	10244(8)	4276(2)
C33	9202(4)	12111(8)	4685(2)
C34	10349(4)	12796(8)	4982(2)
C35	11021(4)	11613(8)	4870(2)

C36	10546(4)	9747(8)	4462(2)
C31	9399(4)	9062(8)	4165(2)
C42	9777(4)	4116(8)	3753(2)
C43	10589(4)	3178(8)	3731(2)
C44	11451(4)	3651(8)	3571(2)
C45	11501(4)	5063(8)	3432(2)
C46	10689(4)	6001(8)	3454(2)
C41	9827(4)	5527(8)	3614(2)
CL1	5538(2)	4974(3)	1748(1)
O1	5854(9)	6495(16)	1697(6)
O2	4421(5)	4682(12)	1733(3)
O3	6235(8)	4993(30)	2135(5)
O4	5624(11)	3514(17)	1320(5)
Molecule 2			
Cu2	-0555(1)	-0437(1)	1517(1)
S4	-1799(2)	1266(3)	1662(1)
S5	-0397(2)	-0822(4)	2226(1)
S6	-1359(2)	-3650(3)	0959(1)
P2	0958(2)	1142(3)	1471(1)
C14	-3276(8)	-3157(13)	0521(4)
C15	-3455(10)	-4010(18)	0006(5)
C16	-3753(11)	-3076(19)	-0239(5)
C17	-3895(10)	-1399(17)	-0032(5)
C18	-3757(9)	-0502(16)	0480(4)
C19	-3433(7)	-1393(12)	0760(3)
C20	-3250(7)	-0307(12)	1314(3)
C21	-1601(9)	1729(13)	2296(4)

C22	-1536(8)	0084(13)	2374(4)
C23	-1052(10)	-3409(15)	1909(4)
C24	-0965(9)	-4491(15)	1404(4)
C25	-2885(8)	-4179(14)	0788(4)
C26	1804(8)	3371(12)	2044(3)
C52	-0487(4)	0907(7)	0627(2)
C53	-0831(4)	1429(7)	0261(2)
C54	-0078(4)	2856(7)	0254(2)
C55	1018(4)	3762(7)	0614(2)
C56	1362(4)	3240(7)	0980(2)
C51	0609(4)	1813(7)	0986(2)
C62	2632(5)	0015(8)	1079(2)
C63	3485(5)	-0834(8)	1056(2)
C64	3722(5)	-1761(8)	1333(2)
C65	3106(5)	-1840(8)	1633(2)
C66	2253(5)	-0991(8)	1656(2)
C61	2016(5)	-0064(8)	1379(2)
CL2	2610(2)	9114(3)	3062(1)
O5	3015(6)	0848(10)	3071(4)
O6	1786(11)	-2215(12)	2617(5)
O7	3444(8)	-1520(13)	3238(5)
O8	1946(11)	-0470(16)	3370(5)

[a]Multiplied by 10^4

Table C8. Hydrogen Atom Parameters[a] for [Cu(TTOB)(PPh_2Me)][ClO_4].

Atom	x	y	z	U[b]
Molecule 1				
H2	6669	4479	5041	86
H3	6932	7439	5692	95
H4	6408	9719	5538	88
H5	5356	8876	4710	78
H7A	4412	4386	3638	61
H7B	4234	6378	3864	61
H8A	5330	5859	2778	49
H8B	4227	5597	2890	49
H9A	4182	2618	2764	49
H9B	4279	2710	2294	49
H10A	5376	-0674	2566	64
H10B	4845	0552	2928	64
H11A	6131	-0274	3363	67
H11B	7055	0527	3205	67
H12A	5587	2015	4180	75
H12B	5019	2512	3776	75
H13A	8208	5989	2790	57
H13B	9286	7768	3126	57
H13C	8110	7974	3122	57
H32	7947	9778	4074	73
H33	8745	12917	4761	92

H34	10672	14067	5260	79
H35	11801	12079	5073	82
H36	11004	8941	4386	73
H42	9190	3793	3862	54
H43	10555	2217	3825	82
H44	12004	3013	3556	92
H45	12088	5385	3323	88
H46	10723	6962	3359	66
Molecule 2				
H15	-3364	-5230	-0166	103
H16	-3869	-3673	-0588	116
H17	-4092	-0795	-0225	106
H18	-3880	0700	0635	94
H20A	-3749	0434	1362	60
H20B	-3392	-1187	1430	60
H21A	-2218	2098	2375	77
H21B	-0917	2756	2519	77
H22A	-1416	0478	2718	71
H22B	-2233	-0924	2165	71
H23A	-1831	-3664	1863	95
H23B	-0699	-3859	2120	95
H24A	-0201	-4460	1461	91
H24B	-1437	-5779	1249	91
H25A	-3063	-3760	1085	82
H25B	-3249	-5521	0574	82
H26A	1345	4158	2137	70
H26B	2401	4014	1990	70

H26C	2112	3112	2306	70
H52	-1000	-0065	0631	55
H53	-1577	0812	0016	67
H54	-0312	3212	0005	78
H55	1531	4734	0609	77
H56	2108	3857	1225	61
H62	2471	0646	0891	62
H63	3904	-0780	0852	75
H64	4303	-2339	1317	72
H65	3267	-2471	1822	69
H66	1834	-1045	1861	57

[a] Multiplied by 10^4. [b] Multiplied by 10^3.

Table C9. Thermal Parameters[a] for $[Cu(TTOB)(PPh_2Me)][ClO_4]$.

Atom	U11	U22	U33	U23	U13	U12
Molecule 1						
Cu1	32.6(5)	39.7(5)	54.9(6)	24.7(5)	19.6(5)	13.7(4)
S1	38.8(11)	40.4(11)	47.7(13)	20.3(10)	18.5(10)	17.2(9)
S2	42.8(11)	42.4(11)	51.2(13)	18.6(10)	22.3(10)	15.5(9)
S3	45.5(12)	54.8(13)	66.5(15)	39.0(12)	23.7(11)	19.5(10)
P1	30.9(10)	36.3(11)	42.0(12)	20.0(10)	13.3(9)	11.0(9)
C1	59(2)					
C2	76(3)					
C3	87(3)					
C4	81(3)					
C5	71(3)					
C6	53(2)					
C7	57(2)					
C8	47(2)					
C9	45(2)					
C10	58(2)					
C11	61(2)					
C12	69(3)					
C13	54(2)					
C32	68(3)					
C33	83(3)					
C34	74(3)					
C35	74(3)					

C36	66(3)					
C31	41(2)					
C42	50(2)					
C43	74(3)					
C44	86(3)					
C45	81(3)					
C46	60(2)					
C41	40(2)					
CL1	47(1)	70(2)	52(1)	37(1)	19(1)	17(1)
O1	138(9)	151(9)	411(21)	194(13)	164(12)	69(7)
O2	46(4)	138(7)	148(8)	93(6)	37(5)	23(4)
O3	79(7)	644(31)	174(12)	289(18)	45(7)	96(12)
O4	203(12)	155(10)	163(12)	29(9)	85(10)	87(9)
Molecule 2						
Cu2	40.2(6)	53.8(6)	56.3(7)	28.2(5)	26.4(5)	20.2(5)
S4	43.3(12)	44.3(12)	66.5(15)	22.1(11)	28.0(11)	19.4(10)
S5	58.9(15)	79.9(17)	58.6(16)	37.8(14)	20.5(12)	25.4(13)
S6	75.4(16)	47.4(13)	62.0(15)	23.9(12)	39.2(13)	32.2(12)
P2	33.7(11)	43.5(12)	46.7(13)	17.5(11)	16.2(10)	13.8(9)
C14	64(3)					
C15	95(4)					
C16	106(4)					
C17	96(4)					
C18	86(3)					
C19	55(2)					
C20	55(2)					
C21	71(3)					

C22	67(3)					
C24	82(3)					
C25	76(3)					
C26	66(3)					
C52	51(2)					
C53	62(2)					
C54	71(3)					
C55	71(3(					
C56	55(2)					
C51	42(2)					
C62	57(2)					
C63	67(3)					
C64	64(3)					
C65	63(2)					
C66	51(2)					
C61	41(2)					
CL2	57(1)	51(1)	81(2)	26(1)	29(1)	12(1)
O5	81(5)	64(5)	189(9)	64(5)	76(6)	30(4)
O6	189(11)	63(6)	175(11)	12(7)	-40(9)	21(7)
O7	88(6)	113(7)	318(16)	116(10)	29(8)	54(6)
O8	236(13)	168(10)	217(13)	136(10)	167(12)	93(10)

[a] Multiplied by 10^3. Note: Where only U_{11} is given, this refers to the isotropic temperature factor.

Table C10. Positional Parameters[a] for $Mo(TTOB)(CO)_3$.

Atom	x	y	z
Mo	4321(1)	2933(1)	4197(1)
S1	2014(2)	2216(1)	4775(1)
S2	1722(2)	3061(1)	2807(1)
S3	5170(2)	1942(1)	3219(1)
C1	5278(9)	0960(3)	4534(5)
C2	7061(10)	0768(4)	4846(5)
C3	7837(11)	0682(4)	5756(7)
C4	6877(12)	0781(4)	6399(6)
C5	5115(10)	0962(4)	6127(5)
C6	4263(9)	1049(3)	5207(5)
C7	2340(9)	1242(4)	4929(6)
C8	-0074(9)	2243(5)	3881(5)
C9	-0203(9)	2891(5)	3275(6)
C10	1770(9)	2252(4)	2143(5)
C11	3660(10)	2073(4)	2103(5)
C12	4484(10)	1063(4)	3547(5)
C13	3613(9)	3732(4)	4844(5)
C14	6265(9)	2740(4)	5278(5)
C15	5884(9)	3630(4)	3816(5)
O13	3219(8)	4223(3)	5241(4)
O14	7406(7)	2646(3)	5918(4)
O15	6793(7)	4073(3)	3646(4)

S4	9149(3)	0150(1)	1998(2)
O4	9875(10)	0658(4)	2816(6)
C16	6782(17)	0313(7)	1749(10)
C17	9522(16)	0574(7)	0980(9)
S5	8304	0769	1971
O5	8303	0900	0992
C18	0484	0598	2616
C19	7372	0000	2000

[a]Multiplied by 10^4

Table C11. Hydrogen Atom Parameters[a] for $Mo(TTOB)(CO)_3$.

Atom	x	y	z	U[b]
H2	7757	0696	4411	58
H3	9059	0552	5946	52
H4	7432	0725	7033	94
H5	4457	1029	6580	76
H7A	1811	1010	4365	50
H7B	1777	1085	5391	50
H8A	-1043	2249	4168	36
H8B	-0146	1827	3511	36
H9A	-1213	2832	2773	39
H9B	-0370	3297	3625	39
H10A	1063	2321	1536	52
H10B	1298	1867	2422	52
H11A	3635	1646	1757	55
H11B	4102	2454	1802	55
H12A	4892	0701	3204	65
H12B	3221	1042	3430	65
Solvent molecule:				
H16A	5598	0147	1512	94
H16B	7251	0480	1257	94
H16C	6777	0692	2170	94
H17A	9971	0716	0470	92
H17B	9217	0081	0926	92
H17C	10408	0651	1533	92

H18A	0265	0126	2802	94
H18B	0271	0614	1966	94
H18C	-0336	0918	2804	94
H19A	6638	-0343	2197	94
H19B	8219	0182	2519	94
H19C	7977	-0220	1592	94

[a] Multiplied by 10^4. [b] Multiplied by 10^3.

Table C12. Thermal Parameters[a] for $Mo(TTOB)(CO)_3$.

Atom	U11	U22	U33	U23	U13	U12
Mo	29.0(4)	42.8(4)	28.2(4)	-3.2(2)	6.1(3)	1.3(2)
S1	34.3(9)	63.5(12)	34.3(10)	-4.6(8)	11.2(7)	-4.0(8)
S2	39.6(10)	60.3(11)	36.5(10)	2.0(8)	3.7(8)	9.3(8)
S3	36.2(9)	48.8(10)	31.3(9)	-3.3(7)	9.8(7)	3.6(7)
C1	48(4)	39(4)	47(4)	-2(3)	9(3)	-5(3)
C2	54(5)	49(4)	61(5)	6(4)	9(4)	11(3)
C3	47(4)	66(5)	81(7)	13(5)	0(5)	3(4)
C4	85(6)	55(5)	46(5)	14(4)	-9(5)	0(4)
C5	69(5)	52(5)	40(4)	2(3)	18(4)	-8(4)
C6	50(4)	37(4)	44(4)	6(3)	4(3)	-2(3)
C7	46(4)	62(5)	59(5)	0(4)	14(4)	-12(3)
C8	34(4)	84(6)	51(5)	-9(4)	14(4)	0(4)
C9	36(4)	98(7)	45(5)	-5(4)	6(3)	16(4)
C10	47(4)	62(4)	28(4)	-4(3)	2(3)	7(3)
C11	50(4)	66(5)	26(4)	-4(3)	10(3)	2(3)
C12	59(4)	51(4)	37(4)	-7(3)	12(3)	-1(4)
C13	47(4)	56(5)	38(4)	8(4)	13(3)	8(3)
C14	41(4)	46(4)	43(4)	0(3)	9(3)	-4(3)
C15	44(4)	54(4)	38(4)	-4(3)	15(3)	6(4)
O13	107(5)	65(4)	61(4)	-9(3)	39(4)	18(3)
O14	56(3)	85(4)	58(4)	8(3)	-25(3)	-6(3)
O15	67(3)	63(4)	77(4)	2(3)	38(3)	-15(3)
S4	61(1)					

O4	81(2)
C16	91(4)
C17	86(4)
S5	66
O5	79
C18	85
C19	85

[a] Multiplied by 10^3. [b] Fixed parameters of solvent molecule at 78 and 22% occupancy.

Table C13. Data for NMR Simulation of TTMB at 300MHz.[a]

($SCH_2CH_2SCH_2CH_2S$ "bracket").

Expt Freq	Calc Freq	Intensity	Error*
632.400	632.413	.021	-.013
652.590	652.585	1.424	.005
653.760	653.795	1.503	-.035
658.110	658.110	.855	.000
658.110	658.110	.855	.000
660.390	660.388	1.751	.002
662.490	662.458	1.900	.032
666.720	666.710	1.145	.010
666.720	666.710	1.145	.010
	670.261	2.576	
	670.770	2.620	
690.420	690.432	.205	-.012
693.780	693.783	.205	-.003
	713.445	2.620	
	713.954	2.576	
717.510	717.505	1.145	.005
717.510	717.505	1.145	.005
721.770	721.757	1.900	.013
723.870	723.827	1.751	.043
726.090	726.105	.855	-.015
726.090	726.105	.855	-.015
730.440	730.420	1.503	.020

731.580	731.631	1.424	-.051
751.800	751.802	.021	-.002

*assigned transitions only. [a]Frequencies are in Hz.

Table C14. Data for NMR Simulation of TTOB at 300MHz.[a] ($SCH_2CH_2SCH_2CH_2S$ "bracket").

Expt Freq	Calc Freq	Intensity	Error*
	758.719	.003	
780.254	780.252	1.234	.002
781.902	781.908	1.382	-.006
	786.972	1.667	
	787.711	.924	
	787.711	.924	
790.416	790.416	1.076	.000
790.416	790.416	1.076	.000
795.038	795.033	2.766	.005
	795.237	1.665	
797.283	797.284	1.434	-.001
816.564	816.565	1.434	-.001
	818.612	1.665	
818.818	818.817	2.766	.001
823.434	823.434	1.076	.000
823.434	823.434	1.076	.000
	825.537	1.849	
	826.139	.924	
	826.139	.924	
	826.878	1.667	
831.949	831.942	1.382	.007
833.590	833.598	1.234	-.008

855.131	.003

*assigned transitions only. [a]Frequencies are in Hz.

CHAPTER 4

The Ditopic Ligands 2,5,8,13,16,19-Hexathia[9.9]-*ortho*-benzenophane, HTOB and 2,5,8,13,16,19-Hexathia[9.9]-*meta*-benzenophane, HTMB.

4.1 Introduction

Macrocyclic structures containing two discrete binding subunits should allow for coordination of two metal ions and thus the formation of binuclear complexes. These complexes may further bind to bridging ligands and, depending on the distance between the two metal ions, may lead to the observation of metal-metal interactions. The low π-acidity of thioether ligands is also likely to increase the nucleophilicity of the metal centers, which may manifest itself in novel reaction chemistry. Only two binuclear complexes in which the metal ions are facially coordinated in a single thioether macrocycle have been reported in the literature[36,49]. The macrocycle in both complexes serves as a tridentate ligand to each of the metal centers on opposite sides of the ring. Neither complex shows any apparent metal-metal interaction.

In this chapter, the synthesis of two ditopic macrocycles incorporating two S-CH_2CH_2-S-CH_2CH_2-S chelating strings bridged by *ortho*- and *meta*-xylyl units is described (Figure 4.1). The *ortho*-xylyl bridged ligand was structurally characterized by X-ray crystallography and complexed to Cu(I).

4.2 Experimental Section

i) Preparation of *ortho*-xylene-bis(1-hydroxy-3-thiapropane)

Na metal (4.91 g, 214 mmol) was dissolved in anhydrous ethanol (250 mL).

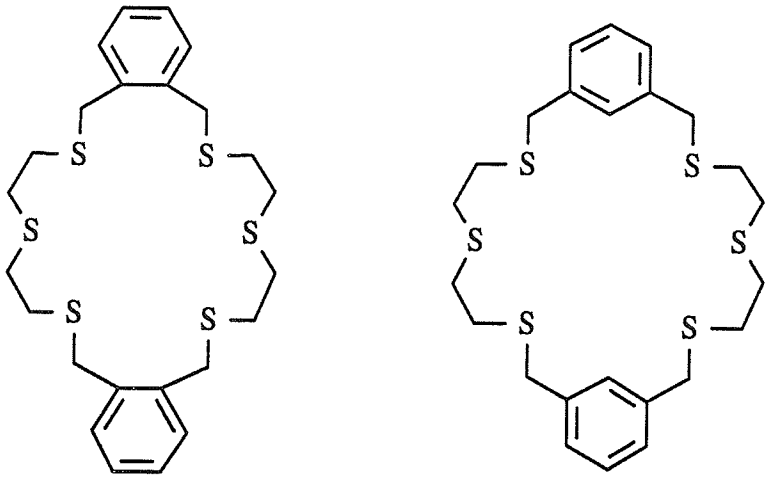

HTOB HTMB

Figure 4.1 Ditopic macrocyclic thioether ligands.

2-Mercaptoethanol (16.71 g, 214 mmol) was added and the resulting solution equilibrated for 1 h. A solution of α,α′-dibromo-*ortho*-xylene (28.23 g, 107 mmol) in anhydrous ethanol (750 mL) was added dropwise over a period of 2 h while refluxing. The mixture was refluxed for another 3 h during which time a white solid precipitated and the solution color changed to yellow. The mixture was cooled to room temperature and stirred overnight. The solvent was removed after filtering and the greenish oily residue extracted with diethylether (400 mL). The extract was filtered and the diethylether removed leaving an oil. The oil solidified upon standing at 10 °C. Yield: 24.78 g (90%). IR: ν(OH) 3380 cm^{-1} (vs, br). $^{13}C\{^1H\}$ NMR ($CDCl_3$): δ 135.95, 130.50, 127.42 (aromatic); 60.61 (CH_2OH), 34.82 (CH_2S), 33.29 (benzylic CH_2); ^1H NMR ($CDCl_3$): δ 7.23 (m, 4H, aromatic); 3.90 (s, 4H, benzylic CH_2); 3.69 (q, 4H, CH_2O); 2.86 (t, 2H, OH); 2.67 (t, 4H, SCH_2). Anal calculated for $C_{12}H_{18}O_2S_2$: C, 55.78; H, 7.02; S, 24.81. Found: C, 55.76; H, 7.07; S, 25.00.

ii) Preparation of *ortho*-xylene-bis(1-chloro-3-thiapropane)

Extreme Caution! Vesicant. Thionyl chloride (19.60 g, 165 mmol; 20% excess) was added dropwise via syringe to *ortho*-xylene-bis(1-hydroxy-3-thiapropane) (17.74 g, 69 mmol) dissolved in CH_2Cl_2 (20 mL) under N_2 in a 50 mL Schlenk flask. During the addition, gas evolved and the solution developed a dark-brown color. The mixture was stirred for 1 h, after which the solvent was removed *in vacuo*. CH_2Cl_2 (30 mL) was added followed by a saturated solution of $NaHCO_3$ (30 mL) and the mixture stirred vigorously. The two phase system was then filtered through phase separation paper and the organic layer dried over Na_2SO_4. After filtration and removal of solvent *in vacuo*, the product was obtained as an orange-brown liquid. Due to the dangerous nature of this compound, no further purification was attempted. Yield: 18 g (88 %). $^{13}C\{^1H\}$ NMR ($CDCl_3$): δ 135.76, 130.65, 127.72 (aromatic); 43.01 (CH_2Cl); 33.80 and 33.78 (CH_2SCH_2). ^1H NMR ($CDCl_3$): δ 7.26 (m, 4H, aromatic); 3.95 (s, 4H, benzylic CH_2); 3.56 (t, 4H, CH_2Cl); 2.82 (t, 4H, SCH_2). An elemental analysis was not performed due to the dangerous nature of the compound.

iii) Preparation of *ortho*-xylene-bis(1-hydroxy-3,6-dithiahexane)

2-Mercaptoethanol (8.78 g, 112 mmol) was added to anhydrous ethanol (350 mL) in which Na metal (2.58 g, 112 mmol) had been dissolved. The resulting solution was equilibrated for 1 h. The mixture was brought to reflux and *ortho*-xylene-bis(1-chloro-3-thiapropane) (16.59 g, 56 mmol) in anhydrous ethanol (200 mL) was added dropwise over a period of 2 h using a constant addition funnel. After the addition was completed, the mixture was refluxed for another 2 h and allowed to cool to room temperature. The work-up was the same as for *ortho*-xylenebis(1-hydroxy-3-thiapropane). Yield: 17.8 g (84 %). The product solidifies upon standing at 10 °C. IR: ν(OH) 3390 cm^{-1}

(vs, br). $^{13}C\{^1H\}$ NMR ($CDCl_3$): δ 136.03, 130.62, 127.51 (aromatic), 60.61 (CH_2OH), 35.33 (benzylic), 33.80, 32.18, 31.78 ($CH_2SCH_2CH_2$ SCH_2). ^1H NMR ($CDCl_3$): δ 7.23 (m, 4H, aromatic), 3.94 (s, 4H, benzylic CH_2), 3.70 (q, 4H, CH_2O), 2.70 (m, 12H, $SCH_2CH_2SCH_2$), 2.33 (t, 2H, OH).

iv) Preparation of *ortho*-xylene-bis(1-chloro-3,6-dithiahexane)

Extreme Caution! Vesicant. *ortho*-Xylene-bis(1-hydroxy-3,6-dithiahexane) (5.24 g, 13.8 mmol) was dissolved in CH_2Cl_2 (25 mL) under N_2. $SOCl_2$ (4.0 g, 33.6 mmol; 20% excess) was added dropwise by syringe. During the addition gas bubbles evolved and the solution turned brown (tea-colored). The mixture was stirred for 1 h at room temperature after which the solvent was removed *in vacuo*. CH_2Cl_2 (20 mL) was added, followed by a saturated $NaHCO_3$ solution (20 mL). The resulting mixture was stirred vigorously for 30 min and filtered through phase separation paper. The organic layer was dried over Na_2SO_4. After removal of the CH_2Cl_2, the product remains as a black viscous liquid which solidifies on standing at 10 °C. Yield: 4.52 g (80%). $^{13}C\{^1H\}$ NMR ($CDCl_3$): δ 135.98, 130.63, 127.54 (aromatic); 43.02 (CH_2Cl); 34.22, 33.77, 32.32, 31.93 ($CH_2SCH_2CH_2SCH_2$). ^1H NMR ($CDCl_3$): δ 7.26 (s, 4H, aromatic), 3.94 (s, 4H, benzylic CH_2), 3.57 (t, 4H, CH_2Cl), 2.67-2.85 (m, 12H, $SCH_2CH_2SCH_2$). Due to its dangerous nature, the product was not characterized further.

v) Preparation of 2,5,8,13,16,19-hexathia[9.9]-*ortho*-benzenophane, HTOB.

Method A: A solution of potassium metal (6.38 g, .16 mol) and 2-mercaptoethanol (12.6 g, 0.08 mol) in anhydrous ethanol (200 mL) was added dropwise to α,α′-dibromo-*ortho*-xylene (21.54 g, 0.08 mol) dissolved in anhydrous ethanol (500 mL) at room temperature under N_2. A white precipitate formed instantly and the addition was

completed in 1 h. Stirring was continued for another 2 h. The mixture was filtered and the solid residue extracted with benzene (300 mL). The product precipitated as white fluffy material, which was recrystallized from a CH_3Cl/hexane mixture as colorless needles. Yield: 1.2 g (5.4%). mp: 152.5-153.5 °C. $^{13}C\{^1H\}$ NMR ($CDCl_3$): δ 135.93, 130.38, 127.65 (aromatic), 33.85, 32.59, 32.39, ($CH_2SCH_2CH_2S$). ^1H NMR ($CDCl_3$): δ 7.29 (m, 8H, aromatic), 3.94 (s, 8H, benzylic CH_2), 2.76 (m, 16H, SCH_2CH_2S). Anal calculated for $C_{24}H_{32}S_6$: C, 56.21; H, 6.29; S, 37.51. Found: C, 55.91; H, 6.05; S, 38.16.

Method B: Cs_2CO_3 (1.9 g, 5.9 mmol) was suspended in DMF (300 mL) at a temperature of 55 °C under N_2. A solution of *ortho*-xylene-α,α′-dithiol (1.00 g, 5.68 mmol) and *ortho*-xylene-bis(1-chloro-3,6-dithiahexane) (2.43 g. 5.68 mmol) in DMF (200 mL) was added dropwise using a constant addition funnel over a period of 24 h, while stirring vigorously. The reaction mixture was cooled to room temperature and the solvent removed on a rotary evaporator. The residue was extracted with CH_2Cl_2 (150 mL) and filtered through Celite. The filtrate was washed with NaOH (0.1 M) (2 x 75 mL), dried over Na_2SO_4 and evaporated *in vacuo*. Yield: 2.68 g (92%). The brown colored residue was recrystallized from $CHCl_3$ giving colorless needles (0.4 g (14%)). The melting point and NMR data are in accordance with those reported in the first synthesis (method A) of this compound.

vi) Preparation of $[Cu_2(CH_3CN)_2(HTOB)][ClO_4]_2$

HTOB (148 mg, 0.29 mmol) was suspended in CH_3CN and CH_2Cl_2 was added until a clear solution resulted. A solution of $[Cu(CH_3CN)_4][ClO_4]$ (189 mg, 0.58 mmol) in CH_3CN (5 mL) was added dropwise by syringe. The mixture was stirred for 3 h, while the temperature was maintained between 45 and 50 °C. Halfway through this period the solution turned foggy and a white solid started to precipitate.. The mixture was cooled to

room temperature and the solvent removed *in vacuo*. The white solid residue was recrystallized from acetonitrile. Yield: 251 mg (94 %). $^{13}C\{^1H\}$ NMR (CD_3CN): δ 135.98, 132.26, 129.30 (aromatic); 35.72, 34.58, 34.43 (aliphatic). ^1H NMR (CD_3CN): δ 7.34 (m, 8H, aromatic), 3.98 (s, 8H, benzylic CH_2), 2.85 (m, 16H, SCH_2CH_2S).

vii) Preparation of $[Cu_2(PPhMe_2)_2(HTOB)][ClO_4]_2$

$[Cu_2(HTOB)(CH_3CN)_2][ClO_4]_2$ was prepared *in situ* as outlined above. Assuming a 100% yield for the above reaction, dimethylphenylphosphine (108 mg, 0.8 mmol) was added by microsyringe. The resulting mixture was stirred overnight at room temperature during which time a white precipitate formed. The solvent was removed *in vacuo* and diethylether (20 mL) was added while stirring vigorously. The diethylether was then syringed off and the white solid dried *in vacuo*. Yield: 410 mg (46%). $^{13}C\{^1H\}$ NMR (CD_3CN): δ 136.03, 132.21, 129.29 (aromatic), 35.64, 34.49, 34.39 (aliphatic); 18.75 (CH_3). ^1H NMR (CD_3CN): δ 7.34 (m, aromatic), 3.97 (s, 8H, benzylic CH_2), 2.82 (m, 16H, SCH_2CH_2S), 1.43 (s, broad. CH_3). Anal calculated for $C_{40}H_{54}Cl_2Cu_2O_8P_2S_6$: C, 43.08; H, 4.88; S, 17.24. Found: C, 43.08; H, 4.94; S, 17.33.

viii) Preparation of $Mo_2(CO)_6(HTOB)$

$Mo(CO)_6$ (398 mg, 1.5 mmol) was refluxed in CH_3CN (20 mL), under N_2, for 4 h. To the resulting yellow solution of *fac*-$Mo(CO)_3(CH_3CN)_3$, HTOB (353 mg, 0.7 mmol) dissolved in CH_2Cl_2 (15 mL), was added by syringe while stirring. A brown solid precipitated. This mixture, was stirred at reflux for 30 min, cooled to room temperature and stirred overnight. The mother liquor was syringed off and the residue dried *in vacuo*. Recrystallization was attempted by slow diffusion of diethylether into a DMSO solution of the product. Yield: 311 mg. ^1H NMR (CD_3CN): δ 7.27 (m, 8H, aromatic), 3.95 (t, 8H,

benzylic CH_2), 2.60-3.00 (m, 16H, CH_2CH_2).

ix) Preparatiom of *meta*-xylene-bis(1-hydroxy-3-thiapropane)

Na (2.04 g, 88.5 mmol) was dissolved in anhydrous ethanol (250 mL) under N_2. 2-Mercaptoethanol (6.92 g, 88.5 mmol) was added and the mixture equilibrated for 1 h. The solution was brought to reflux and a solution of α,α′-dibromo-*m*-xylene (11.69 g, 44.3 mmol) in anhydrous ethanol (250 mL) was added dropwise over a period of 1 h. The mixture was refluxed for 4 h, cooled to room temperature and stirred overnight. The work-up of the product is identical to the ortho analog. Yield: 8.71 g (76%). MS: m/e 240 (M^+-18). IR: ν(OH) 3375 cm^{-1} (vs, br). $^{13}C\{^1H\}$ NMR ($CDCl_3$): δ 138.33, 129.08, 128.60, 127.42 (aromatic); 60.42 (CH_2OH); 35.61, 33.71 (aliphatic); ^1H NMR ($CDCl_3$): δ 7.18 (m, 4H, aromatic); 3.67 (s, 4H, benzylic CH_2); 3.58 (q, 4H, CH_2O); 3.13 (t, 2H, OH); 2.55 (t, 4H, SCH_2). Anal calculated for $C_{12}H_{18}O_2S_2$: C, 55.78; H, 7.02; S, 24.81. Found: C, 55.02; H, 6.90; S, 24.45.

x) Preparation of *meta*-xylene-bis(1-chloro-3-thiapropane)

Extreme Caution! Vesicant. Thionyl chloride (3.64 g, 30.6 mmol; 20% excess) was added dropwise via syringe to *meta*-xylene-bis(1-hydroxy-3-thiapropane) (3.29 g, 12.7 mmol) dissolved in CH_2Cl_2 (15 mL) under N_2 in a 50 mL Schlenk flask. Gas bubbles evolved immediately and the solution turned yellow-brown. The work-up of the product was the same as for ortho analog. Due to the dangerous nature of this compound no further purification was attempted. Yield: 2.89 g (76%). $^{13}C\{^1H\}$ NMR ($CDCl_3$): δ 138.33, 129.17, 128.92, 127.77 (aromatic); 42.86 (CH_2Cl); 36.33 and 33.41 (CH_2SCH_2). ^1H NMR ($CDCl_3$): δ 7.27 (m, 4H, aromatic); 3.75 (s, 4H, benzylic CH_2); 3.53 (t, 4H, CH_2Cl); 2.76 (t, 4H, SCH_2).

xi) Preparation of *meta*-xylene-bis(1-hydroxy-3,6-dithiahexane)

Na (0.23 g, 10.0 mmol) was dissolved in anhydrous ethanol (250 mL) under N_2. 2-Mercaptoethanol (0.78 g, 10.0 mmol) was added and the mixture equilibrated for 1 h. The solution was brought to reflux and a solution of *meta*-xylene-bis(1-chloro-3-thiapropane) (1.48 g, 5.0 mmol) in ethanol (50 mL) was added dropwise over a period of 30 min. The mixture was refluxed for 2 h, cooled to room temperature and stirred overnight. The solvent was removed and the oily residue extracted with H_2O (50 mL). The water was syringed off and the oil dissolved in diethylether (50 mL). This solution was dried over Na_2SO_4. Upon evaporation of the solvent the product is obtained as a thick oil. Yield: 1.32 g (70%). IR: ν(OH) 3390 cm^{-1} (vs, br). $^{13}C\{^1H\}$ NMR ($CDCl_3$): δ 138.36, 129.15, 128.69, 127.57 (aromatic), 60.59 (CH_2OH), 36.15, 35.13, 31.54, 31.39 ($CH_2SCH_2CH_2SCH_2$). ^1H NMR ($CDCl_3$): δ 7.21 (m, 4H, aromatic), 3.72 (s, 4H, benzylic CH_2), 3.65 (q, 4H, CH_2O), 2.63 (m, 12H, $SCH_2CH_2SCH_2$), 2.54 (t, 2H, OH).

xii) Preparation of *meta*-xylene-bis(1-chloro-3,6-dithiahexane)

Extreme Caution! Vesicant. *meta*-Xylene-bis(1-hydroxy-3,6-dithiahexane) (1.31 g, 3.5 mmol) was dissolved in CH_2Cl_2 (10 mL) under N_2. $SOCl_2$ (1.04 g, 7.7 mmol ; 20% excess) was added dropwise by syringe . During the addition gas bubbles evolved and the solution turned brown (tea-colored). The mixture was stirred for 1 h at room temperature after which the solvent was removed in vacuo. CH_2Cl_2 (5 mL) was added, followed by a saturated solution of $NaHCO_3$ (6 mL). The resulting mixture was stirred vigorously for 30 min and filtered through phase separation paper. The organic layer was dried over Na_2SO_4. After removal of the CH_2Cl_2, the product remains as a brownish viscous liquid. Yield: 0.60 g (41.5 %). $^{13}C\{^1H\}$ NMR ($CDCl_3$): δ 138.26, 128.98, 128.54, 127.42 (aromatic); 42.89 (CH_2Cl); 36.01, 34.01, 31.94, 31.25 ($CH_2SCH_2CH_2SCH_2$). ^1H NMR

($CDCl_3$): δ 7.21 (s, 4H, aromatic), 3.72 (s, 4H, benzylic CH_2), 3.66 (t, 4H, CH_2Cl), 2.57-2.71 (m, 12H, $SCH_2CH_2SCH_2$). Due to its dangerous nature, the product was not characterized further.

xiii) Preparation of 2,5,8,13,16,19-hexathia[9.9]-*meta*-benzenophane, HTMB

Cs_2CO_3 (0.49 g, 1.5 mmol) was suspended in DMF (300 mL) at a temperature of 55 °C under N_2. A solution of *meta*-xylene-α,α′-dithiol (0.25 g, 1.45 mmol) and *meta*-xylene-bis(1-chloro-3,6-dithiahexane) (0.60 g. 1.45 mmol) in DMF (30 mL) was added dropwise using a constant addition funnel over a period of 24 h, while stirring vigorously. The product work-up was the same as for the ortho analog. This resulted in the isolation of a colorless oil, which was recrystallized from chloroform. Yield: 0.35 g (46.5 %). $^{13}C\{^1H\}$ NMR ($CDCl_3$): δ 138.57, 129.26, 129.01, 127.73 (aromatic), 36.25, 31.83, 31.31, ($CH_2SCH_2CH_2S$). ^1H NMR ($CDCl_3$): δ 7.23 (m, 8H, aromatic), 3.70 (s, 8H, benzylic CH_2), 2.53 (m, 16H, SCH_2CH_2S).

xiv) General X-ray Diffraction Data Collection, Solution and Refinement.

In order to avoid repetition, the reader is referred to the relevant paragraph in chapter 2 for general comments on X-ray diffraction data collection, solution and refinement.

xv) Structure Determination of 2,5,8,13,16,19-hexathia[9.9]-*ortho*-benzenophane, HTOB

Colorless crystals of HTOB were grown by slow evaporation of a $CHCl_3$ solution of the compound. Preliminary photography was consistent with a monoclinic crystal

system. Observed extinctions were consistent with space group $P2_1/c$. Intensity data ($\pm h,+k,+l$) were collected in one shell ($4.5°<2\theta<45°$). A total of 1382 reflections were collected and 1319 unique reflections with $F_o^2 > 3\sigma(F_o^2)$ were used in the refinement. The three S atom positions were determined by direct methods from the E-map with highest figure of merit. The remaining carbon atoms were located from successive difference Fourier map calculations. In the final cycles of refinement, sulfur atoms were refined anisotropically and the carbon atoms were assigned isotropic thermal parameters. At final convergence this resulted in:

$R = \Sigma||F_o| - |F_c|/\Sigma|F_o|| = 0.0311$ and $R_w = (\Sigma w(|F_o| - |F_c|)^2/\Sigma wF_o^2)^{1/2} = 0.0378$

The Δ/σ values in the final cycle were less than 0.074. A final difference Fourier map calculation showed no peaks of chemical significance; the largest was 0.39 electrons/Å^3 and was associated with the S1 atom. Table 4.1 gives the crystal data and machine and collection parameters. Selected bond distances and angles are summarized in Table 4.2. Atomic positional parameters (Table D1), hydrogen atom parameters (Table D2) and thermal parameters (Table D3) are given in appendix D.

Table 4.1 Crystallographic Data for 2,5,8,13,16,19-Hexathia[9.9]-ortho-benzenophane, HTOB.

Chemical formula	$C_{24}H_{32}S_6$
Crystal color	colorless
Crystal form	needles
Formula weight	512.24
a, Å	5.047(3)
b, Å	8.567(7)
c, Å	29.886(25)
β, deg	98.29(7)

Crystal system	monoclinic
Space group	$P2_1/c$
Vol, Å^3	1278.9(17)
ρ(calcd), g/cm^{-3}	1.33
Z	2
Cryst dimens, mm	.22x.39x.18
μ, abs coeff, cm^{-1}	4.89
Radiation (λ, Å)	MoKα(0.71069)
Temp, °C	24
Scan speed, deg/min	2.0-5.0 (θ-2θ scan)
Scan range, deg	1.0 below Kα_1 and 1.0 above Kα_2
Bkgd/scan time ratio	0.5
Data collected (2θ)	1382 (4.5 to 45°)
hkl range	$\pm h,+k,+l$
Unique data ($F_o^2>3\sigma F_o^2$)	1319
No. of variables	142
R(F_o^2), %	3.11
$R_w(F_o^2)$, %	3.78

4.3 Results.

i) Synthesis

The one-pot synthesis[8,9,12] described in method A (Eq A) to prepare HTOB is simple, but the yields are extremely low. The preferred route (Eq B) to synthesize the large molecules HTOB and HTMB is, without question, via the hydroxy- and

chloro-intermediates followed by ring closure using the cesium ion mediated method[13,14]. For the preparation of HTMB, it is the only available route as the one-pot synthesis yielded only TTMB (the small ring species) and polymer. All intermediates were prepared in good yields and the xylene-dithiols are commercially available. This avoided the cumbersome synthesis of the dithiols.

(A)

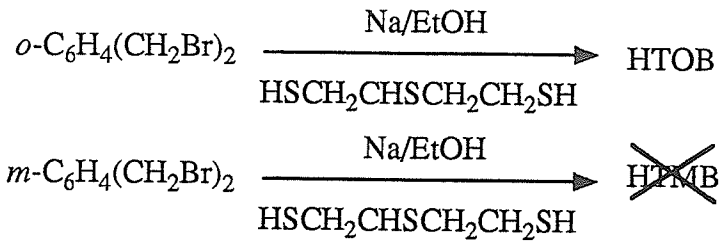

(B)

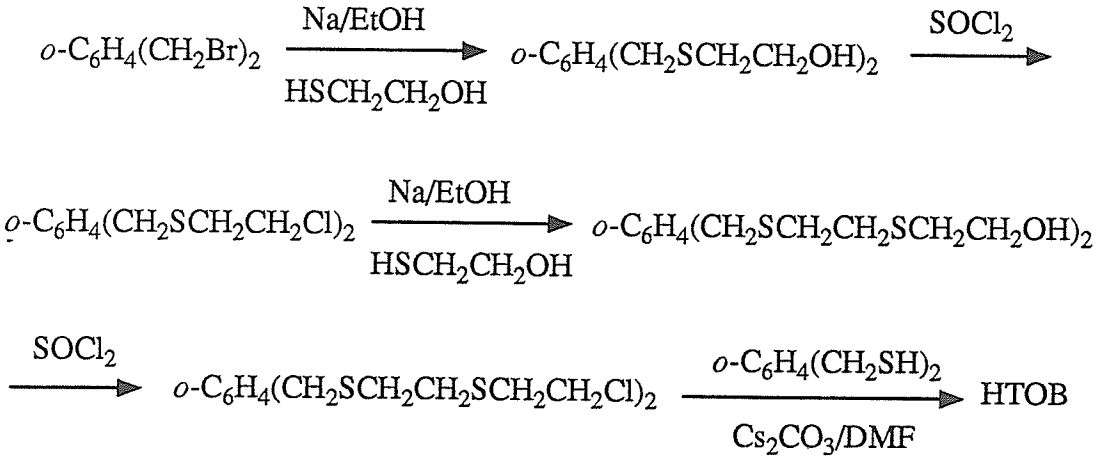

ii) X-ray structure of 2,5,8,13,16,19-hexathia[9.9]-*ortho*-benzenophane, HTOB

The unit cell contains two discrete molecules of HTOB, each on a crystallographic center of inversion. Sulfur-carbon bond distances range from 1.803(3) to 1.819(3) Å and carbon-carbon bond distances from 1.491(4) to 1.520(4) Å for the aliphatic carbons and from 1.367(5) to 1.397(4) Å for the carbons in the aromatic ring. The C-S-C angles range

from 99.2(1)° to 101.0(1)°. These values are in good agreement with those found for other macrocyclic thioethers reported in the literature[18,65] and those reported for 16S6. A listing of selected inter-atomic distances and angles is given in Table 4.2. From the ORTEP diagram (Figure 4.2), it can be seen that the S-CH_2CH_2-S-CH_2CH_2-S linkages do not have the same conformation as the S-CH_2CH_2-S-CH_2CH_2-S "brackets" in TTOB and TTMB. The benzylic S-atoms across the ortho-xylyl linkages are oriented in opposite directions, whereas the S atoms at the end of each "bracket" are pointing in the same direction with respect to the plane through the xylyl aromatic rings. Hence, one "bracket" lies above, whereas the other is below the plane through the xylyl units. The shape of the cavity is rectangular and measures approximately 5.5 by 9.7 Å . The aromatic rings of the ortho-xylyl linkages are parallel to each other, but do not lie in the same plane.

An analysis of the torsional angles, listed in Table 4.3, shows that, although the gauche placement of C-C-S-C fragments is generally satisfied, the S-CH_2CH_2-S-CH_2CH_2-S "bracket" is severely distorted from the ideal conformation. Two of the C-C-S-C fragments have torsional angles (C6-C7-S1-C8 = 165.6° and C9-S2-C10-C11 = 169.2°) that indicate an anti placement around these bonds in contrast to the preferred gauche placement for C-S bonds. Distortion is particularly evident from the S2-C10-C11-S3 torsional angle with a value of 82.8°, indicating gauche instead of the expected anti placement around C-C bonds.

Table 4.2 Selected Bond Distances and Angles for 2,5,8,13,16,19-Hexathia[9.9]-*ortho*-benzenophane, HTOB.

	Distances (Å)		
S1-C7	1.819(3)	C3-C4	1.367(5)
S1-C8	1.809(3)	C4-C5	1.375(5)
S2-C9	1.813(3)	C5-C6	1.385(4)

S2-C10	1.803(3)	C1-C6	1.397(4)
S3-C12	1.814(3)	C6-C7	1.504(4)
C1-C12	1.502(4)	C8-C9	1.491(4)
C1-C2	1.391(4)	C10-C11	1.520(4)
C2-C3	1.379(4)		
	Angles (°)		
C7-S1-C8	101.0(1)	C1-C6-C7	122.1(2)
C9-S2-C10	99.2(1)	C6-C7-S1	109.5(2)
S2-C10-C11	112.5(2)	S1-C8-C9	114.3(2)
S3-C12-C1	108.6(2)	C8-C9-S2	113.3(2)
C12-C1-C6	121.6(2)		

Table 4.3 Torsional Angles for 2,5,8,13,16,19-Hexathia[9.9]-*ortho*-benzenophane, HTOB.

S3'-C12-C1-C6	-88.8	S1-C8-C9-S2	-175.7
C12-C1-C6-C7	1.3	C8-C9-S2-C10	-72.5
C1-C6-C7-S1	87.9	C9-S2-C10-C11	169.2
C6-C7-S1-C8	165.6	S2-C10-C11-S3	82.9
C7-S1-C8-C9	-65.0		

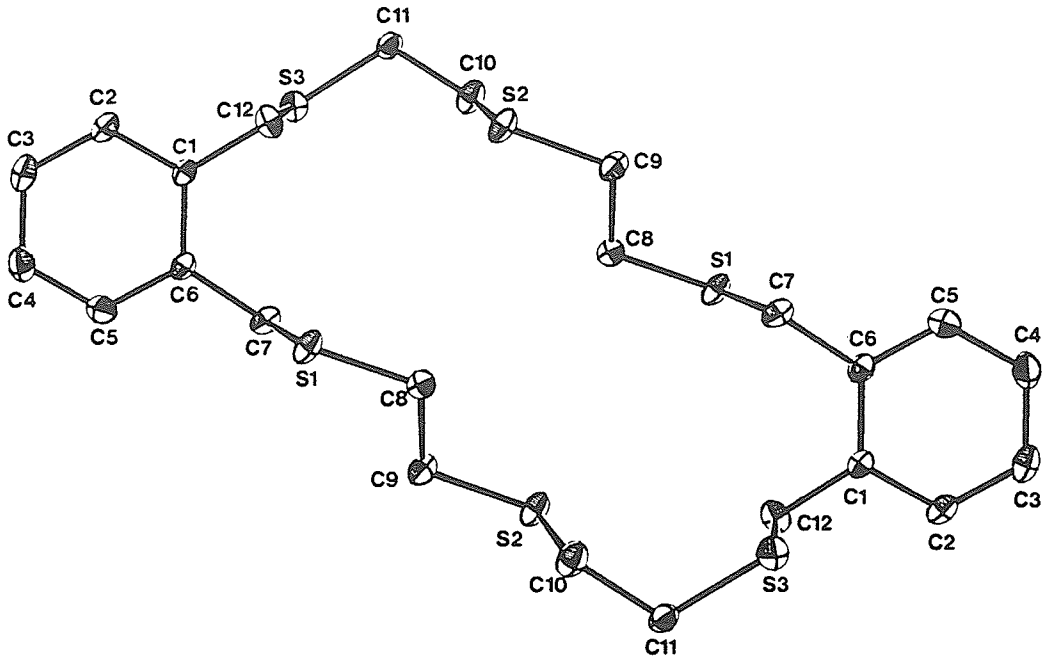

Figure 4.2 Perspective ORTEP drawing of HTOB showing the atom numbering scheme. 20% thermal ellipsoids are shown.

iii) ^{1}H-NMR

The resonance signals of the S-CH_2CH_2-SCH_2CH_2-S "brackets" in the ^{1}H-NMR spectra of the macrocyclic thioethers HTOB and HTMB occur as slightly broadened multiplets at 2.76 and 2.53 ppm respectively. The multiplets are very similar to each other but differ significantly from the spectra observed for the S-CH_2CH_2-SCH_2CH_2-S "brackets" of the small ring species TTOB and TTMB, which both gave sharp, well resolved multiplets of 16 peaks (Figure 3.9). The resonance patterns were found to be very characteristic and hence ^{1}H NMR is an excellent tool to distinguish between the small and large rings of these macrocyclic thioethers (Figure 4.3). The difference between the resonance patterns for the S-CH_2CH_2-SCH_2CH_2-S "brackets" of the small and the large

ring may be due to a greater flexibility of the large ring molecule. However, the X-ray structure also shows that the "bracket" conformations of the small and large ring molecules differ in the solid state, with the ideal "bracket" occuring only for the small rings.

Therefore, the lack of a complex AA'BB' multiplet in the ^{1}H NMR may be an indication that these S-CH_2CH_2-SCH_2CH_2-S linkages also do not have the ideal "bracket" conformation for the large ring macrocycles HTOB and HTMB in solution.

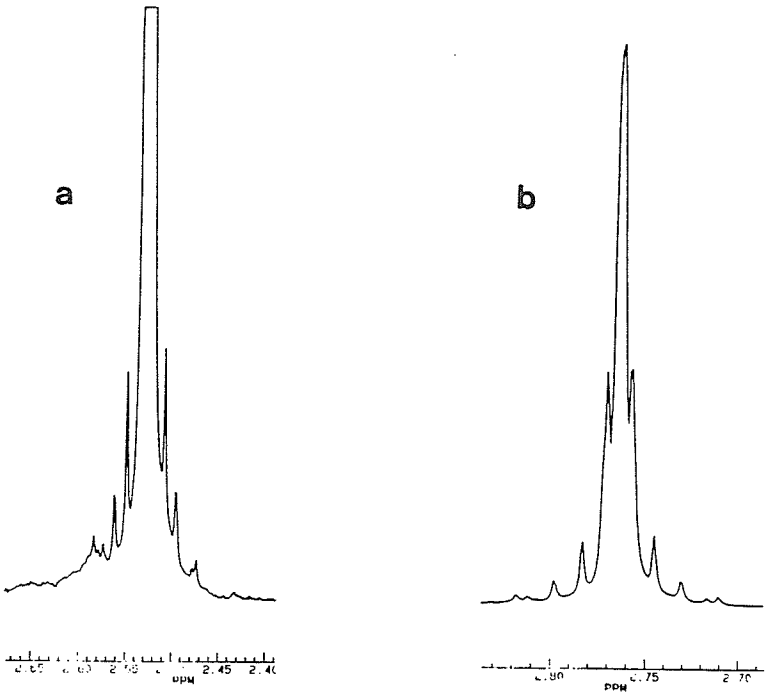

Figure 4.3 ^{1}H NMR spectrum of the $SCH_2CH_2SCH_2CH_2S$ "bracket". a) HTMB and b) HTOB (at 300MHz.)

The ^{1}H NMR spectra of the complexes $[Cu_2(HTOB)(CH_3CN)_2][ClO_4]_2$ and $[Cu_2(HTOB)(PPhMe_2)_2][ClO_4]_2$ differ only in the signals due to the ancillary ligand. The spectra show an identical multiplet around δ 2.8 ppm. The pattern of this multiplet differs significantly from the multiplet assigned to the S-CH_2CH_2-S-CH_2CH_2-S "bracket"

resonance of the uncomplexed ligand (Figures 4.3 and 4.4). The presence of well resolved peaks for the thioether linkages of these complexes probably indicates that the ligand in its complexed form is simply more rigid than when uncomplexed. Also, since the patterns in the spectra of HTOB in both complexes are the same, the nature of the ancillary ligand seems to have little affect on the conformation of the ligand in its complexed form. The ^1H NMR spectrum of the molybdenum complex shows a non-symmetrical resonance pattern for the $SCH_2CH_2SCH_2CH_2S$ "brackets", which is inconclusive with respect to a mono- or binuclear complex.

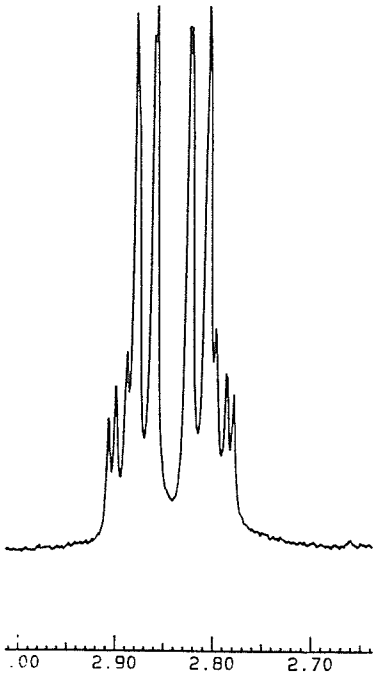

Figure 4.4 ^1H NMR spectrum (at 300MHz.) of the $SCH_2CH_2SCH_2CH_2S$ "bracket" of $[Cu_2(HTOB)(CH_3CN)_2][ClO_4]_2$.

4.4 Discussion

The crystal structure of HTOB shows that in the solid state the benzylic sulfur atoms across the *ortho*-xylene bridge, are directed in opposite directions, whereas the

sulfur atoms at the endpoints of the chelating strings point in the same direction. Hence, the *ortho*-xylyl fragment is very effective in separating the chelating sites. This conformation of the ligand may accommodate the approach of metal ions from opposite sides of the ligand plane. Therefore, the coordination mode of the binuclear complexes is likely "in-and-out". That is, each Cu^+ ion has a tetrahedral geometry and is facially coordinated by the macrocycle, but to opposite sides of the ligand. The same structure is proposed for the complex when the labile CH_3CN ligands are replaced by PMe_2Ph groups (Figure 4.5).

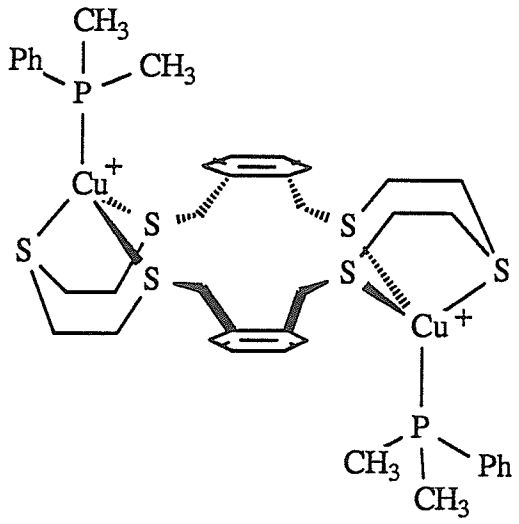

Figure 4.5 "in and out" coordination of $[Cu_2(HTOB)(PPhMe_2)_2]^{2+}$ cation

Although we did succeed in synthesizing the *meta* analog (HTMB), purification of the compound proved to be extremely difficult. X-ray quality crystals could not be obtained, but the $^{13}C\{^1H\}$ and ^1H NMR and the elemental analysis data are consistent with HTMB having the structure shown in Figure 4.1.

4.5 Summary and Conclusions

The large ring thioether HTOB was synthesized and structurally characterized by X-ray crystallography. HTOB is a potentially ditopic ligand. The two chelating strings are the S-CH_2CH_2-S-CH_2CH_2-S brackets, which are separated by ortho-xylyl units. Although no crystal structures have been obtained, we believe that the ligand forms the binuclear complex $[Cu_2(HTOB)(CH_3CN)_2][ClO_4]_2$, with $[Cu(CH_3CN)_4][ClO_4]$, and the labile CH_3CN ligands are easily replaced by phosphine groups analogous to the mononuclear Cu(I) complexes of TTOB.

HTMB, the large ring hexathioether with meta-xylyl units in the ring, is expected to exhibit the same type of complexation results.

Appendix D

Table D1. Positional Parameters[a] for 2,5,8,13,16,19-Hexathia[9.9]-*ortho*-benzenophane, HTOB.

Atom	x	y	z
S1	4490(2)	1350(1)	4454(1)
S2	9371(2)	3760(1)	5604(1)
S3	2893(1)	5477(1)	3286(1)
C1	2727(5)	2330(3)	3308(1)
C2	1804(6)	1705(4)	2885(1)
C3	3077(7)	0457(4)	2716(1)
C4	5279(7)	-0196(4)	2968(1)
C5	6218(6)	0410(4)	3388(1)
C6	4994(5)	1672(3)	3564(1)
C7	6141(6)	2291(3)	4022(1)
C8	5502(6)	2610(4)	4934(1)
C9	8444(6)	2603(4)	5098(1)
C10	8100(7)	2505(4)	6009(1)
C11	9032(7)	2999(4)	6495(1)
C12	1343(6)	3727(3)	3472(1)

[a]multiplied by 10^4.

Table D2. Hydrogen Atom Parameters[a] for 2,5,8,13,16,19-Hexathia[9.9]-*ortho*-benzenophane, HTOB.

Atom	x	y	z	U[b]
H2	0265	2146	2709	61
H3	2413	0048	2426	84
H4	6164	-1055	2853	84
H5	7744	-0053	3562	55
H7A	8013	2080	4078	49
H7B	5856	3386	4031	49
H8A	4594	2280	5175	54
H8B	4981	3648	4850	54
H9A	8997	1556	5161	53
H9B	9351	3009	4865	53
H10A	8708	1472	5968	82
H10B	6193	2528	5954	82
H11A	8818	2083	6678	69
H11B	10978	3305	6541	69
H12A	-0508	3708	3350	49
H12B	1525	3710	3793	49

[a] Multiplied by 10^4. [b] Multiplied by 10^3.

Table D3. Thermal Parameters[a] for 2,5,8,13,16,19-Hexathia[9.9]-*ortho*-benzenophane, HTOB.

Atom	U11	U22	U33	U23	U13	U12
S1	59.3(5)	49.7(5)	33.9(5)	-1.8(3)	0.9(3)	-19.2(4)
S2	60.8(5)	55.9(5)	37.3(5)	-7.0(3)	1.8(4)	-19.2(4)
S3	53.4(5)	45.6(5)	48.3(5)	2.7(3)	13.5(4)	-4.4(3)
C1	40.8(15)	38.7(15)	31.0(16)	0.6(12)	5.8(12)	-5.4(12)
C2	55.3(18)	53.3(18)	32.8(18)	-1.1(14)	-3.6(13)	-5.3(15)
C3	75.7(22)	58.1(21)	38.0(18)	-12.0(16)	7.5(16)	-12.2(17)
C4	76.3(22)	55.7(20)	53.7(22)	-11.3(17)	20.4(18)	4.9(17)
C5	50.1(17)	57.9(21)	52.9(20)	1.2(16)	4.2(15)	10.8(15)
C6	39.6(15)	42.9(15)	32.5(16)	-1.2(13)	5.5(12)	-8.7(13)
C7	44.9(16)	52.3(18)	37.0(17)	3.6(13)	-0.7(12)	-9.8(14)
C8	49.6(18)	52.5(18)	39.2(17)	-2.0(14)	3.3(13)	3.3(14)
C9	47.5(17)	58.9(20)	40.2(17)	-3.7(14)	3.1(13)	-5.8(14)
C10	77.7(22)	44.5(18)	42.9(18)	-1.8(14)	2.4(15)	-12.2(15)
C11	61.9(20)	41.8(18)	39.1(19)	2.3(13)	-2.3(14)	0.3(15)
C12	44.9(16)	46.1(18)	41.8(18)	0.6(13)	9.2(13)	-0.7(12)

[a] Multiplied by 10^3. Note: Where only U_{11} is given, this refers to the isotropic temperature factor.

REFERENCES.

1 Meadow, J. R.; Reid, E. E. *J. Am. Chem. Soc.* **1934**, 56, 2177.

2 Pedersen, C. J. *J. Am. Chem. Soc.* **1967**, 89, 7017.

3 Rosen, W. and Busch, D. H. *Inorg. Chem.* **1970**, 9, 262-265.

4 Cooper, S. R. *Acc. Chem. Res.* **1988**, 21, 141-146, and references therein.

5 Colman, P. M.; Freeman, H. C.; Guss J. M.; Murata, M.; Norris, V. A.; Ramshaw, J. A. M.; Venkatappa, M. P. *Nature(London)*, **1978**, 272, 319-324.

6 Setzer, W, N.; Ogle, C. A.; Wilson, G. S. and Glass, R. S. *Inorg. Chem.* **1983**, 22, 266-271.

7 Pedersen, C. J. *J. Org. Chem.* **1971**, 36, 254-257.

8 Ochrymowycz, L. A.; Ching-Pong Mak; Michna, J. D. *J. Org. Chem.* **1973**, 38, 2079-2084.

9 Vögtle, F. *Tetrahedron* **1969**, 25, 3231-3242.

10 Weber, E.; Vögtle, F. *Chem. Ber.* **1976**, 109, 1803-1831.

11 Weber, E.; Vögtle, F. *Liebigs Ann. Chem.* **1976**, 891-915.

12 Gerber, D.; Chongsawangvirod, P.; Leung, A. K.; Ochrymowycz, L. A. *J. Org. Chem.* **1977**, 42, 2644-2645.

13 Buter, J. and Kellogg, R. M. *J. Chem. Soc. Chem. Commun.* **1980**, 466-467.

14 Buter, J. and Kellogg, R. M. *J. Org. Chem.* **1981**, 46, 4481-4485.

15 Patai, S. *The Chemistry of Ethers, Crown Ethers, Hydroxyl Groups and their Sulphur Analogues. Supplement E, Part 1; Ed. John Wiley &. Sons: New York,* **1980**, *175-211.*

16 Sellmann D.; Frank P. *Angew. Chem. Int. Ed. Eng.* **1986**, 25, 1107-1109.

17 Küppers, H. J.; Raabe E.; Krüger, C.; Wieghardt, K. *Angew. Chem. Int. Ed. Eng.* **1987**, 25, 1101-1102.

18 Hartman, J. R,; Wolf, R. E.; Foxman, B. M. and Cooper, S. R. *J. Am. Chem. Soc.* **1983**, 105, 131-132.

19 Blower, P. J.; Cooper, S. R. *Inorg. Chem.* **1986**, 26, 2009-2010.

20 Wolf, R. E.; Hartman, J. R.;Ochrymowycz L. A.; Cooper, S. R. *Inorg. Chem.* **1987**, 29, 976.

21 Murray, S. G.; Hartley, F. R. *Chem. Rev.* **1981**, 81, 365-414.

22 Rosen, W. and Busch, D. H. *J. Am. Chem. Soc.* **1969**, 91, 4694-4697.

23 Rawle, S. C.; Hartmann, J. R.; Watkin, D. J. and Cooper, S. R. *J. Chem. Soc., Chem. Comm.* **1986**, 1083.

24 Hintsa, E. J.;Hartman, J. R. and Cooper, S. R. *J. Am. Chem. Soc.* **1983**, 105, 3738-3739.

25 Thorne, C. M.; Rawle, S. C.; Admans, G. A. and Cooper, S. R. *Inorg. Chem.* **1986**, 3848-3850.

26 Cooper, S. R.; Rawle, S. C.; Hartman, J. R.; Hintsa, E. J. and Admans, G. A. *Inorg. Chem.* **1988**, 27, 1209-1214.

27 Küppers, H. J.; Wieghardt, K.; Nuber, B.; Weiss, J.; Bill, E.; Trautwein, A. X. *Inorg. Chem.* **1987**, 26, 3762-3769.

28 Wieghardt, K.; Küppers, H. J. and Weiss, J. *Inorg. Chem.* **1985**, 24, 3067-3071.

29 Blake A. J.; Crofts, R. D.; Reid, G. and Schröder, M. *J. Organomet. Chem.* **1989**, 359, 371-378.

30 Küppers, H. J.; Neves, A.; Pomp C.; Ventur, D.; Wieghardt, K.; Nuber, B.; Weiss, J. *Inorg. Chem.* **1986**, 25, 2400-2408.

31 Hintsa, E. J.;Hartman, J. R. and Cooper, S. R. *J. Chem. Soc., Chem. Commun.* **1984**, 386.

32 Jenkinson, J. J.; Levason, W.; Perry, R. J. and Spicer M. D. *J. Chem. Soc. Dalton Trans.* **1989**, 453.

33 Jones, T. E.; Zimmer, L. L.; Diadarrio, L. L.; Rorabacher, D. B.; Ochrymowycz, L. A. *J. Am. Chem. Soc.* **1975**, 97, 7163-7165.

34 Dockal, E. R.; Diadarrio, L. L.; Glick, M. D.; Rorabacher, D. B. *J. Am. Chem. Soc.* **1977**, 99, 4530-4532.

35 Pett, V. B.; Diadarrio, L. L. Jr.; Dockal, E. R.; Corfield, P. W.; Ceccarelli, C.; Glick, M. D.; Ochrymowycz, L. A.; Rorabacher, D. B. *Inorg. Chem.* **1983**, 22, 3661-3670.

36 Gould, R. O.; Lavery, A. J. and Schröder, M. *J. Chem. Soc. Chem. Commun.* **1985**, 1492.

37 Corfield, P. W. R.; Ceccarelli, C.; Glick, M. D.; Wei-Yu Moy I.; Ochrymowycz, L. A.; Rorabacher, D. B. *J. Am. Chem. Soc.* **1985**, 107, 2399-2404.

38 Hartman, J. R. and Cooper, S. R. *J. Am. Chem. Soc.* **1986**, 108, 1202-1208.

39 DeSimone, R. E. and Glick, M. D. *J. Am. Chem. Soc.* **1975**, 942-943.

40 Cragel, J.; Pett, V. B.; Glick, M. D. and DeSimone, R. E. *Inorg. Chem.* **1978**, 17, 2885-2893.

41 Sellmann, D.; Zapf, L.; *Angew. Chem. Int. Ed. Eng.* **1984**, 23, 807-808.

42 Ashby, M. T.; Lichtenberger, D. L. *Inorg. Chem.* **1985**, 636-638.

43 Ashby, M. T.; Enemark, J. H.; Lichtenberger, D. L. and Ortega, R. B. *Inorg. Chem.* **1986**, 25, 3154-3157.

44 Bell, M. N.; Blake, A. J.; Schröder, M.; Küppers, H. J. and Wieghardt, K. *Angew. Chem. Int. Ed. Eng.* **1987**, 26, 250-251

45 Rawle, S. C.; Sewell, T. J. and Cooper, S. R. *Inorg. Chem.* **1987**, 26, 3769-3775.

46 Rawle, S. C. and Cooper, S. R. *J. Chem. Soc. Chem. Commun.* **1987**, 308-309.

47 Sellmann, D.; Knoch, F.; Wronna, C. *Angew. Chem. Int. Ed. Eng.* **1988**, 27, 691-692

48 Bell, M. N.; Blake, A. J.; Schröder, M. and Stephenson, T. A. *J. Chem. Soc. Chem. Commun.* **1986**, 471-472.

49 Riley, D. P.; Oliver, J. D. *Inorg. Chem.* **1983**, 22, 3361-3363.

50 Yoshida, T.; Ueda, T.; Adachi, T.; Yamamoto, K.; Higuchi, T. *J. Chem. Soc. Chem. Commun.* **1985**, 1137-1138.

51 Rawle, S. C.; Yagbasan, R.; Prout, K. and Cooper, S. R. *J. Am. Chem. Soc.* **1987**, 109, 6181-6182.

52 Blake, A. J.; Holder, A. J.; Hyde, T. I.; Schröder, M. *J. Chem. Soc. Chem. Commun.* **1987**, 987-988.

53 Blake, A. J.; Gould, R. O.; Lavery, A. J.; Schröder, M. *Angew. Chem. Int. Ed. Eng.* **1986**, 25, 274-275.

54 Blake, A. J.; Holder, A. J.; Hyde, T. I.; Roberts, Y. V.; Lavery, A. J.;Schröder, M. *J. Organometallics* **1987**, 323, 261-270.

55 Shriver D. F. "The Manipulation of Air-Sensitive Compounds". McGraw-Hill: New York (1969).

56 Jones R. A.; Wright T. C.; Atwood J. L. and Hunter W. E.. Organometallics 2, 470, (1983).

57 Abraham R. J.; Loftus P. "Proton and Carbon-13 NMR Spectroscopy". John Wiley & Sons: New York.

58 Günther H. "NMR Spectroscopy". John Wiley & Sons: New York.

59 Kubas, G. J. *Inorg. Synth.* **1979**, 19, 90-92.

60 Blake, A. J.; Gould, R. O.; Reid, G.; Schröder, M. *J. Organometallics* **1988**, 356, 389-396.

61 Küppers, H. J.; Wieghardt, K.; Nuber, B.; Weiss, J.; Krüger, C.; Yi-Hung Tsay *Angew. Chem. Int. Ed. Eng.* **1987**, 26, 575-576.

62 Clarkson J.; Yagbasan R.; Blower P. J.; Rawle S. C.; Cooper S. R. *J. Chem. Soc. Chem. Commun.* **1987**, 950-951.

63 Blake, A. J.; Gould, R. O.; Holder, A. J.; Hyde, T. I.; Lavery, A. J.; Odulate, M. O.; Schröder, M. *J. Chem. Soc. Chem. Commun.* **1987**, 118-120.

64 Borgen, G.; Dale, J.; Anet, F. A. L. and Krane, J. *J. Chem. Soc.* **1974**, 243-245.

65 Glass, R. S.; Wilson, G. S. and Setzer, W. N. *J. Am. Chem. Soc.* **1980**, 102, 5068-5069.

66 Alcock, N. W.; Herron, N.; Moore, P. *J. Chem. Soc. Chem. Commun.* **1976**, 886-887.

67 Robinson, G. H.; Sangokoya, S. A. *J. Am. Chem. Soc.* **1988**, 110, 1494-1497.

68 Carlin, R. L.; Weissberger, E. *Inorg. Chem.* **1964**, 3, 611

69 Cromer, D. T.; Waber, J. T. *International Tables for X-ray Crystallography*; Kynoch: Birmingham, England, 1974.

70 (a) Cromer, D. T.; Mann, J. B.; *Acta. Crystallogr., Sect. A: Cryst. Phys., Diffr., Theor. Gen. Crystallogr.* **1968**, *A24*, 321. (b) *Ibid.* **1968**, *A24*, 390.

71 Abraham, R. J. "The Analysis of High Resolution NMR Spectra". Elsevier: Amsterdam.

72 Wolf, R. E.; Hartman, J. R.; Storey, . M. E.; Foxman, B. M. and Cooper, S. R. *J. Am. Chem. Soc.* **1987**, 109, 4328-4335.

73 Beach, N. A.; Gray, H. B. *J. Am. Chem. Soc.* **1968**, 90, 5713.

74 Elias, H.; Schmidt, G.; Küppers, H.; Saher, M.; Wieghardt, K.; Nuber, B.; Weiss, J. *Inorg. Chem.* **1989**, 28, 3021-3024.

75 Lecomte, J.; Lehn, J. M.; Parker, D.; Guilhem, J.; Pascard, C. *J. Chem. Soc. Chem. Commun.* **1983**, 296.